Rapid ecological and evolutionary divergence during a poleward range expansion

Monica M. Sheffer[1]*, Linda Zander[1], Brian Schulze[1#], Pierick Mouginot[2], Thomas Naef[3], Jürgen Kreyling[4], Rosemary G. Gillespie[5], Katharina J. Hoff[6,7], Stefan Prost[8,9,10,11], Henrik Krehenwinkel[12] & Gabriele Uhl[1]

[1]General and Systematic Zoology, Zoological Institute and Museum, University of Greifswald, 17489 Greifswald, Germany

[2]PSL Research University, CNRS-EPHE-UPVD, USR 3278 CRIOBE, 66360, Perpignan, France

[3]Applied Zoology and Nature Conservation, Zoological Institute and Museum, University of Greifswald, 17489 Greifswald, Germany

[4]Experimental Plant Ecology, Institute for Botany and Landscape Ecology, University of Greifswald, 17489 Greifswald, Germany

[5]Department of Environmental Science Policy and Management, University of California Berkeley, 94720 Berkeley, CA, USA

[6]Institute of Mathematics and Computer Science, University of Greifswald, 17489 Greifswald, Germany

[7]Center for Functional Genomics of Microbes, University of Greifswald, 17489 Greifswald, Germany

[8]Department of Behavioural and Cognitive Biology, University of Vienna, 1090 Vienna, Austria

[9]Konrad Lorenz Institute of Ethology, University of Veterinary Medicine, A-1160 Vienna, Austria

[10]Natural History Museum Vienna, Central Research Laboratories, 1010 Vienna, Austria

[11]South African National Biodiversity Institute, National Zoological Gardens of South Africa, Pretoria 0001, South Africa

[12]Department of Biogeography, University of Trier, 54296 Trier, Germany

*Indicates corresponding author

[#]Current affiliation: Animal Ecology, Zoological Institute and Museum, University of Greifswald, 17489 Greifswald, Germany

Abstract

Anthropogenic climate change is rapidly altering ecosystems, driving range shifts, range contractions, dwindling population sizes and local extinctions in many species. Some species, however, are expanding their ranges and seem to benefit from warming temperatures. This is the case for the wasp spider, *Argiope bruennichi*, which has undergone a range expansion from its historic range in the Mediterranean ("core"), now reaching as far as the Baltic states and Scandinavia ("edge"). The rate of this range expansion cannot be attributed to climate change alone, and it has been hypothesized that adaptive introgression lent the genetic variation upon which selection could act, enabling the rapid range expansion. In the present study, we first quantify the degree of local adaptation and phenotypic plasticity in cold tolerance in edge relative to core populations, and secondly investigate genomic and phenotypic turnover across the proposed introgression zone. With a reciprocal transplant common garden experiment, we provide strong support for the hypothesis that edge populations are locally adapted to colder winter conditions. We also find evidence of seasonal plasticity in the core populations, while edge populations have lost this plasticity. Our genome-wide analysis, using a combination of F_{ST} outlier and genetic-environment association tests, supports the hypothesis that adaptive introgression played a role in environmental adaptation.

Keywords

Range expansion, local adaptation, phenotypic plasticity, cold tolerance, spider, adaptive introgression

Introduction

Organisms experience changing environments from season to season, but also in the long term, and less predictably, facing global climate change. Global change is massively altering ecosystems, leading to extinction events, dwindling population sizes, and range contractions in many species worldwide. However, some species seem to profit from these changes, displaying dramatic poleward range expansions (reviewed in i.e. Parmesan *et al.*, 1999; Hickling *et al.*, 2006; Chen *et al.*, 2011). Such range expansions have long been explained by environmental change alone. Recent work shows that range-expanding populations differentiate from core populations during the process of expansion. Environmental change may make a new habitat suitable in one dimension, such as sufficiently warm summer temperatures for development, while other dimensions, such as colder winter temperatures at the expanding front, may require genetic adaptation or adaptive phenotypic plasticity (Sexton *et al.*, 2009; Colautti & Barrett, 2013). This is the case, for example, in the range-expanding damselfly, *Ischnura elegans*, which has maintained its heat tolerance but altered its lower thermal tolerances, likely through evolutionary adaptation, during a poleward range expansion (Lancaster *et al.*, 2015, 2016). The rapid establishment and phenotypic differentiation of range-expanding species offers the opportunity to investigate the roles of plasticity and evolutionary adaptation in responses to novel environments, and to obtain information on the underlying genomic basis of adaptation. This is especially true for species with passive dispersal, such as seeds or spiders dispersing in the wind, with little to no control over where they land.

Phenotypic plasticity, the potential for a single genotype to produce differing phenotypes in response to differing environmental conditions (see Fordyce, 2006; Whitman & Agrawal, 2009), can facilitate range expansion, enabling dispersing organisms to persist wherever they arrive. However, even if plasticity is sufficient for initial survival and establishment, local adaptation may subsequently arise, i.e. if there is a cost to plasticity (Ghalambor *et al.*, 2007; Auld, Agrawal & Relyea, 2010; Hoffmann & Bridle, 2021). Common garden and reciprocal transplant experiments allow for disentangling plastic and adaptive responses, by manipulating the environment while controlling for genetic background. Such experiments have demonstrated that local genetic adaptation is widespread in nature (i.e. Clausen, Keck & Hiesey, 1941; Leimu & Fischer, 2008; Hereford, 2009; Fraser *et al.*, 2011). However, the relative importance of novel mutations or standing genetic variation providing the substrate for selection, enabling genetic adaptation, cannot be derived from those experiments (Barrett & Schluter, 2008; Hedrick, 2013; Hoban *et al.*, 2016), and is rarely studied in conjunction with the relative importance of adaptation and phenotypic plasticity in organismal responses to novel environments.

In theory, adaptation from standing genetic variation should take place more quickly than adaptation from novel mutations. This has a number of reasons; for instance, variants which may be adaptive under novel environments are already present in the gene pool and occur at reasonably high frequencies, while novel mutations seldom arise and start at low frequencies, which are more susceptible to genetic drift (reviewed in Barrett & Schluter, 2008). A third avenue through which adaptive variants can arise in a genepool is via introgression, admixture or intraspecific hybridization of previously isolated populations. Traditionally, hybridization has often been associated with deleterious effects, such as outbreeding depression (Muhlfeld *et al.*, 2009). More recently, however, studies have increasingly begun to identify cases of adaptive introgression. For example, introgression plays a strong role in wing coloration in the *Heliconius* butterfly mimicry complex (Zhang *et al.*, 2016; Moest *et al.*, 2020). Adaptive introgression can be especially rapid, when it involves the sharing of alleles that are under very strong selection in a novel

environment, as has been demonstrated in the case of rapid pesticide resistance in an African mosquito species (Norris *et al.*, 2015). Another interesting example for adaptive introgression is the increased fitness at higher altitudes found in Tibetan humans, which has been shown to stem from introgression of Denisovan-like DNA into humans (Huerta-Sánchez *et al.*, 2014; Racimo *et al.*, 2015).

Argiope bruennichi is an orb-weaving spider species with a Palearctic distribution, which has undergone a rapid latitudinal range expansion within Europe in the last century (Follner & Klarenberg, 1995; Algo, 2010; Krehenwinkel & Tautz, 2013; Krehenwinkel, Rödder & Tautz, 2015; Wawer *et al.*, 2017). Krehenwinkel & Tautz (2013) attributed the range expansion to climate-mediated adaptive introgression, with individuals from eastern Asia mixing with the European gene pool via Russia, providing genetic variation that enabled rapid adaptation to the colder, previously unsuitable conditions in northern Europe. Indeed, as a consequence of their latitudinal range expansion, individuals in the expanding populations prefer colder temperatures (Krehenwinkel & Tautz, 2013) and have a colder climatic niche, as they must endure much more extreme winter temperatures and higher seasonality than their counterparts in the core of the range (Krehenwinkel *et al.*, 2015). What remains unclear is whether the observed differences are due to phenotypic plasticity or genetic adaptation, and where, precisely, adaptive introgression occurred geographically and within the genome.

To address the first hypothesis, we set out to quantify the level of genetic adaptation and phenotypic plasticity in edge relative to core populations in a suite of life history and physiological traits which may enhance their ability to endure the colder winter conditions at the expanding edge. We did this using a reciprocal transplant common garden experiment, overwintering juvenile spiders ("spiderlings") from replicated core or edge populations in either native or foreign conditions. At two time points, mid-winter and post-winter, we measured their survival, mass, body size, and several cold tolerance metrics: namely supercooling point, lower lethal temperature, and chill coma recovery time.

To address the second hypothesis, we investigated phenotypic traits and genomic patterns across latitude. Our sampling scheme focused on core and edge populations and the area of suspected introgression. We quantified how adult phenotypes (body size, clutch size, hatching success, and pigmentation) vary with latitude. We assessed population genomic patterns across latitude, and scanned for signatures of adaptive introgression in the genome, to test if introgression truly provided the substrate for selection enabling range expansion in this species.

Material and Methods

Population samples

We collected adult *A. bruennichi* females in a transect from southern France to Estonia, with dense sampling in Germany cutting across the admixture zone proposed by Krehenwinkel & Tautz (2013) from July 29th-August 10th, 2018. We timed the collecting trip according to the mating season, when the females had mated (indicated by the lack of males, which had been cannibalized) but not yet laid egg sacs (indicated by the lack of egg sacs in the field). We filled in the gaps between southern France, Germany, and Estonia using DNA extracts from samples previously used in Krehenwinkel & Tautz (2013). Similarly, we used DNA extracts from that study for outgroup populations from Russia and Japan (Figure 1). We aimed to collect 10 individuals per site, although we included populations with as few as three individuals when population densities were low. Our transect within Europe spans 15 degrees of latitude. Exact collecting locations with GPS coordinates and sample sizes can be found in Table 1.

In addition to the ~10 animals per site collected from the NE-SW transect, we collected 94 more adult *A. bruennichi* females from the three sites in Estonia and 80 more from the four sites in southern France to increase the sample size for our reciprocal transplant common garden experiment (henceforth "common garden experiment").

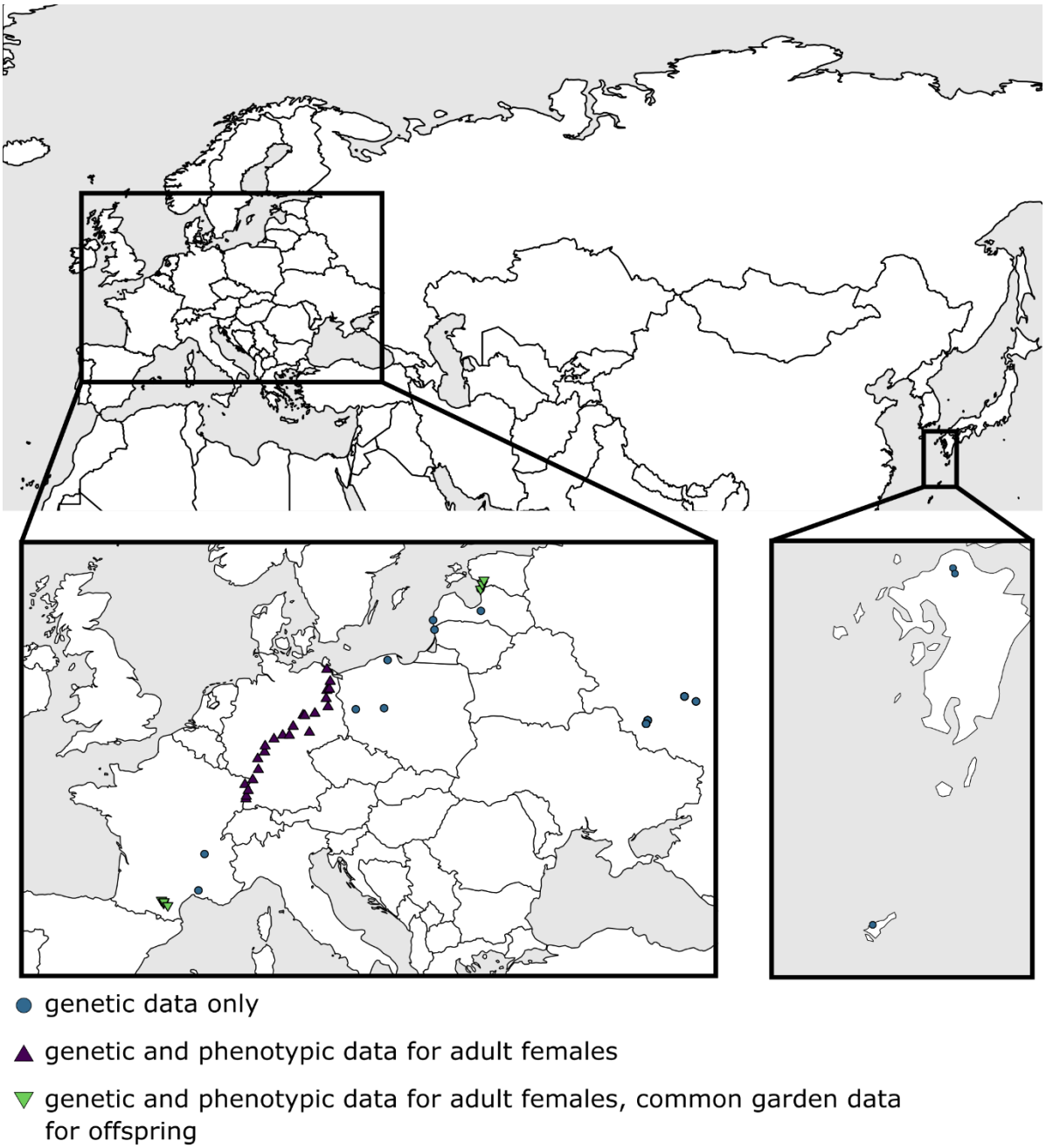

Figure 1. **Collecting sites included in this study**. Each point represents a collecting locality; point shape and color corresponds to the data collected at each site.

Table 1. **Collecting sites included in this study**. The "Use" column contains a sub-column for the two aspects of our study: the common garden experiment (CG) and the transect sampling. The transect sub-column contains either "P" (data for adult phenotypes) and/or "G" (genetic data), or "O" (outgroup genetic data). In the sample size column ("N"), the number in [square brackets] indicates additional females collected to achieve reasonable sample sizes for the common garden experiment. Populations in **bold text** have data for both aspects (transect and common garden).

Population Number	Population Name	Use		Country	N	Latitude (˚N)	Longitude (˚E)
		CG	Transect				
1	**Belflou**	✓	P&G	France	10 [7]	43.32287	1.786019
2	**Casties**	✓	P&G	France	10 [7]	43.18677	1.939997
3	**Mireval**	✓	P&G	France	10 [51]	43.25358	1.961534
4	**Perry**	✓	P&G	France	10 [15]	43.07072	2.231319
5	Nimes	-	G	France	10	43.78	4.4
6	Lyon	-	G	France	10	45.48	4.83
8	Umkirch	-	P&G	Germany	10	48.05299	7.758187
9	Kenzingen	-	P&G	Germany	10	48.17536	7.783603
10	Offenburg	-	P&G	Germany	10	48.44384	7.919677
11	Brumath	-	P&G	France	11	48.72702	7.689943
12	Au Am Rhein	-	P&G	Germany	10	48.95041	8.243427
13	Heidelberg	-	P&G	Germany	10	49.42313	8.638357
14	Graefenhause	-	P&G	Germany	10	49.93076	8.594512
15	Buedingen	-	P&G	Germany	10	50.24868	9.078187
16	Schotten	-	P&G	Germany	10	50.5284	9.117785
17	Bad Hersfeld	-	P&G	Germany	10	50.85265	9.743685
18	Eisenach	-	P&G	Germany	8	51.02786	10.35974
19	Gierstadt	-	P&G	Germany	10	51.02483	10.82997
20	Kelbra	-	P&G	Germany	10	51.44596	11.10118
21	Pegau	-	P&G	Germany	10	51.16905	12.25069
22	Zeits	-	P&G	Germany	4	51.97261	11.8048
23	Barby	-	P&G	Germany	3	51.94881	11.9164
24	Rabenstein	-	P&G	Germany	10	52.056	12.636
25	Schulzendorf	-	P&G	Germany	10	52.36082	13.56633
26	Wandlitz	-	P&G	Germany	10	52.74649	13.4346
27	Templin	-	P&G	Germany	4	53.12951	13.48775
28	Mittenwald	-	P&G	Germany	7	53.1869	13.66299
29	Strasburg	-	P&G	Germany	10	53.54765	13.72238
30	Ludwigsburg	-	P&G	Germany	10	54.11404	13.48225
32	Grodziszcze	-	G	Poland	7	52.25	15.533
33	Poznan	-	G	Poland	10	52.3	17.5333
34	Lebork	-	G	Poland	10	54.55	17.78
35	Palanga	-	G	Lithuania	10	55.97	21.1
36	Liepaja	-	G	Latvia	10	56.42	21
37	Salaspils	-	G	Latvia	10	56.85	24.38
38	Ainazi	-	G	Latvia	10	57.87	24.35
39	**Ikla**	✓	P&G	Estonia	10 [6]	57.87248	24.35843
40	**Pulgoja**	✓	P&G	Estonia	10 [9]	58.10143	24.48833
41	**Paernu**	✓	P&G	Estonia	10 [79]	58.29702	24.59738
42	Selikhovy Dvory Village	-	O	Russia	10	51.57	36.07
43	Khytor Stepnoy Village	-	O	Russia	10	51.73333	36.18333
44	Donskoye Village	-	O	Russia	10	52.85	38.78333
45	Yablonevoye Village	-	O	Russia	3	52.61667	39.6
46	Amami oshima Island	-	O	Japan	7	28.33	129.32
47	Amami oshima Island	-	O	Japan	9	28.33	129.32
48	Fukuoka	-	O	Japan	10	33.65	130.6833

Animal husbandry

After collection, we brought the spiders into a climate controlled chamber at the University of Greifswald, Germany, where they produced one to two egg sacs under shared conditions (80 % relative humidity, 26°C day temperature, 20°C night temperature, with 12 hours of full day, 10 hours of full night, and one hour to transition between the day and night temperatures). The spiders were stored in plastic containers (height: 13 cm, diameter: 12 cm) with a hole filled with cotton on the top for ventilation; additional humidity was provided by spraying the cotton with water every evening. We fed the spiders with adults or larvae of *Lucilia caesar* and *Calliphora vomitoria* flies twice a week.

After the period for oviposition was over, the adult females were anesthetized using CO_2, then preserved in pure ethanol and stored at -80°C. Females that died of natural causes in the lab were not used for sequencing, as they were not immediately preserved, and thus the DNA could have degraded over night until they were checked the next day.

Common garden experiment

Timing of experiments

Egg sacs were laid over a period of one month and 15 days, between August 4, 2018 and September 19, 2018. We will henceforth refer to the number of days between collection and oviposition as "oviposition latency." In the field, *A. bruennichi* females lay their eggs into round flask-shaped egg sacs, placed ~20 cm above the ground, in the grass (Wawer *et al.*, 2017; MM Sheffer, personal observation). Females do not guard or tend their egg sacs for extended periods of time, and a single female can produce multiple egg sacs; we refer to the eggs in each egg sac as a "clutch." Females in our study laid up to two egg sacs. The day following oviposition, we placed the egg sacs into 5 x 5 x 3.5 cm plastic boxes with mesh on two sides, and moved them into climate cabinets programmed with the same day/night conditions under which they were laid, until the onset of winter treatments. Eggs develop, hatch and molt within two to four weeks following oviposition (Leborgne & Pasquet, 2005; Schneider, Fromhage & Uhl, 2005; Welke & Schneider, 2010). These molted spiderlings overwinter within the egg sac. Here, it is important to note that because the egg sacs were laid before we began the winter treatments, and hatching occurs shortly after oviposition, clutch size and hatching success will not be affected by the winter treatments.

On October 1st, 2018, we changed the climate conditions in the climate cabinets, one with a "warm" winter treatment, corresponding to the natural conditions in southern France (climate cabinet: Panasonic Pflanzenzucht- und Klimatestkammer MLR-352H, Ewald Innovationstechnik GmbH, Bad Nenndorf, Germany), and the other a "cold" winter treatment, corresponding to the natural conditions in Estonia (climate cabinet: Percival Tieftemperaturkammer LT-36VL mit Fernkondensator, CLF PlantClimatics GmbH, Wertingen, Germany). The egg sacs from each origin (France "core", or Estonia "edge") were randomly assigned to warm or cold winter treatments, while ensuring approximately equal sample sizes per origin and treatment (Table 2)**.** For details on the winter regimens, see Supplemental File 1: Figure S1. All egg sacs from a single mother (up to two) were placed into the same winter treatment.

At mid-winter (February 4-March 19, 2019) and post-winter (April 4-May 19, 2019) intervals, we opened a subset of the egg sacs and counted the number of eggs, dead spiderlings, and living spiderlings, and performed cold tolerance experiments, described below. Egg sacs opened at mid-winter were opened six

months (183 +/- 2 days) after the oviposition date, while post-winter egg sacs were opened eight months (243 +/- 1 days) after oviposition.

Table 2. Sample sizes for the common garden experiment. Egg sacs laid by adult female spiders from French (core) and Estonian (edge) populations were placed into either warm or cold winter treatments. The egg sacs were opened at mid- (February-March) or post-winter (April-May). Some, but not all, mothers laid two egg sacs.

	Experimental group			
Origin	Winter treatment	Season	# 1st Egg sacs	# 2nd Egg sacs
Core	Warm	Mid-Winter	31	16
Core	Warm	Post-Winter	31	7
Core	Cold	Mid-Winter	30	8
Core	Cold	Post-Winter	28	9
Edge	Warm	Mid-Winter	33	26
Edge	Warm	Post-Winter	30	20
Edge	Cold	Mid-Winter	31	19
Edge	Cold	Post-Winter	30	10

For egg sacs with sufficient numbers of living spiderlings, we allotted 15 spiderlings for body size measurements, 20 spiderlings for lower lethal temperature measurements, 10 spiderlings for chill coma recovery time measurements, and 8 spiderlings for supercooling point measurements. In some families with low survival, small clutch size, or low hatching success, slightly fewer spiderlings were used in some measurements. Precise descriptions of the measurements taken follow below.

Response variables for common garden experiment

Life history traits and survival

We calculated the clutch size of egg sac as the sum of eggs, dead spiderlings, and living spiderlings. Hatching success was calculated as the sum of dead and living spiderlings ("hatched" spiderlings) divided by the total clutch size. Survival was calculated as the number of living spiderlings divided by the total number of hatched spiderlings.

Mass and body size (spiderlings)

After counting the spiderlings, we immediately took the mass of 15 individual spiderlings per clutch using a Sartorius ME5 scale (Sartorius AG, Goettingen, Germany). After weighing, the spiderlings were stored individually in 80% ethanol at room temperature. Later, the preserved spiderlings were removed from ethanol, and the first leg on the right side was removed and photographed using a Zeiss Discovery V20 Microscope in combination with a Zeiss AxioCam MRc camera with a 0.63X objective (Zeiss AG, Oberkochen, Germany). From the photos, we measured the length from the proximal end of the patella to the distal end of the tibia ("Tibia-Patella length"), using the Carl Zeiss AxioVision SE64 Software (v.4.9.1.2, Zeiss AG, Oberkochen, Germany). Tibia-patella length is a commonly-used proxy for body size in spiders (Uhl & Vollrath, 2000).

Chill coma recovery time

10 spiderlings per clutch were placed individually into a 3D-printed microwell plate. The wells were painted bright white with non-toxic water-based paint to increase the contrast between the well and the

spiderlings. The wells were covered with a glass slide to prevent the spiderlings from escaping, and then the plate was placed into a -9°C freezer for one hour, to induce chill coma. After one hour, the plate was carefully removed from the freezer, and placed into a climate chamber (15°C, 80% humidity). The glass slide was changed to prevent fogging, and then the spiderlings were filmed in the plate for one hour using an iPhone 6 camera. Analysis of the videos was done manually, with the IDs obscured, by scanning through the video while watching a single spider, until the first movement. Then the video was re-watched at normal speed from a few seconds before the first movement, and the time of the very first movement (i.e. a leg twitch, shift in body position) was marked down as the chill coma recovery time, in seconds. All videos from the mid-winter experiments were re-watched to determine the repeatability of the measurements; the CCR time did not differ significantly between the first and second watching, therefore we did not re-watch the post-winter videos.

Supercooling point

An organism's supercooling point is the temperature at which the body water freezes. This point can be detected by the heat of crystallization released upon ice formation (Sinclair, Coello Alvarado & Ferguson, 2015). In order to determine *A. bruennichi* supercooling points, eight spiderlings per clutch were placed individually into a pipette tip, which had been sealed at the tip. A thermocouple (Type K) was inserted into the pipette tip until it came into contact with the spiderling, and was then held in place with a piece of cotton, so that neither the spiderling nor the thermocouple could move. The pipette tips were placed into well-fitting holes drilled into a custom-made aluminum block, and the block was then placed into a dynamic climate chamber (Modell MKT 115, Binder GmbH, Tuttlingen, Germany). Temperature data from the thermocouples was gathered by Pico USB TC-08 thermocouple data loggers (Pico Technology, Cambridgeshire, United Kingdom) once every second for the duration of the trial. Trials started at 5°C and ramped down at a rate of approximately -0.4°C/minute for a total of 150 minutes. Data was copied from the data logger output program into Excel, and then analyzed with a custom R script (Supplemental File 2). The supercooling point was calculated as the temperature immediately before a temperature increase above the threshold of 0.3°C/second. The threshold was determined by running the script on several sets of data with different thresholds; 0.3°C/second was sensitive enough to detect the more gradual peaks, but not so sensitive that background changes in temperature were recorded as supercooling points. Each batch of peaks with supercooling points marked was visually inspected before being entered into the final datasheet.

Lower lethal temperature

Of the 20 spiderlings taken from each clutch, 10 were used as test subjects, and 10 were used as a control group, to account for mortality unrelated to the test. The tube containing test spiderlings was placed into a freezer at either -10°C, -18°C, -26°C, or -32°C, for one hour, then placed into a climate chamber held at 15°C, 80% humidity, to recover. The control spiderlings were handled in the same way (carried to the freezer, but not placed inside, and then carried to the climate chamber), but remained at the recovery temperature for the duration of the test (2 hours). After the recovery period, the test and control tubes were opened (blind to treatment, ID, and test/control status) and the number of live and dead spiderlings was recorded. A spiderling was considered dead only if it did not respond to any stimulus (touch with a paintbrush or submersion in ethanol). Of the 1,738 spiderlings in control groups, only 15 died.

Statistical analysis of common garden data

Explanatory variables

In order to assess phenotypic plasticity and genetic adaptation in the common garden experiment, our explanatory variables of central interest were "origin" (southern France or Estonia) and "winter treatment" (warm or cold). We also investigated seasonal differences with the explanatory variable "season" (mid-winter or post-winter). All starting models included the interaction of these three variables, except for clutch size and hatching success, as these could not be affected by the winter treatments (see "Timing of experiments," above). For the lower lethal temperature experiments, exposure temperature (-10°C, -18°C, -26°C, or -32°C) was also included as an explanatory variable. Additional, potentially biologically relevant, variables were oviposition latency (time from collection to oviposition), mother's body size, clutch size, and whether the individual came from a first or second clutch. Continuous explanatory variables were centered and scaled in order to allow for interpretation of effects on the same scale (Schielzeth, 2010).

Random effects

The population from which a spider was collected (three populations in Estonia, four populations in southern France) was included as a random effect. For response variables measured at the individual spiderling level, the clutch (first or second) and mother's ID were included as nested random effects within population – specified in the model as (1 | Population / Mother ID / Clutch). If measurements were done at the clutch level, only population was included as a random effect (1 | Population).

Modeling approach

We analyzed all common garden data using (generalized) linear mixed models in R, using the package 'glmmTMB' (Brooks *et al.*, 2017) for non-Gaussian distributions and the package 'lme4' for Gaussian distributions (Bates *et al.*, 2015). Details of the models for each response variable follow below.

For the data on clutch size, we used a negative binomial distribution with default link function and linear parameterization ("nbinom1" in R). Hatching success was modeled using a betabinomial distribution with default link. The hatching success data showed zero inflation due to oviposition latency, so we included a zero inflation formula to account for the excess of zero hatching success in late-laid egg sacs. We used a betabinomial distribution with default link for the survival model. As for hatching success, we also found zero inflation due to oviposition latency (an excess of zero survival in late-laid egg sacs). Therefore, we included oviposition latency as a zero inflation formula. Mass and body size were modeled using a Gaussian distribution.

The distribution of chill coma recovery times was highly skewed, and attempts to find an appropriate distribution family and model to handle the skewness proved unsuccessful. Therefore, we log-transformed the raw data, allowing us to model with a Gaussian distribution. Due to the characteristic multimodal distribution of supercooling points (i.e. Sinclair *et al.*, 2003), we followed the common practice in the field, and split the data into "low group" (LG) and "high group" (HG) supercooling points at -25.5°C, chosen according to visual inspection of a break in the distribution of the raw data (Supplemental File 1: Figure S2). The LG SCPs had a normal distribution, and were modeled as a single response variable with a Gaussian distribution. The HG SCPs were much rarer, and did not allow for modeling directly. Thus, we calculated the per-clutch ratio of HG:LG SCPs, to test whether any of our treatment groups had a tendency toward more HG SCPs. This HG:LG comparison was modeled with a binomial distribution and logit link.

Finally, the lower lethal temperature data were modeled with a betabinomial distribution and default link. These data were recorded as the number surviving or dying within a subset of one clutch. The exposure temperature was added as an explanatory variable, along with all other aforementioned explanatory variables.

For each full starting model, we performed a backward stepwise model selection using AIC, with random factors always included in the compared models. We did not remove any fixed effects, only the interactions, according to AIC. The model with the lowest AIC was then assessed further. For models with a ΔAIC of less than four, we always proceeded with the most parsimonious (i.e. least complex) model within those criteria. Model assumptions were checked using the R package 'DHARMa', which uses simulated residuals to provide easily interpretable checks of assumptions for many model and distribution types (Hartig, 2021).

Where possible, we used the Nakagawa & Schielzeth method (Nakagawa & Schielzeth, 2013) to calculate a pseudo-R^2, implemented in the 'performance' R package (Lüdecke *et al.*, 2021), to assess how much of the variation in the data was explained by the full model (conditional pseudo-R^2), and by the model without random effects (marginal pseudo-R^2). The Nakagawa & Schielzeth method is not reliable for betabinomial models, thus we used a crude calculation suggested in the 'glmmTMB' FAQs (https://bbolker.github.io/mixedmodels-misc/glmmFAQ.html) to understand the goodness of fit for our betabinomial models (hatching success, overwintering survival, and lower lethal temperature); precisely, we calculated the squared correlation of the predicted values with the observed values of the response variable (calculated in R: cor(model.response(model.frame(model)), predict(model, type = "response"))^2) . This does not provide a comparison of conditional and marginal R^2, thus for betabinomial models we only report the conditional R^2. We refer to "significant" effects as those where the 95% confidence interval (CI) does not cross zero.

To visualize the results, we used the 'ggpredict' function from the 'ggeffects' R package (Lüdecke, 2018) to compute estimated marginal means and 95% CI of the response variable for specific model terms. This allows us to visualize results on the observed scale, making biological interpretation more straightforward. Likewise, although within the model continuous fixed effects were centered and scaled, we plotted the model estimates with the unscaled values.

Historical climate data across transect

We extracted historical climate data for all collecting sites along the transect, excluding the outgroups in Russia and Japan, using an R script and data for the 19 standard bioclimatic variables downloaded from WorldClim at 30 second (~1km^2) resolution (Fick & Hijmans, 2017). To summarize and reduce the number of environmental variables in downstream analyses, we summarized the 19 variables into fewer dimensions using a principal components analysis (PCA) using the R package 'FactoExtra' (Kassambara & Mundt, 2020) (Supplemental File 3), following the recommendation of Hoban *et al.* (2016). The first five principle components (PCs) accounted for 97.6% of the variation in the climate data, and were used as explanatory variables for phenotype-environment and genotype-environment associations.

Transect data – adult female phenotypes

For the females from the study by Krehenwinkel & Tautz (2013), we have genetic data but do not have phenotype data, as we directly used their previously extracted DNA and the physical specimens were not

available. Thus, we collected phenotype data for the females collected in 2018 from southern France, Germany and Estonia, described in detail below.

Adult female body size

We removed and photographed the first leg on the right side from each female using a Zeiss Discovery V20 Microscope in combination with a Zeiss AxioCam MRc camera with a 0.63X objective (Zeiss AG, Oberkochen, Germany). From the photos, we measured tibia-patella length as a proxy for body size, as described above for spiderlings.

Opisthosoma pigmentation

To characterize the pigmentation of the dorsal opisthosoma, we photographed each female in the field, using an Olympus Tough F2.0 camera with a ring light flash attachment mounted on a wooden box lined with aluminum foil and blue paper bottom. The spiders were anesthetized using CO_2 so that we could position them for the photograph. When the camera was mounted, no light could enter the box other than the diffused light from the ring light, thus standardizing the lighting conditions in the field. The images were processed in Gimp (v.2.10): we cut out the opisthosoma, added a blue background, and reduced the number of colors in the image to six, using the "posterize" function. The six colors were then characterized as dark (black, red, green, or violet) or light (white or yellow), and we calculated the number of light and dark pixels per spider in R.

Clutch size and hatching success

Egg sacs laid by German females were opened approximately two months after oviposition (64 +/- 13 days). As above, we calculated the clutch size as the sum of eggs, dead spiderlings, and living spiderlings. Hatching success was calculated as the sum of dead and living spiderlings ("hatched" spiderlings) relative to the total clutch size. For the transect, we only include data from the first clutch.

Statistical analysis of transect phenotype data

To test if the female traits (body size, pigmentation, clutch size and hatching success) varied with the environment, we used generalized linear mixed models in R, using the package 'glmmTMB' (Brooks *et al.*, 2017). The female traits were used as response variables, and the five environmental principle components were used as explanatory variables. Body size was modeled with a Gaussian distribution, clutch size with a negative binomial distribution with quadratic parameterization ("nbinom2" in R), pigmentation with a binomial (light vs dark pixels) distribution, and hatching success with a betabinomial distribution. Sampling site was included as a random effect. All models fit linear assumptions.

Transect data – population genomics and signatures of adaptation

Library preparation and sequencing

We extracted genomic DNA from the four left legs of the adult female spiders using a plate extraction protocol, as follows: the legs were placed into single well of a 96-well plate containing 3mm steel beads, cell lysis buffer (made of 10mM Tris pH 8, 100mM NaCl, 10mM EDTA pH 8, 0.5% SDS, and double distilled water) and Proteinase K. The plate was then shaken in a GenoGrinder 2010 (OPS Diagnostics) at 1,200 hz for 2 minutes for physical tissue lysis, followed by overnight incubation at 55°C. The next day, RNAse A was added to digest RNA. We then added NaCl to precipitate the proteins, and spun the plate down. We retained the supernatant, containing DNA, and discarded the insoluble protein phase. We used isopropanol to precipitate the DNA from the supernatant, then washed the DNA pellet twice with 70%

ethanol. The ethanol was allowed to evaporate, leaving only DNA. The extracted DNA was rehydrated in 50 µl of TE Buffer. DNA quantification was carried out using a Qubit fluorimeter (Thermo Scientific, Waltham, USA) according to the manufacturer's protocol.

We prepared dual-indexed libraries using a double digest restriction-enzyme-associated DNA sequencing (ddRADseq) library preparation protocol, based on the Peterson method (Peterson *et al.*, 2012), as adapted in Maas *et al.* (2018), with 500ng of DNA as starting material for most samples. Some samples started with lower input, but library preparation succeeded nonetheless. We digested the DNA using the restriction enzymes NlaIII (frequent cutter) and SbfI-HF (rare cutter). These enzymes were chosen based on their GC content, to avoid over-digestion of the AT-rich genome. We tested the digestion with *in silico* digestions of the *A. bruennichi* genome assembly (Sheffer *et al.*, 2021b) using SimRAD (Lepais & Weir, 2014), as well as testing digestions in the lab according to the Peterson protocol. We indexed each individual with unique barcodes, then pooled the individuals into 19 libraries of 24 individuals each. Another round of indexing was performed, to give each library of individuals a unique identifier. We quantified the indexed libraries using RT-qPCR, then pooled all of the libraries together. We used a Sage Science Pippen Prep to size select 475-696 bp fragments (including internal adapters), with a peak at 570 bp. The fragment size range was confirmed with a Bioanalyzer High Sensitivity chip (Agilent). We then sequenced 150 bp single-end reads on three lanes of Illumina HiSeq 4000 at UC Berkeley's Vincent J. Coates Genomics Sequencing Lab.

Sequence processing and SNP filtering

We demultiplexed the raw reads based on the individual barcode sequences, then used Trimmomatic (v.0.39) (Bolger, Lohse & Usadel, 2014) to remove adapter sequences. We mapped the reads of each sample onto the genome assembly using BWA-MEM (v.0.7.12-r1039) with default settings (Li, 2013), then sorted and indexed the mapped reads using SAMtools sort and SAMtools index (SAMtools v.1.3.1) (Li *et al.*, 2009).

We generated a VCF file for all samples using SAMtools mpileup. We then filtered the SNP data using SNPcleaner (v.2.24) (Fumagalli *et al.*, 2014). SNPs were retained for downstream analyses if they had a minimum coverage of 3x per individual, no more than 40**%** of missing data for individual sites, and a maximum coverage of 240x per individual. The cutoff for maximum coverage is ~10 times higher than the average coverage per individual, and helps to avoid SNP calls that fall in highly repetitive regions of the genome.

We used a custom pipeline to further filter the SNPs based on their position inside/outside of exons and introns. Intergenic SNPs, which did not fall within introns or exons, were used for population genomic analyses that call for neutral loci. We will refer to these as "neutral SNPs" henceforth. For analyses which included all data, including those SNPs falling within genes, we will refer to "all SNPs." To account for uncertainty in SNP and genotype calls based on allele counts, which might introduce noise or bias into downstream analyses (Johnson & Slatkin, 2008; Lynch, 2008), we used an empirical Bayesian framework, implemented in ANGSD (analysis of next-generation sequencing data; Korneliussen, Albrechtsen & Nielsen, 2014) to calculate genotype likelihoods instead of generating SNP genotype calls whenever possible.

Population genetic structure and demography

Because our sampling covered a broad geographic area, it was important to quantify the underlying demographic patterns and population genetic structure before searching for genomic signatures of adaptation. To this end, we used several methods: using neutral SNPs, we performed a PCA on the genotype likelihoods, as implemented in ngsTools "PCAngsd" (Fumagalli *et al.*, 2013). Also using the neutral SNPs, we calculated the per-individual inbreeding coefficients, as well as the pairwise relatedness of all individuals included in the study, using ngsF (Vieira *et al.*, 2013) and ngsRelate (Korneliussen & Moltke, 2015). Using all SNPs, we calculated the pairwise F_{ST} for each sampling site in ANGSD (Fumagalli *et al.*, 2013). We interpreted the F_{ST} results using a heatmap, calculated in R (R Core Team, 2017), as well as a neighbor-joining tree calculated in the R package 'ape' (Paradis & Schliep, 2019)**,** visualized with FigTree (Rambaut & Drummond, 2018).

Further, using all SNPs from a random subset of five individuals per population (to reduce run time), we calculated a phylogenetic tree with a combination of ngsDist (Vieira *et al.*, 2016) and FastME (v.2.1.6.1) (Lefort, Desper & Gascuel, 2015). We then looked for signatures of admixture at the individual level using ngsAdmix (Skotte, Korneliussen & Albrechtsen, 2013). Due to the stochastic nature of simulation-based clustering programs like ngsAdmix and the like (i.e. STRUCTURE and ADMIXTURE (Pritchard, Stephens & Donnelly, 2000; Alexander, Novembre & Lange, 2009)), for the ngsAdmix analysis, we ran 50 replicate analyses with values of *K* ranging from *K*=2 to *K*=20. The results of all replicates were summarized using the program CLUMPAK, which identifies the most common results across replicates for each value of *K* (Kopelman *et al.*, 2015). The summarized data was then used to visualize individual admixture proportions in R.

We used the results of the PCA and ngsAdmix analysis to identify larger groups within our data, for downstream genome-wide analyses that rely on pairwise comparisons, i.e. F_{ST}. Running such pairwise comparisons for all sampling sites across the genome becomes difficult to interpret, while grouping at i.e. the country level is not biologically meaningful. Therefore, we used a data-informed approach and assigned the sampling sites into four groups, following the nomenclature of Krehenwinkel & Tautz (2013): "native" (all sampling sites from France, as well as thirteen southwestern German sampling sites), "invasive" (all sampling sites from Estonia, Latvia, Lithuania, Poland, and ten northeastern German sampling sites), "Russian," and "Japanese."

Genome-wide measurements

Two common ways of detecting adaptation at the genomic level are (i) genetic differentiation outlier tests and (ii) environmental association tests (i.e. Hoban *et al.*, 2016; Ahrens *et al.*, 2018). In these tests, one assumes that sites which show (i) much higher than average genetic differentiation, i.e. F_{ST}, among populations, or (ii) high correlation with environmental variables, may play a role in local (environmental) adaptation. To identify genomic regions of interest in *A. bruennichi*, we used both of these methods, with an additional criterion: given the hypothesis that admixture played a role in driving the range expansion, we additionally scanned the genome for regions where the invasive/expanding populations show greater similarity (i.e. lower F_{ST}) to our Japanese populations, relative to the native/core populations. The coincidence of high environmental association with high differentiation between native and invasive populations <u>and</u> relatively low differentiation between invasive and Japanese populations would be taken as support for the hypothesis that introgression provided the substrate for selection in *A. bruennichi*.

For the genetic differentiation outlier approach, using all SNPs, we analyzed genome-wide patterns in F_{ST} as implemented in ANGSD (Fumagalli *et al.*, 2013). We calculated F_{ST} in sliding windows, with 50kb windows and 10kb steps, with our sampling sites grouped into three populations: native, invasive and Japanese. We do not perform an explicit significance test with F_{ST}, but look at positions with values above the genome-wide average F_{ST}. We performed association tests in ANGSD using the **-**doAsso method, which uses a generalized linear framework to associate genotype likelihoods with binary, count, or continuous variables (Skotte, Korneliussen & Albrechtsen, 2012); in this case, we tested the association of genotypes with continuous environmental variables, namely the first five PCs from the historical climate data (see section "Historical climate data" above). This test calculates a likelihood ratio test (LRT) score, and we use a significance cutoff of 0.0005 based on a chi-square distribution, corresponding to an LRT of 12.116 as our significance threshold.

Results

Common garden

To help understand how well our models represent the data, we calculated a pseudo-R^2 value. The pseudo-R^2 value can be interpreted as the amount of variation in the data, which is explained by the model. The conditional pseudo-R^2 includes random effects, while the marginal pseudo-R^2 includes only the fixed effects. A model with perfect fit to the data would have a pseudo-R^2 of 1.

The model for clutch size had a conditional pseudo-R^2 of 0.773 and marginal pseudo-R^2 of 0.617 (Table 3). Spiders from the core of the range had larger clutches than spiders from the edge of the range; clutch size increased with increasing body size, and decreased with longer oviposition latency (Supplemental File 1: Figure S3A-C, Table 3). Estimated at average oviposition latency, second clutches had slightly higher clutch sizes than first clutches, with the marginal means differing by ~19 spiderlings (Supplemental File 1: Figure S3C). The hatching success model had a significant effect of origin and oviposition latency, with higher hatching success in clutches from the core of the range and with shorter latency (Supplemental File 1: Figure S3D). The effects of mother's body size and clutch (first or second) on hatching success were not significant (Table 3). The conditional pseudo-R^2 was 0.224 (calculating the pseudo-R^2 for betabinomial models is not straightforward, thus we do not report a marginal pseudo-R^2; see methods).

Our model for overwintering survival had a pseudo-R^2 of 0.262. The interaction of winter treatment and origin showed a significant effect: under the cold winter treatment, spiderlings from edge populations survived at higher percentages than spiderlings from core populations (Figure 2A, Table 3). Survival was higher overall under the warm winter treatment (Figure 2A), and decreased over the course of winter (Figure 2B). We observed lower survival for clutches with longer oviposition latencies. Origin on its own was not significant, as it only played a role in interaction with the winter treatment. The remaining fixed effects, mother's body size and clutch, were not significant (Table 3).

Table 3: Model table for life history traits: clutch size, hatching success, and overwintering survival. Estimates are reported on the latent scale, with 95% confidence intervals. Fixed effects are considered to be significant if their confidence interval does not cross zero; these are indicated in **bold text**. Fixed effects separated by a colon indicate an interaction of those effects. Reference level of fixed effects is given in [square brackets].

Response Variable	Sample size	Pseudo-R^2 (cond.)	Pseudo-R^2 (marg.)	Fixed effects	Estimate	2.5%	97.5%
Clutch size	359	0.773	0.617	**Origin [edge]**	-0.19213	-0.35238	-0.03187
				Mother's body size*	0.20021	0.14292	0.25750
				Clutch [2]	0.11179	0.00232	0.22127
				Oviposition latency*	-0.49744	-0.55604	-0.43884
Hatching success	359	0.224	NA	**Origin [edge]**	-0.7730	-1.42442	-0.12164
				Mother's body size*	-0.05427	-0.31531	0.20678
				Clutch [2]	0.06178	-0.47923	0.60279
				Oviposition latency*	-0.94689	-1.30692	-0.58687
Survival	359	0.262	NA	**Winter treatment [cold]: Origin [edge]**	0.49163	1.56800	1.03031
				Winter treatment [cold]	-1.88981	-1.06448	-1.47714
				Origin [edge]	-0.80683	0.16345	-0.32169
				Season [post-winter]	-0.76410	-0.22459	-0.49434
				Clutch [2]	-0.62737	0.20182	-0.21278
				Mother's body size*	-0.18149	0.18805	0.00328
				Oviposition latency*	-0.55753	-0.11039	-0.33396

*centered and scaled

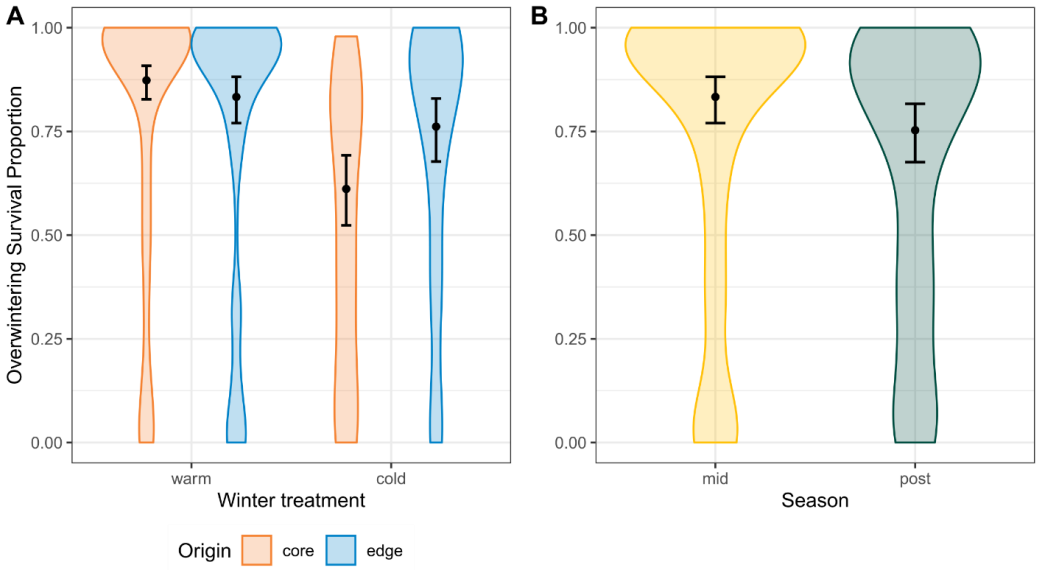

Figure 2: Overwintering survival of spiderlings according to winter treatment and origin (A) and season (B). (A) Survival according to winter treatment and origin. Under warm winter conditions, there is high survival fromboth origins. Under cold conditions, edge spiderlings have higher survival than core spiderlings. (B) Survival is higher at mid-winter and declines in post-winter. Violin plots represent the distribution of the raw data; black points with error bars represent estimated marginal means and 95% confidence intervals for discrete predictor variables. Model predictions are back-transformed to the observed scale.

The model for lower lethal temperature had a pseudo-R^2 of 0.719. As expected, survival decreased with decreasing exposure temperatures. The interaction of exposure temperature and origin showed that at the lowest temperatures, spiderlings from the edge of the range had higher survival than spiderlings from the core (Figure 3A). The three-way interaction of exposure temperature, winter treatment, and season

shows that post-winter, spiderlings have a lower survival at low exposure temperatures if they have experienced a warm winter treatment (Figure 3B**,** Table 4).

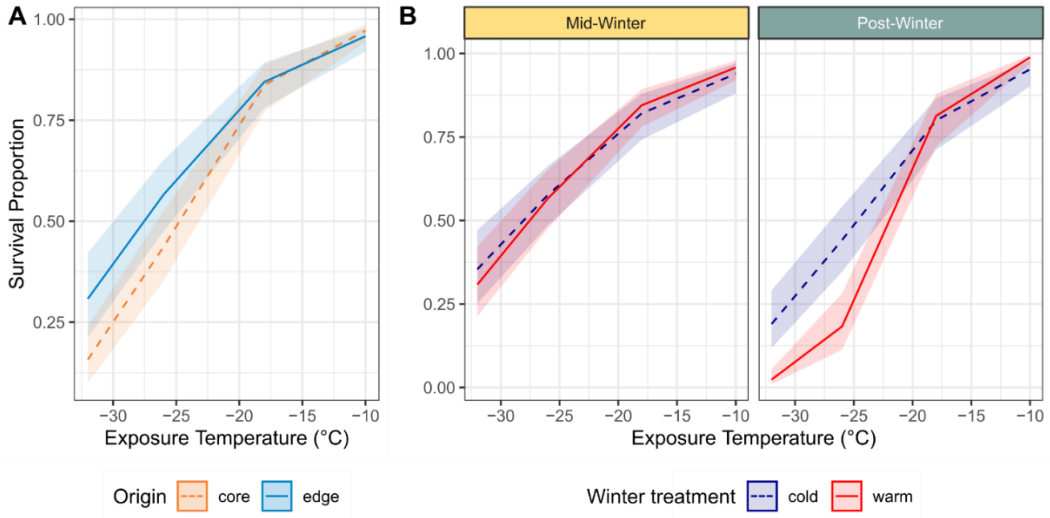

Figure 3: Lower lethal temperature according to (A) origin and exposure temperature and (B) the interaction of exposure temperature with season (mid- or post-winter) and warm or cold winter treatments. Lines represent model predictions flanked with their 95% confidence intervals. Model predictions are back-transformed to the observed scale. (A) Regardless of experimental treatment, edge spiderlings have higher survival at the coldest exposure temperatures. (B) At mid-winter (left), there is no difference in survival between warm and cold winter treatments. Post-winter (right), survival at the lowest exposure temperatures decreases dramatically for spiderlings in the warm winter treatment.

We analyzed the data on supercooling points in two models, due to multimodality of the raw data: firstly, we analyzed the "low group" (LG) SCPs as a continuous variable, measured at the spiderling level. SCPs were classified into the LG if they were below -25.5°C. Secondly, we analyzed the per-clutch ratio of LG to "high group" (HG) SCPs (SCPs higher than -25-5°C, see methods and Supplemental File 1: Figure S2). For the LG SCPs, our had a conditional pseudo-R^2 of 0.301 and a marginal pseudo-R^2 of 0.245. This relatively low R^2 may be due to the arbitrary splitting of the data into groups. Overall, spiderlings from the edge populations had lower SCPs than spiderlings from the core (Figure 4A). The SCP increased post-winter, and was notably higher in the post-winter warm treatment Table 4. The model comparing the ratio of LG:HG SCPs had a pseudo-R^2 of 0.841. Post-winter, across all treatments, there is a shift toward more HG SCPs. For egg sacs from the core of the range, post-winter, under a warm winter treatment, the ratio dips strongly toward more HG SCPs (Figure 4B, Table 4).

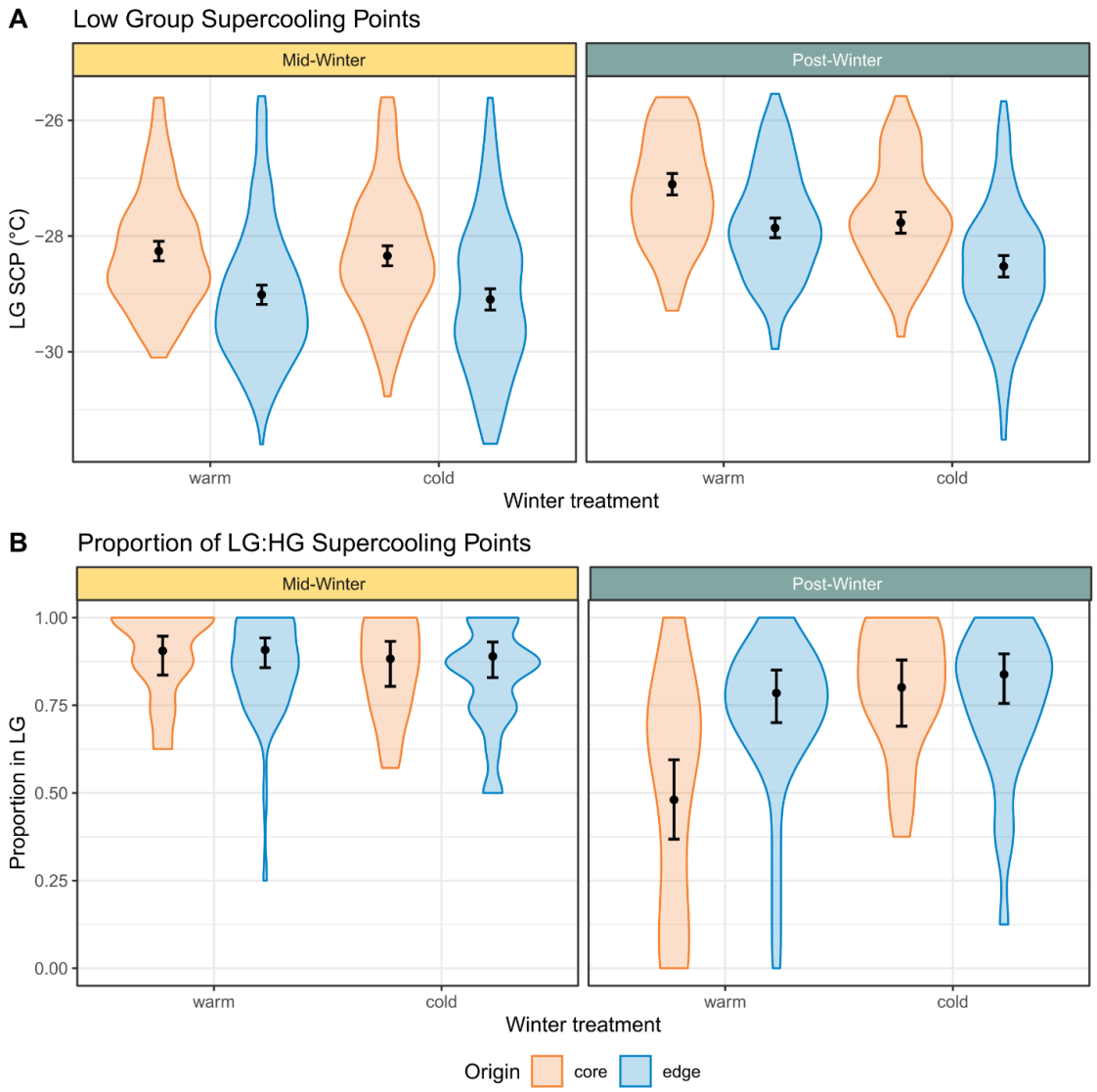

Figure 4. Supercooling points according to winter treatment, origin and season. "Low group" (LG) supercooling points are plotted in (A), while the ratio (see methods) of LG:HG ("high group") supercooling points is plotted in (B). Violin plots represent the distribution of the raw data; black points with error bars represent estimated marginal means and 95% confidence intervals for discrete predictor variables. Model predictions are back-transformed to the observed scale.

As the last cold-tolerance-related trait, we analyzed the chill coma recovery time of spiderlings, in response to the interaction of winter temperature, origin and season, and the two-way interactions of those fixed effects, along with clutch, mother's leg length, fecundity of the egg sac, and oviposition latency. The conditional pseudo-R^2 was 0.010, and the marginal pseudo-R^2 was 0.002. Nearly all effects were significant, but given the extremely low R^2 values, we will not interpret the results of the model. Estimates and confidence intervals are nonetheless presented in Table 4.

Table 4: Model table for cold-tolerance-related traits in offspring. Estimates are reported on the latent scale, with 95% confidence intervals. Fixed effects are considered to be significant if their confidence interval does not cross zero; these are indicated in **bold text.** Fixed effects separated by a colon indicate an interaction of those effects. Reference level of fixed effects is given in [square brackets].

Response Variable	Sample size	Pseudo-R^2 (cond.)	Pseudo-R^2 (marg.)	Fixed effects	2.5%	97.5%	Estimate
Lower lethal temperature survival	371	0.719	NA	**Exposure temperature: Winter treatment [warm]: season [post-winter]**	0.04335	0.239335	0.14134
				Exposure temperature: Origin [edge]	-0.10268	-0.01348	-0.05807
				Winter treatment [warm]: season [post-winter]	0.17541	4.73690	2.45615
				Exposure temperature: season [post-winter]	-0.00914	0.11022	0.05054
				Exposure temperature: winter treatment [warm]	-0.02695	0.08140	0.02722
				Oviposition latency*	-0.46991	0.00162	-0.23415
				Clutch [2]	-0.70801	0.24224	-0.23289
				Origin [edge]	-2.11262	0.13284	-0.98989
				Season [post-winter]	-0.70449	2.24726	0.77138
				Winter treatment [warm]	-0.66658	1.99523	0.66433
				Exposure temperature	0.16124	0.25850	0.20987
Low-group supercooling point	1493	0.301	0.245	**Winter treatment warm: season [post-winter]**	0.31763	0.84627	0.58195
				Oviposition latency*	-0.24258	-0.00054	-0.12156
				Mother's body size*	-0.03738	0.16173	0.06218
				Clutch size*	-0.08836	0.11005	0.01085
				Clutch [2]	-0.13729	0.28251	0.07261
				Origin [edge]	-0.96994	-0.53823	-0.75409
				Season [post-winter]	0.37844	0.76854	0.57349
				Winter treatment [warm]	-0.09594	0.25923	0.08164
Ratio of low-group to high-group supercooling points	245	0.841	NA	Winter treatment [warm]: Origin [edge]: Season [post-winter]	-0.19075	2.51019	1.15972
				Origin [edge]: Season [post-winter]	-0.81417	1.17615	0.18099
				Winter treatment [warm]: Season [post-winter]	-2.78383	-0.64061	-1.71222
				Winter treatment [warm]: Origin [edge]	-1.04706	0.97327	-0.03690
				Oviposition latency*	0.14192	0.75032	0.44612
				Mother's body size*	-0.19871	0.29809	0.04969
				Clutch size*	-0.30033	0.14671	-0.07681
				Clutch [2]	-0.92664	0.14684	-0.38990
				Season [post-winter]	-1.41845	0.17110	-0.62367
				Origin [edge]	-0.73061	0.86961	0.06950
				Winter treatment [warm]	-0.58626	1.06673	0.24023
Chill coma recovery time	2072	0.010	0.002	**Winter treatment [warm]: Origin [edge]: Season [post-winter]**	-0.17466	-0.03670	-0.10568
				Origin [edge]: Season [post-winter]	0.01149	0.11814	0.06482
				Winter treatment [warm]: Season [post-winter]	0.06088	0.16448	0.11268
				Winter treatment [warm]: Origin [edge]	-0.00049	0.09734	0.04842
				Oviposition latency*	0.01005	0.03846	0.02425
				Mother's body size*	-0.02633	-0.00047	-0.01340
				Clutch size*	0.00579	0.03019	0.01799
				Clutch [2]	-0.05448	-0.00392	-0.02920
				Season [post-winter]	-0.12642	-0.04683	-0.08662
				Origin [edge]	-0.06334	0.02267	-0.02033
				Winter treatment [warm]	-0.09988	-0.02591	-0.06289

*centered and scaled

The conditional pseudo-R^2 for the offspring mass model was 0.794, with a marginal pseudo-R^2 of 0.307 (Table 5). Core offspring had higher mass than edge offspring irrespective of season or treatment, and the warm winter treatment resulted in lower mass overall. Mass decreased over the course of winter (Figure 5A). In egg sacs with higher clutch sizes, offspring mass was slightly lower. Additionally, offspring from later-laid egg sacs had lower body mass, while second clutches had higher body mass (Table 5).

For the leg length model, we could not include the sampling population as a random effect because of singular fit, due to the very high variance explained by mother's ID and egg sac. The model had a conditional pseudo-R^2 of 0.817, with a marginal pseudo-R^2 of only 0.060 (Table 5). Evidently, offspring body size has a very strong maternal component. Offspring from the edge of the range are smaller than offspring from the core of the range (Figure 5B)

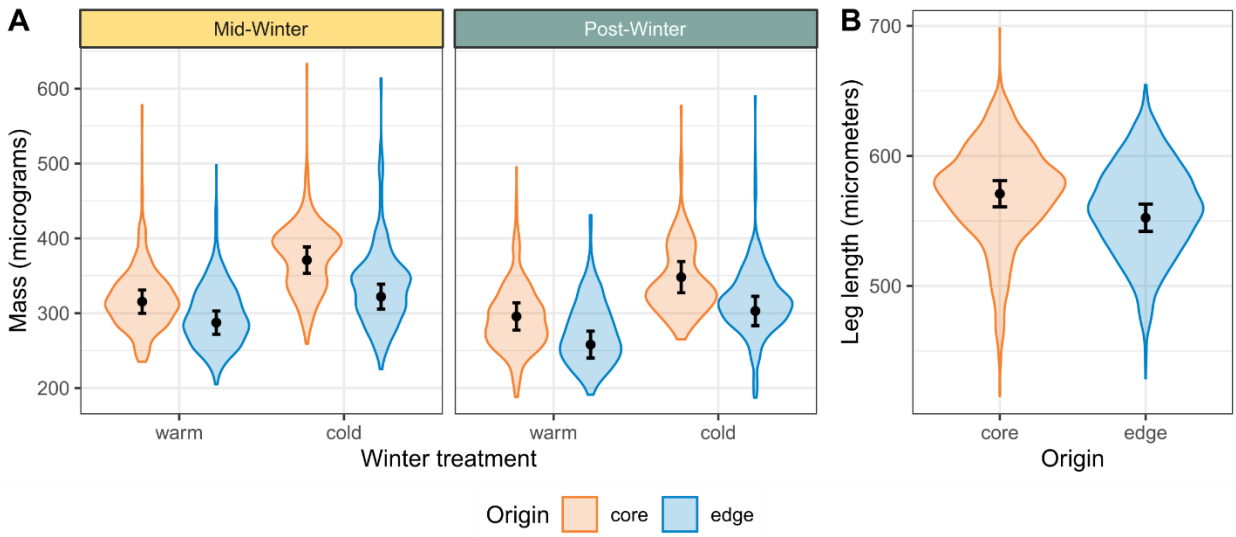

Figure 5. Body size of offspring according to winter treatment and origin. (A) Body mass decreased from mid- to post-winter, and is lower following a warm winter treatment. (B) Spiderlings from the core of the range are larger than those from the edge of the range. Transparent points represent the raw data; black points with error bars represent estimated marginal means and 95% confidence intervals for discrete predictor variables. Model predictions are back-transformed to the observed scale.

Table 5. Model table for offspring body size. Estimates are reported on the latent scale, with 95% confidence intervals. Fixed effects are considered to be significant if their confidence interval does not cross zero; these are indicated in **bold text.** Fixed effects separated by a colon indicate an interaction of those effects. Reference level of fixed effects is given in [square brackets].

Response Variable	Sample size	Pseudo-R^2 (cond.)	Pseudo-R^2 (marg.)	Fixed effects	2.5%	97.5%	Estimate
Offspring mass	3539	0.794	0.307	Winter treatment [warm]: Origin [edge]: Season [post-winter]	-51.08397	26.81681	-13.28800
				Origin [edge]: Season [post-winter]	-21.82160	36.49953	3.67300
				Winter treatment [warm]: Season [post-winter]	-26.18663	32.26970	3.01500
				Winter treatment [warm]: Origin [edge]	-6.92649	44.57374	20.85400
				Winter treatment [warm]	-74.86328	-35.33104	-55.53500
				Origin [edge]	-67.48434	-22.59316	-48.81600
				Season [post-winter]	-45.91207	-1.31285	-22.76000

				Clutch [2]	5.51927	35.04812	19.82900
				Clutch size*	-13.72314	-0.23715	-6.72100
				Mother's body size*	-0.55694	14.51010	5.76000
				Oviposition latency*	-22.97329	-3.05954	-12.74300
Offspring body size	3539	0.817	0.060	Winter treatment [warm]: Origin [edge]: Season [post-winter]	-43.8826	25.60044	-9.2694
				Origin [edge]: Season [post-winter]	-29.1719	22.78383	-3.1507
				Winter treatment [warm]: Season [post-winter]	-12.98791	39.09495	13.1046
				Winter treatment [warm]: Origin [edge]	-5.73829	39.98230	17.1617
				Winter treatment [warm]	-32.89174	2.32406	-15.2201
				Origin [edge]	-45.18832	-5.20747	-25.2248
				Season [post-winter]	-22.01804	17.68051	-2.2011
				Clutch [2]	-14.16640	12.25400	-0.953
				Clutch size*	-5.74777	7.69614	0.9909
				Mother's body size*	-10.76298	1.28542	-4.7659
				Oviposition latency*	-18.65102	-0.88816	-9.8212

*centered and scaled

Phenotype-environment associations across transect

We characterized the environmental variation across our sampling sites using PCA. The first five environmental PCs accounted for 97.6% of the variation in the climate data. PC1 alone accounted for 51.9% of the variation, and varies almost perfectly with latitude (Supplemental File 1: Figure S4). The strongest loadings of this PC were temperature-related, such as the mean temperature of the coldest quarter, the minimum temperature of the coldest month, annual mean temperature, isothermality, and temperature seasonality, although almost all environmental variables had strong contributions to this PC. PC2 accounted for 24.4% of variation, and separated sites more according to precipitation than temperature, with the strongest loadings being the precipitation of the warmest quarter, precipitation of the wettest quarter, annual precipitation, and precipitation of the driest month. PC3 accounted for 11.2% of variation, with the strongest loadings relating to seasonality in temperature and precipitation, as well as the annual temperature range. PC4, which accounted for 6.7% of variation, was strongly related to the mean temperature of the wettest quarter. The strongest loadings for PC5, which accounted for 3.4% of environmental variation, were similar to PC3, but temperature and seasonal precipitation contributed in opposite directions for this PC. See Supplemental File 3 for PCA biplots and loadings of each PC.

Using those 5 PCs, we assessed how adult female traits (leg length, opisthosoma pigmentation, fecundity, and hatching success) vary with the environment. Sampling site was always included as a random effect. Female fecundity and the hatching success of their egg sacs had no significant associations with environmental PCs. Female leg length, however, had a significant association with PC1: leg length is shorter, i.e. spiders mature at a smaller body size, in environments characterized by lower temperatures and greater seasonality. Opisthosoma pigmentation had a significant relationship with PC4, but did not vary with latitude (i.e. PC1) (Figure 6**,** Table 6).

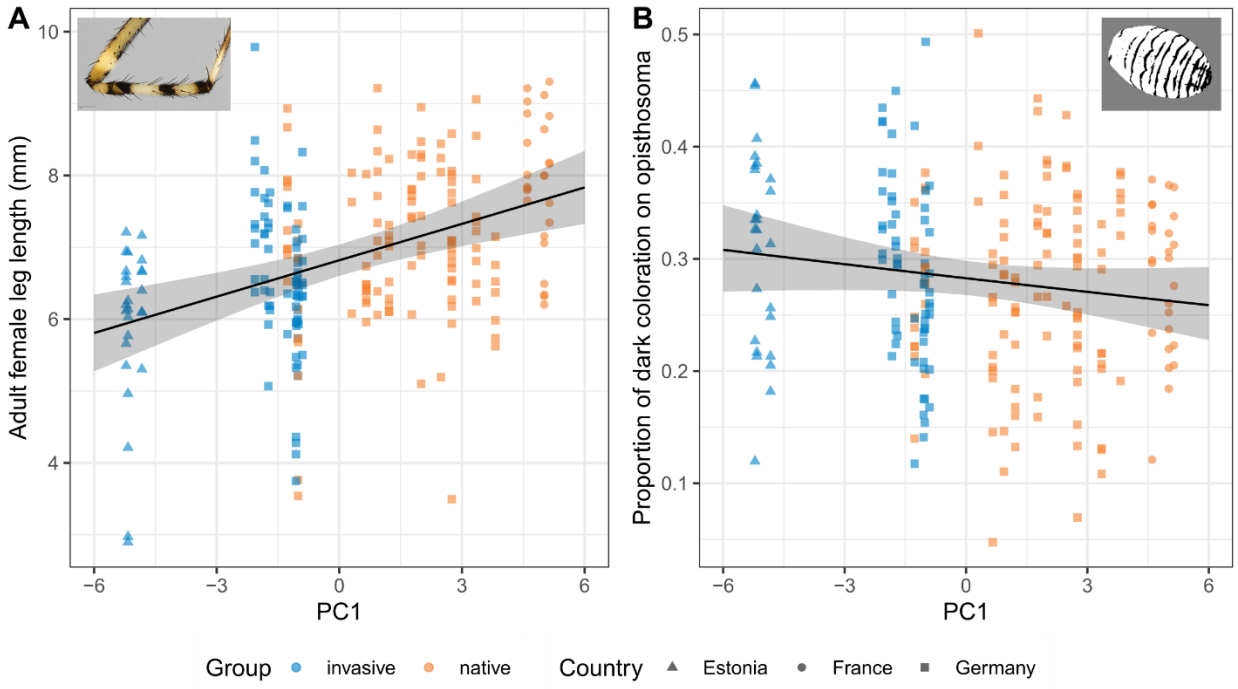

Figure 6: Female traits according to the environment. Points are colored according to their assignment to "invasive" or "native" genetic clusters (see population genetic results, i.e. Figure 7, below), and shaped according to the sampling country. (A) Adult female tibia-patella length, a body size proxy, increases with environmental PC1, i.e. we observe larger body sizes under the warm temperatures at lower latitudes. (B) Opisthosoma pigmentation does not vary according to PC1.

Table 6. Model table for adult female traits according to environmental principle components. Estimates are reported on the latent scale, with 95% confidence intervals. Fixed effects are considered to be significant if their confidence interval does not cross zero; these are indicated in **bold text.**

Response Variable	Sample size	Pseudo-R^2 (cond.)	Pseudo-R^2 (marg.)	Fixed effects	2.5%	97.5%	Estimate
Adult female body size	273	0.419	0.187	**PC1**	87.21212	250.541	168.93
				PC2	-58.018	161.5652	51.46
				PC3	-260.58	192.3862	-33.77
				PC4	-44.8432	378.1135	167.04
				PC5	-226.937	496.4214	133.94
Opisthosoma pigmentation	262	0.280	NA	PC1	-0.04675	0.006182	-0.02029
				PC2	-0.06909	0.003372	-0.03286
				PC3	-0.06669	0.08155	0.007431
				PC4	0.026992	0.164237	0.095615
				PC5	-0.01846	0.215921	0.098732
Clutch size	273	0.323	0.012	PC1	-0.05979	0.033122	-0.01333
				PC2	-0.08344	0.039135	-0.02215
				PC3	-0.11297	0.14434	0.015687
				PC4	-0.08279	0.155782	0.036496
				PC5	-0.18293	0.227001	0.022036
Hatching success	273	0.009	NA	PC1	-0.12185	0.033268	-0.04429
				PC2	-0.05821	0.147993	0.04489
				PC3	-0.23168	0.205299	-0.01319
				PC4	-0.34267	0.045613	-0.14853
				PC5	-0.63409	0.058033	-0.28803

*centered and scaled

Genomic data

SNP calling and filtering

After demultiplexing and trimming adapters, the ddRAD libraries for 423 adult females yielded more than 362 million reads, with an average of 815,796 reads per sample (min: 5,296 reads, max: 12,597,258 reads). An average (mean) of 86.89% of reads per sample mapped to the reference genome, with a mean coverage of 4.94X for each of the 13 chromosome-level superscaffolds (Sheffer *et al.*, 2021b). SNP calling resulted in 22,372 biallelic SNPs. We then filtered the SNPs according to their position within exons and introns: 13,832 "neutral" SNPs did not fall within exons or introns.

Population genetic structure and demography

We performed several analyses to understand the underlying population structure and demographic processes in *A. bruennichi*. Firstly, we used the neutral SNP subset to perform a principal components analysis (PCA) using PCAngsd (Meisner & Albrechtsen, 2018), with three subsets of the samples: (i) all populations, including Japan; (ii) all populations, excluding Japan; and (iii) all European populations, excluding Japan and Russia, as the main focus of our study is the transect through Europe. Results for the PCA including Japan, and the PCA excluding Japan but including Russia, can be found in the supplementary material (Supplemental File 1: Figure S5, Figure S6). In the Europe-only PCA, PC1 accounted for 17.4% of genetic variation, separating French and southwestern German populations from the northeastern European populations, while PC2 accounted for 3.4% of the variation, separating Estonian populations from the remaining European populations (Figure 7).

Using ngsAdmix (Skotte *et al.*, 2013), we calculated individual admixture proportions, with values of *K* ranging from *K*=2 to *K*=20. Plots for *K*=4-8 can be found in the supplementary material (Supplemental File 1: Figure S7); here, we present the results for *K*=2, to correspond with the previous STRUCTURE analysis from Krehenwinkel & Tautz (2013), and *K*=3, which best shows the transition between native and invasive populations (Figure 7B). In the analysis with *K* set to 2, we find, as in Krehenwinkel & Tautz (2013), that the proportion of assignment to the "Japanese" cluster gradually increases with latitude, and is highest in Russian populations. The *K*=3 results show a rapid turnover within Germany: in southwestern Germany, individuals are assigned to the "native" genetic cluster, and in the center of Germany, there is turnover to individuals being assigned to the "invasive" cluster. The turnover occurs between populations 20 and 21, which are just 85 kilometers apart.

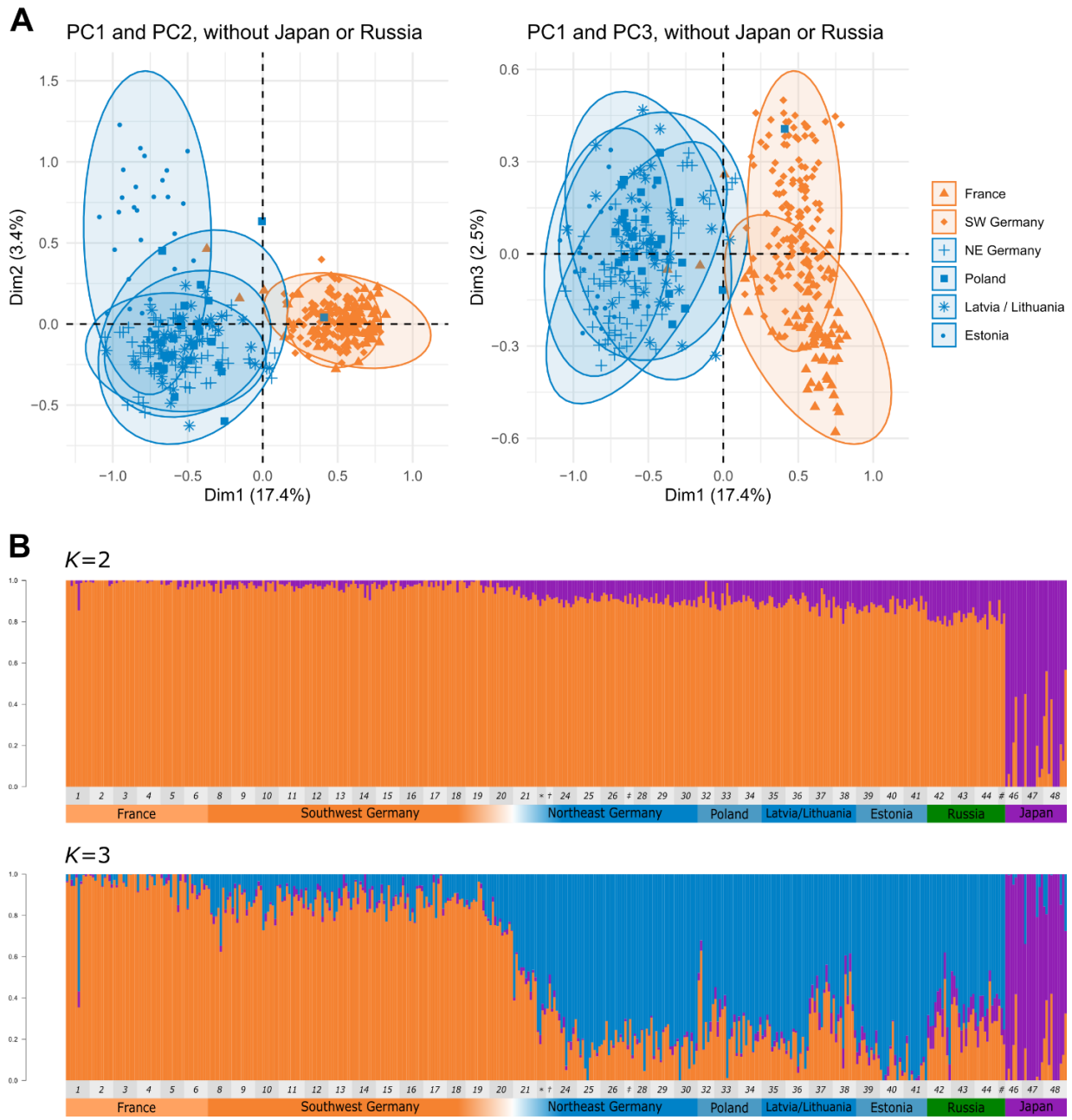

Figure 7. Population genetic structure. (A) Principal components analysis of European populations using neutral SNPs. Ellipses represent 95% confidence intervals; points represent individual samples, with shape indicating the sampling country. Points and ellipses are colored according to the site's "native" (orange) or "invasive" (blue) assignment. (B) Stacked barplots of individual ancestry assignment, using ngsAdmix results for *K*=2 and *K*=3. Numbers below the bars show the sampling sites. For small sampling sites where a number did not fit, * represents population number 22, † represents 23, ‡ represents 27, and # represents 45.

We calculated the levels of inbreeding at every sampling site, to gain insight into the levels of isolation of our populations. The Japanese populations showed high levels of inbreeding, while the remaining populations were mostly outbreeding, especially the Russian populations (Figure 8A). Interestingly, the populations at the edge of the range in Estonia (population numbers 39, 40, and 41) show a linear increase in the level of inbreeding with latitude.

We also calculated the pairwise F_{ST} between all sampling sites, which ranged from 0.018 between two Russian sampling sites to 0.358 between a site in Japan and a site in southern France. As in the PCA, the highest differentiation was found between Japanese and all other populations (Supplemental File 1: Table S1). Within the European (native and invasive) populations, F_{ST} was quite low, ranging from 0.025-0.130. F_{ST} was lower among "native" populations (max: 0.074) than among "invasive" populations (max: 0.130) (Figure 8B), and F_{ST} was very low among Russian populations (max: 0.036) (Supplemental File 1**:** Table S1). As an additional visualization, we used the pairwise F_{ST} matrix to calculate a neighbor-joining tree in the R package 'ape' (Paradis & Schliep, 2019), which showed the native populations in one cluster, while the invasive populations did not cluster as clearly, and were more similar to the Russian and Japanese populations (Figure 8C).

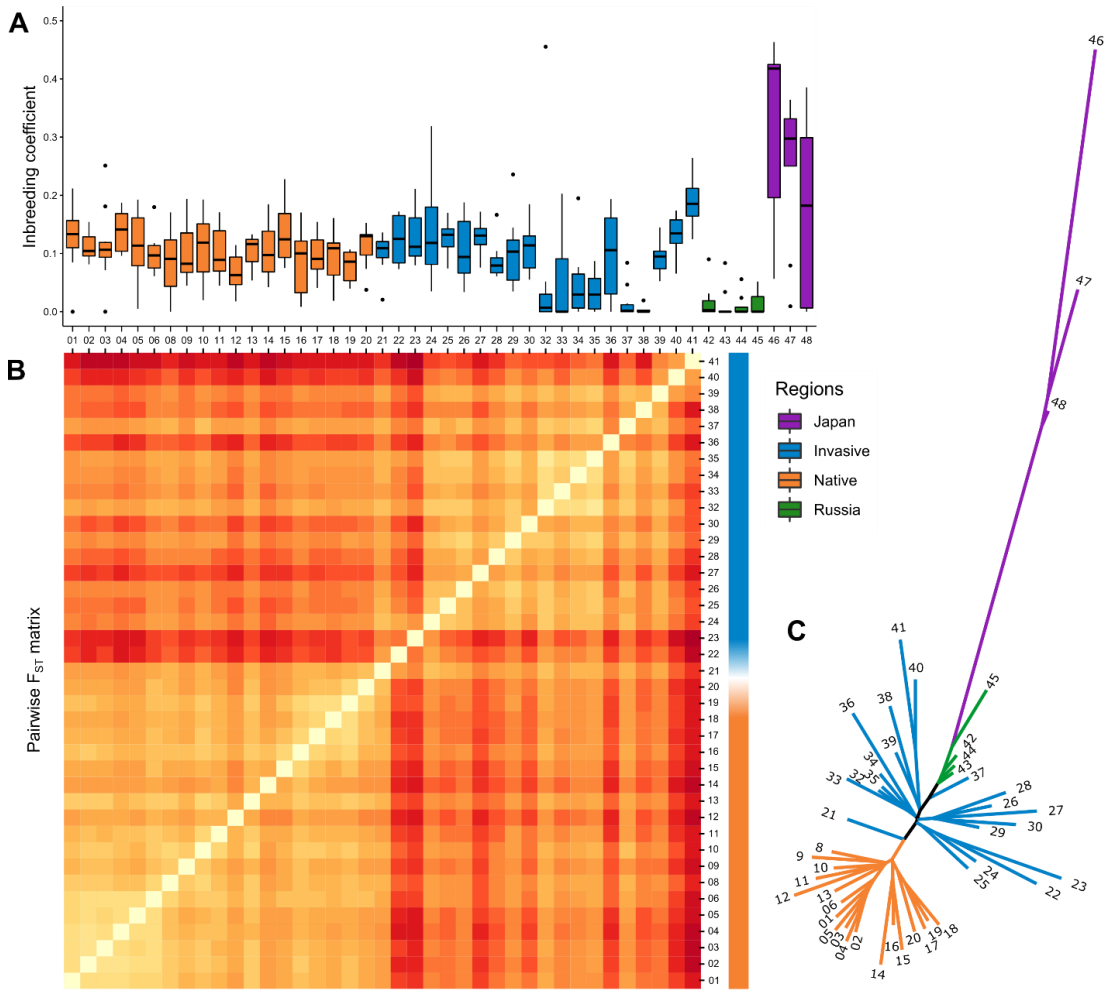

Figure 8. Demography and differentiation. (A) Boxplots of individual inbreeding coefficients for every sampling site. Boxes encompass the 1st and 3rd quartiles of the data and are colored according to sampling region. Thick horizontal lines represent the median, thin vertical lines represent 1.5 times the upper and lower interquartile range, and black points represent outliers. (B) Symmetrical heat-map of pairwise F_{ST} between all European populations. The color scale runs from light yellow (lowest differentiation) to dark red (highest differentiation). Color blocks on the right side of the heat-map represent the groupings of populations into "native" and "invasive" clusters. (C) Neighbor-joining tree of F_{ST} matrix. Branch labels represent the population numbers, and branches are colored by their regional groupings. In (A) and (B), populations are ordered in the same way, to directly compare between the two different statistics.

We constructed another phylogenetic tree using ngsDist (Vieira *et al.*, 2016) and FastME (v.2.1.6.1) (Lefort *et al.*, 2015), which revealed the same large-scale groupings of native, invasive, Russian and Japanese populations as the PCA, admixture, and F_{ST} analyses (Supplemental File 1: Figure S8). Bootstrap support was high for the splits between the Japanese, Russian, and European clades, but was quite low within Europe.

Genome-wide evidence for environmental adaptation

We analyzed genome-wide patterns of genetic differentiation (F_{ST}) and genotype-environment associations to identify potential regions of adaptive introgression. Using the output of both tests, we searched for genomic regions where F_{ST} between native and invasive populations was particularly high, association with the environment was strong, and F_{ST} between invasive and Japanese sites was relatively low. We will interpret this pattern as a signature of adaptive introgression.

Firstly, we looked at associations with environmental PC1, which represents the environmental variables that vary with latitude, mostly relating to cold temperatures. 589 SNPs had significant associations with this latitudinal environmental variation. We found windows showing signatures of adaptive introgression on almost all chromosomes, with particularly strong signatures on chromosome 9. Two regions on chromosome 9, centered at around 29Mbp and 58Mbp, show exactly the pattern we would expect for adaptive introgression: high association with the environment, high differentiation within Europe, and lower differentiation between invasive and Japanese populations. There is another region on chromosome 9, centered at around 107 Mbp, which shows very high environmental association and high differentiation within Europe, but the last criterion of similarity between invasive and Japanese populations is less striking in this region. We also found a very interesting region on chromosome 2; while the range of values on this chromosome was lower, there is an approximately 30 Mbp-long region showing a possible signature of adaptive introgression (Figure 10). Boxplots of significant LRT values per chromosome can be found in Supplemental File 1: Figure S10.

For the other environmental principal components, PC2-5, we found relatively few significant associations: 84 for PC2, 186 for PC3, 53 for PC4, and 109 for PC5. For PC2 and PC4, there were no characteristic patterns of adaptive introgression, and indeed few areas where outliers were found between both the environmental associations and F_{ST}. Environmental PCs 2 and 4 are characterized by variables related to precipitation. On the other hand, environmental PC3 is driven by seasonality in temperature and precipitation, and in that case, we see more significant associations, and more signatures of adaptive introgression. Similarly, PC5 is also related to seasonality, in a slightly different way, as it differentiates between precipitation seasonality and temperature seasonality. The genomic regions displaying signatures of adaptive introgression for PC3 and PC5 are the same as those for PC1.

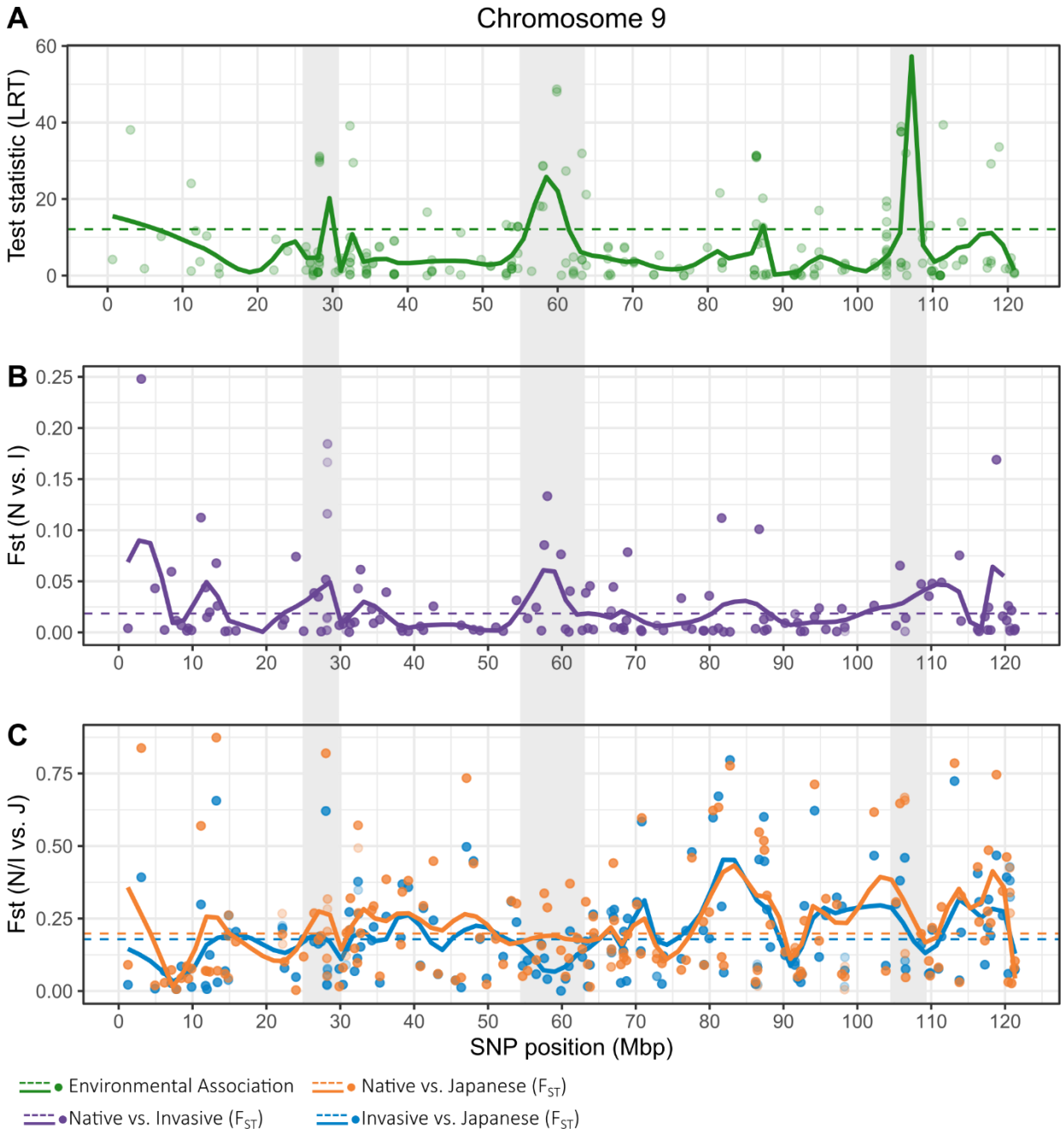

Figure 9. Genomic signatures of adaptation on chromosome 9. Genomic regions underlain with grey bars represent interesting patterns when comparing among the three panels. (A) Association of SNPs with the first environmental principle component. On the y-axis is the likelihood ratio test statistic, x-axis SNP position. The points represent single SNP association statistics; the solid line represents a locally estimated scatterplot smoothing (LOESS) curve to identify patterns in the data. The dashed line represents the significance threshold of p=0.0005 based on a chi-square distribution with one degree of freedom. (B) F_{ST} between native and invasive populations. Points represent sliding window F_{ST} estimates. Again, the solid line represents a LOESS curve, while the dashed line represents the mean genome-wide F_{ST} between the two groups. (C) F_{ST} between native and Japanese populations in orange, between invasive and Japanese in blue. Points represent sliding window F_{ST} estimates, solid lines are LOESS curves, and dashed lines represent the mean genome-wide F_{ST} between the given groups.

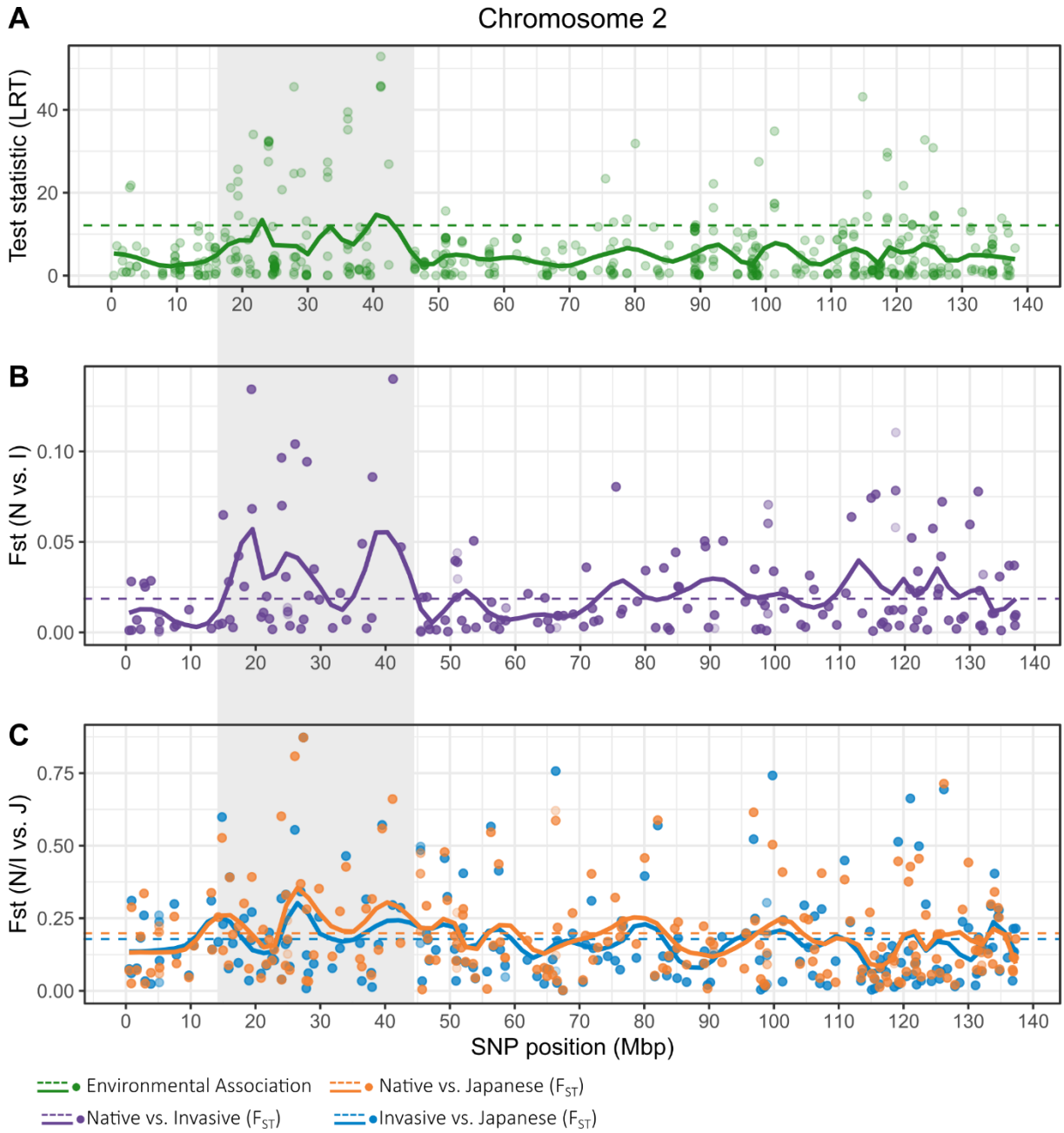

Figure 10. Genomic signatures of adaptation on chromosome 2. Genomic regions underlain with grey bars represent interesting patterns when comparing among the three panels. (A) Association of SNPs with the first environmental principle component. On the y-axis is the likelihood ratio test statistic, x-axis SNP position. The points represent single SNP association statistics; the solid line represents a LOESS curve to identify patterns in the data. The dashed line represents the significance threshold of p=0.0005 based on a chi-square distribution with one degree of freedom. (B) F_{ST} between native and invasive populations. Points represent sliding window F_{ST} estimates. Again, the solid line represents a LOESS curve, while the dashed line represents the mean genome-wide F_{ST} between the two groups. (C) F_{ST} between native and Japanese populations in orange, between invasive and Japanese in blue. Points represent sliding window F_{ST} estimates, solid lines are LOESS curves, and dashed lines represent the mean genome-wide F_{ST} between the given groups.

Discussion

We found strong evidence that the wasp spider range expansion was facilitated by adaptive introgression, and that range edge populations are locally adapted to endure cold and highly seasonal environments at the northern range edge. We observed a latitudinal cline in adult body size and substantial genetic turnover over a very short geographic distance, suggesting very strong selection to maintain this differentiation.

Core versus edge: Common garden experiment

Oviposition latency: The earlier the better

In nearly all investigated traits, we found a significant negative effect of oviposition latency: clutches that were laid later had lower clutch sizes, lower hatching success, reduced survival, and higher SCPs. Seemingly, early oviposition is advantageous in core and edge populations. The consequence of late oviposition has been documented in *A. bruennichi* in the field (Leborgne & Pasquet, 2005). That study also showed that body condition, affected by feeding, has an effect on clutch size. Thus, the negative effect of late oviposition found in our study may be a combination of an inherent decrease in clutch viability with time, as well as a lab effect due to less frequent prey acquisition in the lab. For survival and SCP, in addition to a lab effect, the effect of oviposition latency could also be explained by the time until onset of winter: with more time to prepare for winter, i.e. by accumulating cryoprotectants, offspring from earlier clutches may show greater cold tolerance and overwintering survival. In the few spider species in which seasonal variation in supercooling points has been thoroughly investigated, the accumulation of putative cryoprotectants and thermal hysteresis factors begins ahead of winter, i.e. around September in the northern hemisphere (Kirchner & Kestler, 1969; Tanaka, 1995a). Thus, spiderlings that hatch late in September have less time to accumulate the necessary substances to suppress their supercooling points.

Reproductive success

Because egg sacs were laid and offspring hatched before we began the winter treatments, we cannot disentangle the effects of genetic adaptation and phenotypic plasticity in clutch size and hatching success, and only look at differences between origins. Females from the core of the range had larger clutches and higher hatching success than females from the edge of the range. Populations at the edge of a species range face very different selective pressures than those at the core of the range. In range-expanding species, low population densities at the expanding front, as well as predator release, are hypothesized to select for higher reproductive investment (Phillips, Brown & Shine, 2010). In birds, clutch size generally increases with latitude, the cause of which has been the focus of many competing classical hypotheses (i.e. Lack's rule, Ashmole's hypothesis, reviewed in Lundblad & Conway, 2021). This background led us to expect that clutch size in *A. bruennichi* would increase with latitude, which makes it all the more interesting that we find the opposite pattern. In life-history theory, clutch size is often considered in the context of a trade-off between clutch size and the level of offspring provisioning (approximated with egg size in many species) (Tanaka, 1995b; Hassall *et al.*, 2006). However, we found that edge spiders not only have smaller clutches, they also have smaller offspring, so this tradeoff is not apparent at the full geographic scale. However, in the data overall, we did find a slight negative effect of clutch size on offspring mass: offspring from large clutches had slightly lower mass, suggesting that there is a tradeoff (Table 5). It could thus be hypothesized that edge spiders have smaller clutch sizes to optimize the per-offspring size, if resources are limited by the shorter reproductive season in northern latitudes, and that this tradeoff operates at a local scale rather than range-wide.

Our result for clutch size contrasts with the findings of Wolz *et al.* (2020), where they found equal clutch size between origins in *A. bruennichi*; in that study, the authors suggested that because core females are larger, reproductive investment, relative to body size, is higher in edge females. In our study, we explicitly include female body size as an explanatory variable, and estimate the effects of core vs. edge at median body size. While we do find that larger females have higher clutch sizes, this is true in both populations, and core females have higher clutch sizes overall. While clutch size might naturally vary between years, one difference in our study from that of Wolz *et al.* is the inclusion of multiple clutches per female, and of oviposition latency as a fixed effect. If we exclude all second clutches from our data set and do not account for oviposition latency, we find the same results, that clutch size, relative to body size, is higher in edge females (Supplemental File 1: Table S2, Figure S9). Because in our study, core spiders tended to lay their egg sacs later, we may be overcorrecting for oviposition latency and inflating the estimate of core females' clutch size. However, looking at the raw data (Supplemental File 1: Figure S3A-B), our results appear to reflect the differences well: although the core females started to oviposit later, there is still substantial overlap, and their early egg sacs have higher clutch sizes than edge spiders' early egg sacs, and this is consistent over time. Oviposition latency has a very strong effect in *A. bruennichi* and needs to be included when investigating reproductive success in this species, to avoid drawing potentially incorrect conclusions.

Genetic adaptation in cold tolerance

We found that overwintering survival was highest under warm winter conditions for both core and edge spiderlings. However, under the cold winter treatment, edge spiderlings had higher survival than core spiderlings (Figure 2A). This suggests that the edge populations have adapted to cope with the colder winters, and plasticity does not allow the core spiderlings to cope as well under these conditions. Likewise, in our lower lethal temperature assays, edge spiderlings had higher survival at the lowest exposure temperatures. While survival was similar between origins at exposures to temperatures between -10 and -18°C, at more extreme cold temperatures, edge spiderlings had significantly higher survival. Across all treatments, edge spiderlings had lower LG SCPs. Slightly more nuanced is the difference in the proportion of LG:HG SCPs. At mid-winter, across both treatments and both origins, the majority of spiderlings have LG SCPs. However, post-winter, in the warm winter treatment, spiderlings from the core switch to having a majority of HG SCPs, possibly indicating a switch in strategy depending on environmental cues. This is likely adaptive for the spiderlings from the core of the range, as they can respond to environmental cues in the spring and decrease their investment in maintaining their cold tolerance when it is no longer necessary. We discuss this aspect in more detail below, in the section, "Seasonal variation in cold tolerance plasticity."

Determination of an organism's cold tolerance strategy (chilling intolerant, freeze avoidant, or freeze tolerant) requires data on the lower lethal temperature and supercooling point (Sinclair *et al.*, 2015). Due to methodological constraints, we could not assess lethal temperature and supercooling points simultaneously in a single assay per individual. Thus, we have to compare between the two different assays to determine the *A. bruennichi* cold tolerance strategy. Pooling all of the data across treatment groups, the median SCP in *A. bruennichi* was -27.93°C. Using our model for lower lethal temperature survival, we predict 50% survival at -27.5°C. Thus, the median supercooling point is very similar to the average lethal temperature, suggesting that *A. bruennichi* is a freeze avoidant species: they survive until freezing, and do not succumb to the effects of cold temperatures before that point. This is consistent with

all other reports on cold tolerance strategies of spiders from temperate habitats (Kirchner, 1973, 1987; Cubillos *et al.*, 2018; Anthony, 2019; Anthony *et al.*, 2019).

We also found significant differences in body size between core and edge spiderlings: edge spiderlings were smaller both in leg length and in mass. Mass varied with winter treatment, according to expectation: spiderlings had lower mass following a warm winter treatment than a cold winter treatment. Due to the linear relationship between metabolic rate and temperature in arthropods, and the fact that the spiderlings do not feed over the course of winter (Turnbull, 1973; Welke & Schneider, 2012), they use up more of their energy reserves under warm conditions. This loss of mass continued over the course of winter, with lowest mass post-winter in the warm treatment. Edge spiderlings had consistently lower mass than core spiderlings across treatments. Lower mass in spiderlings from the edge of the range may allow for greater cold tolerance, as body size is linked to cold tolerance in many freeze avoidant arthropods: smaller individuals contain less water, and the probability of ice nucleation is directly related to the number of water molecules in the body (Lee, 2010). Thus, producing smaller offspring at the range edge may be beneficial in *A. bruennichi.* Another possibility is that lower mass in edge spiderlings indicates lower resource provisioning from mothers to offspring. Even if this is the case, the offspring do not seem to have lower quality (i.e. demonstrate lower survival or poorer cold tolerance capacity). Furthermore, the edge spiderlings, under their native cold winter treatment, have almost exactly the same mass as core spiderlings under their native warm winter treatment (Figure 5). Thus, edge spiderlings may have exactly the resources they need given the predictably cold winter in Estonia. However, if winter temperatures increase due to global climate change, this may prove maladaptive (Williams, Henry & Sinclair, 2015b). We found a very strong contribution of our random effects in the model for leg length – with a conditional pseudo-R^2 of 0.817 and almost no contribution of the fixed effects (marginal pseudo-R^2 = 0.060), mother identity seems to determine offspring body size more than anything else.

Taken together, our results indicate that the edge spiderlings have evolved greater cold tolerance and smaller body size than their counterparts in the core of the range. Given that the *A. bruennichi* expansion began in the 1960s, and the species first arrived in Estonia in 2006 (Algo, 2010), this adaptation to the colder winter temperatures in northeastern Europe arose over the course of decades. With one generation per year, this corresponds to only a few dozen generations. Local adaptation in cold tolerance has been found in other species with large latitudinal ranges, correlated with greater variability and seasonality towards the poles (Addo-Bediako, Chown & Gaston, 2000; Lancaster *et al.*, 2015).

Seasonal variation in cold tolerance plasticity

In addition to the observed differences between origins, many traits showed seasonal differences, and especially seasonal differences in the degree of plasticity. For example, at mid-winter, there are no differences between the warm and cold winter treatments in lower lethal temperature. However, post-winter, survival decreases dramatically in the warm treatment at the lower exposure temperatures. This coincides closely with the SCP results. At mid-winter, there is no plasticity, i.e. no winter treatment effects, in the LG SCPs or in the proportion of LG:HG SCPs; at post-winter, there is plasticity, with higher LG SCPs in the warm treatment, and more HG SCPs in general, with a significant switch to HG SCPs in core spiderlings under the warm treatment. This is further evidence that the lower lethal temperature is related to the SCP. Furthermore, the fact that the switch toward HG SCPs was not observed in edge spiderlings suggests that adaptations have arisen to suppress plasticity in this trait and maintain a low SCP even with an early, warm spring, whereas the core spiderlings are plastic. According to theory, plasticity

is favored under predictably variable environments, where no single phenotype has higher fitness in all environments (Ghalambor *et al.*, 2007). Thus, plasticity loss, such as that seen in the LG:HG SCP ratio in edge spiderlings under warm conditions, should only arise when a trait is under very strong selection.

Latitudinal variation in adult phenotypes and genotypes across transect

Female body size, but not pigmentation, clutch size, or hatching success, varies with latitude

We found that adult body size varies with latitudinally varying climatic variables. *A. bruennichi* females are smaller under colder, more seasonal environments. *A. bruennichi*, as many other arthropod species, follows the Converse Bergmann's rule (Mousseau, 1997; Blanckenhorn & Demont, 2004; Chown & Gaston, 2010; Williams, Chick & Sinclair, 2015a). Whether this is due to a shorter growing season or a faster development time cannot be discerned in this study, but it is interesting to note that the smaller body size of edge spiders is already present at the spiderling stage.

Contrary to our expectation, given the fact that many ectothermic animals (i.e. reptiles, insects) show darker coloration at northern latitudes (Watt, 1968; Guppy, 1986; Svensson & Waller, 2013; Martínez-Freiría *et al.*, 2020), we did not find darker opisthosoma pigmentation with increasing latitude. However, we did find a significant association of pigmentation with one environmental principal component (PC4). This PC is strongly related to the mean temperature of the wettest quarter – populations with low temperatures in the wettest quarter had less dark coloration. This effect is very difficult to interpret, and is also not particularly strong. One possible explanation for why we found no latitudinal variation, is that spiders may perform some degree of behavioral thermoregulation by orienting either their dorsal or ventral side toward the sun, as has been documented in some other spider species and within the *Argiope* genus (Robinson & Robinson, 1978; Tolbert, 1979). In *A. bruennichi*, as in many other spider species, the ventral opisthosoma is much darker than the dorsal opisthosoma. By measuring the pigmentation of the dorsal side, we may have missed variation in ventral pigmentation, or there is simply no adaptive variation in pigmentation, as behavioral thermoregulation may be sufficient across the range. It is also possible that opisthosoma pigmentation is plastic, and may vary according to the presence or absence of sun. Some spiders are able to very rapidly alter their coloration in response to environmental stimuli, although this has never been documented in any *Argiope* species (reviewed by Holl, 1987). Given that we measured pigmentation from photographs taken in the field, at varying times of day and under varying environmental conditions, we are not able to test this with our data. Alternatively, although the dorsal opisthosoma pattern is a striking feature in this species, the pigmentation of the legs and/or prosoma may be more important, as these body parts contain more muscles. Darker pigmentation would allow the muscles to warm up, which may be important to optimize foraging success on sunny days, when prey insects are more active. Lastly, the dorsal opisthosoma pattern may have evolved under different, non-thermoregulatory, selection pressures, i.e. to prevent the formation of a searching image for predators, or to attract insect prey (Bond, 2007; Bush, Yu & Herberstein, 2008).

We also did not find any pattern in hatching success or clutch size according to environmental factors. Although our results from the core and edge show that edge spiders have lower clutch sizes and hatching success, this seems not to be consistent across the whole transect. It is possible that the populations at the very edge of the range suffer from edge effects that are not reflected in intermediate populations along the transect. Another possibility is that hatching success and clutch size are highly variable within populations, and our sample size along the transect, of 10 females per population, was not high enough

to detect a signal, given the noise. The very low pseudo-R^2 values of our models for clutch size and hatching success suggest that this is likely to be the case (Table 6), and thus we prefer to interpret the core and edge results, above, where the sample sizes are much higher, as are the pseudo-R^2 values (Table 2**,** Table 3).

Population genetic statistics show strong differentiation over a short geographic distance

Our population clustering analyses revealed that the "native" and "invasive" populations are genetically differentiated, and this differentiation arises over a very short geographic distance. Along our transect, the turnover from "native" to "invasive" occurs over an 85 km stretch within the middle of Germany (Figure 7), and is far less gradual than might be expected, given the level of gene flow possible in such a dispersive species that shows overall low genetic variation across the Palearctic (Krehenwinkel *et al.*, 2016). Our results provide strong support, in great detail, to the hypothesis presented by Krehenwinkel & Tautz (2013): introgression occurred in populations within central Germany. We demonstrate this here by showing that there is greater genetic diversity in the "invasive" populations, and more genetic similarity of invasive populations to the Russian and Japanese populations than found in the French populations.

We calculated individual-level inbreeding coefficients, and compared these across populations. The Japanese populations were highly inbred, while Russian populations were outbred, and there were intermediate inbreeding levels within European populations (Figure 8). High inbreeding of the Japanese populations is unsurprising; *A. bruennichi* spiderlings disperse via aerial ballooning, which should be selected against in island populations, as the likelihood of dispersing into unsuitable areas, i.e. the ocean, is very high. Within the populations at the edge of the range in Estonia, we observed a linear increase in inbreeding levels with latitude. This may be explained by the lower dispersal propensity of edge populations of *A. bruennichi* found by Wolz *et al.* (2020). In that study, edge spiderlings were less dispersive than core spiderlings, which was in contrast to the authors' expectations of spatial sorting and Olympic village effects considered typical at the leading edge of a range expansion (Shine, Brown & Phillips, 2011). Wolz *et al.* hypothesized that there may be strong selection against dispersal at the edge of the range in this case, due to possibly fragmented habitat patches and/or low population densities. Lower dispersal propensity may then lead to increased inbreeding, or vice versa. In light of our results for the lower lethal temperature and supercooling points, we find the explanation for selection against dispersal highly plausible. Further north and inland of our collecting sites, temperatures can dip below -32°C when arctic cold fronts move over Estonia. Such low temperatures are likely fatal for *A. bruennichi* spiderlings, even for short exposure times, based on our data. Thus, it seems that the populations in Estonia are no longer an expansion front, but have reached a range border, beyond which survival over winter is unlikely. This is consistent with the findings of many studies, that poleward range limits are set by direct environmental limitations, where adverse conditions exceed species' tolerance levels (MacArthur, 1972; Root, 1988; Parmesan *et al.*, 2005; Mazaris *et al.*, 2013).

Support for adaptive introgression

Throughout the genome, we found genomic windows with strong environmental associations, high differentiation of native/invasive populations in F_{ST}, and relatively lower F_{ST} between invasive and Japanese populations. This pattern suggests that in *A. bruennichi*, adaptive introgression may have truly provided the genomic substrate for selection, enabling adaptation to colder winters. We found that the same regions of the genome were associated with multiple environmental principal components. In order

to parse apart the precise environmental drivers of adaptation, we will need to test the associations with single bioclimatic variables, rather than summarized principal components. This will also allow us to see if the same genomic regions are associated with adaptation to multiple environmental factors, or if there are different patterns given different, more specific, environmental variables. Further investigation into the genes present in these regions is needed, to shed light on their potential functions. What is clear from our results is that precipitation, strongly represented in PCs 2 and 4, does not exert a strong selection pressure in this system. Temperature and seasonality, on the other hand, show more and stronger genetic associations. Although the sampling design in our study is not intended to identify the precise donor population for introgression, based on our results and those of previous studies (Krehenwinkel & Tautz, 2013; Krehenwinkel *et al.*, 2015), it is highly likely that the introgression came from the east, as represented here by Japanese populations, through Russia. The *A. bruennichi* populations in Russia are characterized by a strongly seasonal climate, with an annual temperature range of 35-40°C, and very cold winters. Thus, it stands to reason that admixture of the European and Russian populations could have enabled introgression of alleles from eastern populations that evolved under cold and seasonal environments.

One very interesting aspect of our results is the high level of differentiation and environmental association we found on chromosome 9, which has recently been identified as an X chromosome (Sheffer *et al.*, 2021a). *A. bruennichi* possesses a multiple X chromosome system, where males are hemizygous for two X chromosomes (9 and 10), meaning females have two copies of each X chromosome while males have one copy of each. Therefore, the effective population size and recombination rate for X chromosomes should be lower than autosomes. This leads to the theoretical prediction of increased evolutionary rates of X chromosomes under natural selection, especially in the case of recessive variants (Charlesworth, Coyne & Barton, 1987; Ellegren, 2009; Bechsgaard *et al.*, 2019). In the case of *A. bruennichi*, it seems that at least one of the X chromosomes has indeed evolved more quickly than autosomes. Chromosome 10 shows weaker patterns than chromosome 9, and does not stand out in its range of LRT or F_{ST} values in the same way (Supplemental File 1: Figure S10). Although they have a different sex determination system, there are interesting introgression patterns in X chromosomes found at the house mouse (*Mus musculus/M. domesticus*) hybrid zone. One central region of the X chromosome in the house mouse has been identified as an area of reduced gene flow, and is thought to be a candidate region for reproductive isolation, while another region shows a signature of adaptive introgression (Payseur, Krenz & Nachman, 2004). Our work builds on the existing evidence that sex chromosomes can – and do – evolve rapidly.

Conclusion

Our study had two central aims: first, to quantify genetic adaptation and phenotypic plasticity in cold tolerance in edge relative to core populations, and second, given a strong role of genetic adaptation in enabling the establishment and persistence of expanding populations, to test if the range expansion and subsequent adaptation was enabled by adaptive introgression. Our reciprocal transplant common garden experiment revealed that the edge populations are clearly locally adapted in cold tolerance. Although there is significant plasticity, especially in the spring, edge spiderlings are more cold tolerant across all investigated traits. Our population genomic analysis revealed striking differentiation over a short geographic distance, suggesting strong selection. Going deeper, looking at genome-wide population genetic outliers and environmental associations, we find compelling, if correlative, evidence for adaptive introgression providing the substrate for selection to the colder, more seasonal environments in

northeastern Europe. Taken together, all of our results suggest that *A. bruennichi* populations in Estonia are no longer an expanding front, but have reached a poleward range limit.

Data availability

The scripts for filtering SNPs in and outside of exons were written by KJH and can be shared upon reasonable request. The genome-wide results for all chromosomes for each environmental PC (65 graphs, thus excluded from the supplement for brevity) can be shared by MMS upon request. Observed means and variances of spider traits will be uploaded to the World Spider Trait Database (https://spidertraits.sci.muni.cz/) for utility in meta-analyses.

Acknowledgements

We would like to thank Lydia Smith and Natalie Graham at UC Berkeley for their invaluable advice on ddRAD library preparation and sequencing. We are grateful to Cynthia Wang for her work on adapting the library preparation protocol. Many thanks to Heidi Land for her incredible organizational skills helping with the coordination of animal caretaking, and more. We also thank Alexandra Machnis, Timon Möller, Birte Schadlowski, Anja Junghanns, and Julia Balk for their help with spider husbandry, counting, and measuring offspring. We also thank Marina Wolz for her very helpful advice on the overwintering procedure and how to count and measure offspring.

Author contributions

GU, HK, SP, and MMS designed the study. Samples were collected by GU, HK, LZ, BS, and MMS. DNA was extracted by HK and MMS. MMS performed the library preparation and sequencing. With help from SP and KJH, MMS performed all population genomic analyses. LZ, BS, GU and MMS photographed the spiders in the field. Phenotyping of adult spiders was done by LZ, BS and MMS. The common garden experiment and subsequent physiological/phenotypic measurements of offspring were designed and run by MMS, with help from LZ and BS. MMS performed all statistical analysis of the adult phenotypes, environmental variables, and common garden data, with input from PM and TN.

References

Addo-Bediako, A., Chown, S.L. & Gaston, K.J. (2000). Thermal tolerance, climatic variability and latitude. *Proc. R. Soc. London. Ser. B Biol. Sci.* **267**, 739–745.

Ahrens, C.W., Rymer, P.D., Stow, A., Bragg, J., Dillon, S., Umbers, K.D.L. & Dudaniec, R.Y. (2018). The search for loci under selection: trends, biases and progress. *Mol. Ecol.* **27**, 1342–1356.

Alexander, D.H., Novembre, J. & Lange, K. (2009). Fast model-based estimation of ancestry in unrelated individuals. *Genome Res.* **19**, 1655–1664.

Algo, R.-J. (2010). Herilasämblik (*Argiope bruennichi*) ja tema sissetung Eestisse (Wasp spider *Argiope bruennichi* and his invasion of Estonia). *Õpilaste Tead.* **2**, 4–26.

Anthony, S. (2019). *Thermal biology of temperate and high-latitude arachnids*. *Electron. Thesis Diss. Repos.* University of Western Ontario, London, Ontario.

Anthony, S.E., Buddle, C.M., Høye, T.T. & Sinclair, B.J. (2019). Thermal limits of summer-collected *Pardosa* wolf spiders (Araneae: Lycosidae) from the Yukon Territory (Canada) and Greenland. *Polar*

Biol. **42**, 2055–2064.

Auld, J.R., Agrawal, A.A. & Relyea, R.A. (2010). Re-evaluating the costs and limits of adaptive phenotypic plasticity. *Proc. R. Soc. B Biol. Sci.* **277**, 503–511.

Barrett, R.D.H. & Schluter, D. (2008). Adaptation from standing genetic variation. *Trends Ecol. Evol.* **23**, 38–44.

Bates, D., Mächler, M., Bolker, B.M. & Walker, S.C. (2015). Fitting linear mixed-effects models using lme4. *J. Stat. Softw.* **67**, 1–48.

Bechsgaard, J., Schou, M.F., Vanthournout, B., Hendrickx, F., Knudsen, B., Settepani, V., Schierup, M.H. & Bilde, T. (2019). Evidence for faster X chromosome evolution in spiders. *Mol. Biol. Evol.* **36**, 1281–1293.

Blanckenhorn, W.U. & Demont, M. (2004). Bergmann and converse Bergmann latitudinal clines in arthropods: Two ends of a continuum? *Integr. Comp. Biol.* **44**, 413–424.

Bolger, A.M., Lohse, M. & Usadel, B. (2014). Trimmomatic: a flexible trimmer for Illumina sequence data. *Bioinformatics* **30**, 2114–2120.

Bond, A.B. (2007). The evolution of color polymorphism: Crypticity, searching images, and apostatic selection. *Annu. Rev. Ecol. Evol. Syst.* **38**, 489–514.

Brooks, M.E., Kristensen, K., van Benthem, K.J., Magnusson, A., Berg, C.W., Nielsen, A., Skaug, H.J., Mächler, M. & Bolker, B.M. (2017). glmmTMB balances speed and flexibility among packages for zero-inflated generalized linear mixed modeling. *R J.* **9**, 378–400.

Bush, A.A., Yu, D.W. & Herberstein, M.E. (2008). Function of bright coloration in the wasp spider *Argiope bruennichi* (Araneae: Araneidae). *Proc. R. Soc. B Biol. Sci.* **275**, 1337–1342.

Charlesworth, B., Coyne, J.A. & Barton, N.H. (1987). The relative rates of evolution of sex chromosomes and autosomes. *Am. Nat.* **130**, 113–146.

Chen, I.C., Hill, J.K., Ohlemüller, R., Roy, D.B. & Thomas, C.D. (2011). Rapid range shifts of species associated with high levels of climate warming. *Science (80-.).* **333**, 1024–1026.

Chown, S.L. & Gaston, K.J. (2010). Body size variation in insects: A macroecological perspective. *Biol. Rev.* **85**, 139–169.

Clausen, J., Keck, D.D. & Hiesey, W.M. (1941). Regional differentiation in plant species. *Am. Nat.* **75**, 231–250.

Colautti, R.I. & Barrett, S.C.H. (2013). Rapid adaptation to climate facilitates range expansion of an invasive plant. *Science (80-.).* **342**, 364–366.

Cubillos, C., Cáceres, J.C., Villablanca, C., Villarreal, P., Baeza, M., Cabrera, R., Graether, S.P. & Veloso, C. (2018). Cold tolerance mechanisms of two arthropods from the Andean Range of Central Chile: *Agathemera crassa* (Insecta: Agathemeridae) and *Euathlus condorito* (Arachnida: Theraphosidae). *J. Therm. Biol.* **74**, 133–139.

Ellegren, H. (2009). The different levels of genetic diversity in sex chromosomes and autosomes. *Trends Genet.* **25**, 278–284.

Fick, S.E. & Hijmans, R.J. (2017). WorldClim 2: new 1-km spatial resolution climate surfaces for global

land areas. *Int. J. Climatol.* **37**, 4302–4315.

Follner, K. & Klarenberg, A.J. (1995). Aeronautic behaviour in the wasp-like spider, *Argiope bruennichi* (Scopoli) (Araneae, Argiopidae). *Proc. 15th Eur. Colloq. Arachnol.* **72**, 66–72.

Fordyce, J.A. (2006). The evolutionary consequences of ecological interactions mediated through phenotypic plasticity. *J. Exp. Biol.* **209**, 2377–2383.

Fraser, D.J., Weir, L.K., Bernatchez, L., Hansen, M.M. & Taylor, E.B. (2011). Extent and scale of local adaptation in salmonid fishes: Review and meta-analysis. *Heredity (Edinb).* **106**, 404–420.

Fumagalli, M., Vieira, F.G., Korneliussen, T.S., Linderoth, T., Huerta-Sánchez, E., Albrechtsen, A. & Nielsen, R. (2013). Quantifying population genetic differentiation from next-generation sequencing data. *Genetics* **195**, 979–992.

Fumagalli, M., Vieira, F.G., Linderoth, T. & Nielsen, R. (2014). ngsTools: Methods for population genetics analyses from next-generation sequencing data. *Bioinformatics* **30**, 1486–1487.

Ghalambor, C.K., McKay, J.K., Carroll, S.P. & Reznick, D.N. (2007). Adaptive versus non-adaptive phenotypic plasticity and the potential for contemporary adaptation in new environments. *Funct. Ecol.* **21**, 394–407.

Guppy, C.S. (1986). Geographic variation in wing melanism of the butterfly *Parnassius phoebus* F. (Lepidoptera: Papilionidae). *Can. J. Zool.* **64**, 956–962.

Hartig, F. (2021). DHARMa: Residual diagnostics for hierarchical (multi-level / mixed) regression models.

Hassall, M., Walters, R.J., Telfer, M. & Hassall, M.R.J. (2006). Why does a grasshopper have fewer, larger offspring at its range limits? *J. Evol. Biol.* **19**, 267–276.

Hedrick, P.W. (2013). Adaptive introgression in animals: examples and comparison to new mutation and standing variation as sources of adaptive variation. *Mol. Ecol.* **22**, 4606–4618.

Hereford, J. (2009). A quantitative survey of local adaptation and fitness trade-offs. *Am. Nat.* **173**, 579–588.

Hickling, R., Roy, D.B., Hill, J.K., Fox, R. & Thomas, C.D. (2006). The distributions of a wide range of taxonomic groups are expanding polewards. *Glob. Chang. Biol.* **12**, 450–455.

Hoban, S., Kelley, J.L., Lotterhos, K.E., Antolin, M.F., Bradburd, G., Lowry, D.B., Poss, M.L., Reed, L.K., Storfer, A. & Whitlock, M.C. (2016). Finding the genomic basis of local adaptation: Pitfalls, practical solutions, and future directions. *Am. Nat.* **188**, 379–397.

Hoffmann, A.A. & Bridle, J. (2021). The dangers of irreversibility in an age of increased uncertainty: revisiting plasticity in invertebrates. *Oikos*.

Holl, A. (1987). Coloration and chromes. In *Ecophysiology of Spiders*: 16–25. Nentwig, W. (Ed). . Berlin Heidelberg New York Tokyo: Springer-Verlag.

Huerta-Sánchez, E., Jin, X., Asan, Bianba, Z., Peter, B.M., Vinckenbosch, N., Liang, Y., Yi, X., He, M., Somel, M., Ni, P., Wang, B., Ou, X., Huasang, Luosang, J., Cuo, Z.X.P., Li, K., Gao, G., Yin, Y., Wang, W., Zhang, X., Xu, X., Yang, H., Li, Y., Wang, J., Wang, J. & Nielsen, R. (2014). Altitude adaptation in Tibetans caused by introgression of Denisovan-like DNA. *Nature* **512**, 194–197.

Johnson, P.L.F. & Slatkin, M. (2008). Accounting for bias from sequencing error in population genetic

estimates. *Mol. Biol. Evol.* **25**, 199–206.

Kassambara, A. & Mundt, F. (2020). FactoExtra: Extract and visualize the results of multivariate data analyses.

Kirchner, W. (1973). Ecological aspects of cold resistance in spiders (a comparative study). In *Effects of temperature on ectothermic organisms*: 271–279. Wieser, W. (Ed). . Berlin, Heidelberg: Springer.

Kirchner, W. (1987). Behavioural and Physiological Adaptations to Cold. In *Ecophysiology of Spiders*: 66–77. Nentwig, W. (Ed). . Berlin, Heidelberg: Springer.

Kirchner, W. & Kestler, P. (1969). Untersuchungen zur Kälteresistenz der Schilfradspinne *Araneus cornutus* (Araneidae). *J. Insect Physiol.* **15**, 41–53.

Kopelman, N.M., Mayzel, J., Jakobsson, M., Rosenberg, N.A. & Mayrose, I. (2015). CLUMPAK: A program for identifying clustering modes and packaging population structure inferences across K. *Mol. Ecol. Resour.* **15**, 1179–1191.

Korneliussen, T.S., Albrechtsen, A. & Nielsen, R. (2014). ANGSD: Analysis of Next Generation Sequencing Data. *BMC Bioinformatics* **15**, 356.

Korneliussen, T.S. & Moltke, I. (2015). NgsRelate: a software tool for estimating pairwise relatedness from next-generation sequencing data. *Bioinformatics* **31**, 4009–4011.

Krehenwinkel, H., Graze, M., Rödder, D., Tanaka, K., Baba, Y.G., Muster, C. & Uhl, G. (2016). A phylogeographical survey of a highly dispersive spider reveals eastern Asia as a major glacial refugium for Palaearctic fauna. *J. Biogeogr.* **43**, 1583–1594.

Krehenwinkel, H., Rödder, D. & Tautz, D. (2015). Eco-genomic analysis of the poleward range expansion of the wasp spider *Argiope bruennichi* shows rapid adaptation and genomic admixture. *Glob. Chang. Biol.* **21**, 4320–4332.

Krehenwinkel, H. & Tautz, D. (2013). Northern range expansion of European populations of the wasp spider *Argiope bruennichi* is associated with global warming-correlated genetic admixture and population-specific temperature adaptations. *Mol. Ecol.* **22**, 2232–2248.

Lancaster, L.T., Dudaniec, R.Y., Chauhan, P., Wellenreuther, M., Svensson, E.I. & Hansson, B. (2016). Gene expression under thermal stress varies across a geographical range expansion front. *Mol. Ecol.* **25**, 1141–1156.

Lancaster, L.T., Dudaniec, R.Y., Hansson, B. & Svensson, E.I. (2015). Latitudinal shift in thermal niche breadth results from thermal release during a climate-mediated range expansion. *J. Biogeogr.* **42**, 1953–1963.

Leborgne, R. & Pasquet, A. (2005). Time of oviposition and reproductive success in *Argiope bruennichi* (Araneae: Araneidae). *Eur. J. Entomol.* **102**, 169–174.

Lee, R.E. (2010). A primer on insect cold-tolerance. In *Low Temperature Biology of Insects*: 3–34. Denlinger, D.L. & Lee, R.E. (Eds). . Cambridge University Press.

Lefort, V., Desper, R. & Gascuel, O. (2015). FastME 2.0: A comprehensive, accurate, and fast distance-based phylogeny inference program. *Mol. Biol. Evol.* **32**, 2798–2800.

Leimu, R. & Fischer, M. (2008). A meta-analysis of local adaptation in plants. *PLoS One* **3**, e4010.

Lepais, O. & Weir, J.T. (2014). SimRAD: An R package for simulation-based prediction of the number of loci expected in RADseq and similar genotyping by sequencing approaches. *Mol. Ecol. Resour.* **14**, 1314–1321.

Li, H. (2013). Aligning sequence reads, clone sequences and assembly contigs with BWA-MEM. *arXiv*.

Li, H., Handsaker, B., Wysoker, A., Fennell, T., Ruan, J., Homer, N., Marth, G., Abecasis, G. & Durbin, R. (2009). The Sequence Alignment/Map format and SAMtools. *Bioinformatics* **25**, 2078–2079.

Lüdecke, D. (2018). ggeffects: Tidy data frames of marginal effects from regression models. *J. Open Source Softw.* **3**, 772.

Lüdecke, D., Ben-Shachar, M., Patil, I., Waggoner, P. & Makowski, D. (2021). performance: An R package for assessment, comparison and testing of statistical models. *J. Open Source Softw.* **6**, 3139.

Lundblad, C.G. & Conway, C.J. (2021). Ashmole's hypothesis and the latitudinal gradient in clutch size. *Biol. Rev.* **96**, 1349–1366.

Lynch, M. (2008). Estimation of nucleotide diversity, disequilibrium coefficients, and mutation rates from high-coverage genome-sequencing projects. *Mol. Biol. Evol.* **25**, 2409–2419.

Maas, D.L., Prost, S., Bi, K., Smith, L.L., Armstrong, E.E., Aji, L.P., Toha, A.H.A., Gillespie, R.G. & Becking, L.E. (2018). Rapid divergence of mussel populations despite incomplete barriers to dispersal. *Mol. Ecol.* **27**, 1556–1571.

MacArthur, R.H. (1972). *Geographical Ecology: Patterns in the Distribution of Species*. Princeton: Princeton University Press.

Martínez-Freiría, F., Toyama, K.S., Freitas, I. & Kaliontzopoulou, A. (2020). Thermal melanism explains macroevolutionary variation of dorsal pigmentation in Eurasian vipers. *Sci. Rep.* **10**, 1–10.

Mazaris, A.D., Kallimanis, A.S., Pantis, J.D. & Hays, G.C. (2013). Phenological response of sea turtles to environmental variation across a species' northern range. *Proc. R. Soc. B Biol. Sci.* **280**.

Meisner, J. & Albrechtsen, A. (2018). Inferring population structure and admixture proportions in low-depth NGS data. *Genetics* **210**, 719–731.

Moest, M., Van Belleghem, S.M., James, J.E., Salazar, C., Martin, S.H., Barker, S.L., Moreira, G.R.P., Merot, C., Joron, M., Nadeau, N.J., Steiner, F.M. & Jiggins, C.D. (2020). Selective sweeps on novel and introgressed variation shape mimicry loci in a butterfly adaptive radiation. *PLoS Biol.* **18**.

Mousseau, T.A. (1997). Ectotherms Follow the Converse to Bergmann's Rule. *Evolution (N. Y).* **51**, 630.

Muhlfeld, C.C., Kalinowski, S.T., McMahon, T.E., Taper, M.L., Painter, S., Leary, R.F. & Allendorf, F.W. (2009). Hybridization rapidly reduces fitness of a native trout in the wild. *Biol. Lett.* **5**, 328–331.

Nakagawa, S. & Schielzeth, H. (2013). A general and simple method for obtaining R2 from generalized linear mixed-effects models. *Methods Ecol. Evol.* **4**, 133–142.

Norris, L.C., Main, B.J., Lee, Y., Collier, T.C., Fofana, A., Cornel, A.J. & Lanzaro, G.C. (2015). Adaptive introgression in an African malaria mosquito coincident with the increased usage of insecticide-treated bed nets. *Proc. Natl. Acad. Sci. U. S. A.* **112**, 815–820.

Paradis, E. & Schliep, K. (2019). ape 5.0: An environment for modern phylogenetics and evolutionary analyses in R. *Bioinformatics* **35**, 526–528.

Parmesan, C., Gaines, S., Gonzalez, L., Kaufman, D.M., Kingsolver, J., Peterson, A.T. & Sagarin, R. (2005). Empirical perspectives on species borders: from traditional biogeography to global change. *Oikos* **108**, 58–75.

Parmesan, C., Ryrholm, N., Stefanescu, C., Hill, J.K., Thomas, C.D., Descimon, H., Huntley, B., Kaila, L., Kullberg, J., Tammaru, T., Tennent, W.J., Thomas, J.A. & Warren, M. (1999). Poleward shifts in geographical ranges of butterfly species associated with regional warming. *Nature* **399**, 579–583.

Payseur, B.A., Krenz, J.G. & Nachman, M.W. (2004). Differential patterns of introgression across the X chromosome in a hybrid zone between two species of house mice. *Evolution (N. Y).* **58**, 2064–2078.

Peterson, B.K., Weber, J.N., Kay, E.H., Fisher, H.S. & Hoekstra, H.E. (2012). Double digest RADseq: An inexpensive method for de novo SNP discovery and genotyping in model and non-model species. *PLoS One* **7**.

Phillips, B.L., Brown, G.P. & Shine, R. (2010). Life-history evolution in range-shifting populations. *Ecology* **91**, 1617–1627.

Pritchard, J.K., Stephens, M. & Donnelly, P. (2000). Inference of Population Structure Using Multilocus Genotype Data. *Genetics* **155**, 945–959.

R Core Team. (2017). R: A language and environment for statistical computing.

Racimo, F., Sankararaman, S., Nielsen, R. & Huerta-Sánchez, E. (2015). Evidence for archaic adaptive introgression in humans. *Nat. Rev. Genet.* **16**, 359–371.

Rambaut, A. & Drummond, A. (2018). FigTree: Tree figure drawing tool.

Robinson, M.H. & Robinson, B.C. (1978). Thermoregulation in orb-web spiders: New descriptions of thermoregulatory postures and experiments on the effects of posture and coloration. *Zool. J. Linn. Soc.* **64**, 87–102.

Root, T. (1988). Environmental factors associated with avian distributional boundaries. *J. Biogeogr.* **15**, 489–505.

Schielzeth, H. (2010). Simple means to improve the interpretability of regression coefficients. *Methods Ecol. Evol.* **1**, 103–113.

Schneider, J.M., Fromhage, L. & Uhl, G. (2005). Extremely short copulations do not affect hatching success in *Argiope bruennichi* (Araneae, Araneidae). *J. Arachnol.* **33**, 663–669.

Sexton, J.P., McIntyre, P.J., Angert, A.L. & Rice, K.J. (2009). Evolution and ecology of species range limits. *Annu. Rev. Ecol. Evol. Syst.* **40**, 415–436.

Sheffer, M.M., Cordellier, M., Forman, M., Grewoldt, M., Hoffmann, K., Jensen, C., Kotz, M., Král, J., Kuss, A.W., Líznarová, E. & Uhl, G. (2021a). Identification of sex chromosomes using genomic and cytogenetic methods in a range-expanding spider, *Argiope bruennichi* (Araneae: Araneidae). *bioRxiv* 1–26.

Sheffer, M.M., Hoppe, A., Krehenwinkel, H., Uhl, G., Kuss, A.W., Jensen, L., Jensen, C., Gillespie, R.G., Hoff, K.J. & Prost, S. (2021b). Chromosome-level reference genome of the European wasp spider *Argiope bruennichi*: A resource for studies on range expansion and evolutionary adaptation. *Gigascience* **10**, 1–12.

Shine, R., Brown, G.P. & Phillips, B.L. (2011). An evolutionary process that assembles phenotypes through space rather than through time. *Proc. Natl. Acad. Sci.* **108**, 5708–5711.

Sinclair, B.J., Coello Alvarado, L.E. & Ferguson, L. V. (2015). An invitation to measure insect cold tolerance: Methods, approaches, and workflow. *J. Therm. Biol.* **53**, 180–197.

Sinclair, B.J., Klok, C.J., Scott, M.B., Terblanche, J.S. & Chown, S.L. (2003). Diurnal variation in supercooling points of three species of Collembola from Cape Hallett, Antarctica. *J. Insect Physiol.* **49**, 1049–1061.

Skotte, L., Korneliussen, T.S. & Albrechtsen, A. (2012). Association testing for next-generation sequencing data using score statistics. *Genet. Epidemiol.* **36**, 430–437.

Skotte, L., Korneliussen, T.S. & Albrechtsen, A. (2013). Estimating individual admixture proportions from next generation sequencing data. *Genetics* **195**, 693–702.

Svensson, E.I. & Waller, J.T. (2013). Ecology and sexual selection: Evolution of wing pigmentation in calopterygid damselflies in relation to latitude, sexual dimorphism, and speciation. *Am. Nat.* **182**.

Tanaka, K. (1995a). Seasonal change in glycogen and inositol/sorbitol contents of the house spider, *Achaearanea tepidariorum* (Araneae: Theridiidae). *Comp. Biochem. Physiol. -- Part B Biochem.* **110**, 539–545.

Tanaka, K. (1995b). Variation in offspring size within a population of the web-building spider *Agelena limbata*. *Res. Popul. Ecol. (Kyoto).* **37**, 197–202.

Tolbert, W.W.. (1979). Thermal stress of the orb-weaving spider *Argiope trifasciata* (Araneae). *Oikos* **32**, 386–392.

Turnbull, A.L. (1973). Ecology of the true spiders (Araneomorphae). *Annu. Rev. Entomol.* **18**, 305–348.

Uhl, G. & Vollrath, F. (2000). Extreme body size variability in the golden silk spider (*Nephila edulis*) does not extend to genitalia. *J. Zool.* **251**, 7–14.

Vieira, F.G., Fumagalli, M., Albrechtsen, A. & Nielsen, R. (2013). Estimating inbreeding coefficients from NGS data: Impact on genotype calling and allele frequency estimation. *Genome Res.* **23**, 1852–1861.

Vieira, F.G., Lassalle, F., Korneliussen, T.S. & Fumagalli, M. (2016). Improving the estimation of genetic distances from Next-Generation Sequencing data. *Biol. J. Linn. Soc.* **117**, 139–149.

Watt, W.B. (1968). Adaptive signficance of pigment polymorphisms in *Colias* butterflies. I. Variation of melanin pigment in relation to thermoregulation. *Int. J. Org. Evol.* **22**, 437–458.

Wawer, W., Rutkowski, R., Krehenwinkel, H., Lutyk, D., Pusz-Boscheńska, K. & Bogdanowicz, W. (2017). Population structure of the expansive wasp spider (*Argiope bruennichi*) at the edge of its range. *J. Arachnol.* **45**, 361–369.

Welke, K.W. & Schneider, J.M. (2010). Males of the orb-web spider *Argiope bruennichi* sacrifice themselves to unrelated females. *Biol. Lett.* **6**, 585–588.

Welke, K.W. & Schneider, J.M. (2012). Sexual cannibalism benefits offspring survival. *Anim. Behav.* **83**, 201–207.

Whitman, D. & Agrawal, A.A. (2009). What is Phenotypic Plasticity and Why is it Important? In

Phenotypic plasticity of insects: Mechanisms and consequences: 1–63. Whitman, D. & Ananthakrishnan, T.N. (Eds). . Enfield: Science Publishers, Inc.

Williams, C.M., Chick, W.D. & Sinclair, B.J. (2015a). A cross-seasonal perspective on local adaptation: Metabolic plasticity mediates responses to winter in a thermal-generalist moth. *Funct. Ecol.* **29**, 549–561.

Williams, C.M., Henry, H.A.L. & Sinclair, B.J. (2015b). Cold truths: How winter drives responses of terrestrial organisms to climate change. *Biol. Rev.* **90**, 214–235.

Wolz, M., Klockmann, M., Schmitz, T., Pekár, S., Bonte, D. & Uhl, G. (2020). Dispersal and life-history traits in a spider with rapid range expansion. *Mov. Ecol.* **8**, 1–11.

Zhang, W., Dasmahapatra, K.K., Mallet, J., Moreira, G.R.P. & Kronforst, M.R. (2016). Genome-wide introgression among distantly related *Heliconius* butterfly species. *Genome Biol.* **17**, 25.

Supplemental File 1

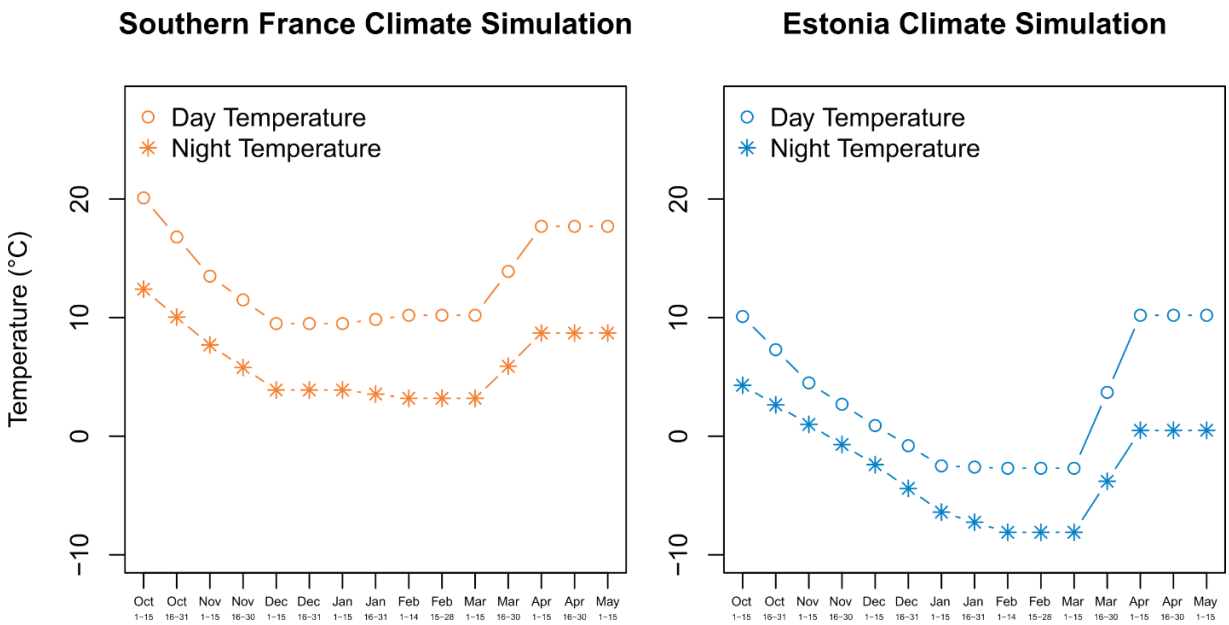

Figure S1. Climate simulations used for overwintering in our reciprocal common garden transplant. Spiderlings were placed under either conditions found at the core of the range (Southern France) or at the edge of the range (Estonia). Simulations are based on data averaged over 10 years (2004-2014), derived from www.weatheronline.co.uk

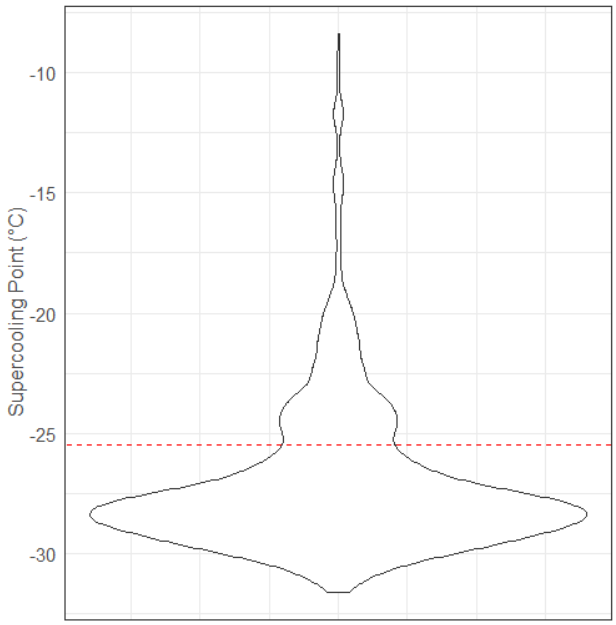

Figure S2. Multimodal distribution of supercooling points (SCPs). We split the data into two groups: low group (LG) SCPs, below -25.5°C (dashed red line), and high group (HG) SCPs, above -25.5°C. The LG distribution was Gaussian, and we only used the HG SCPs to calculate a per-family ratio of LG:HG SCPs.

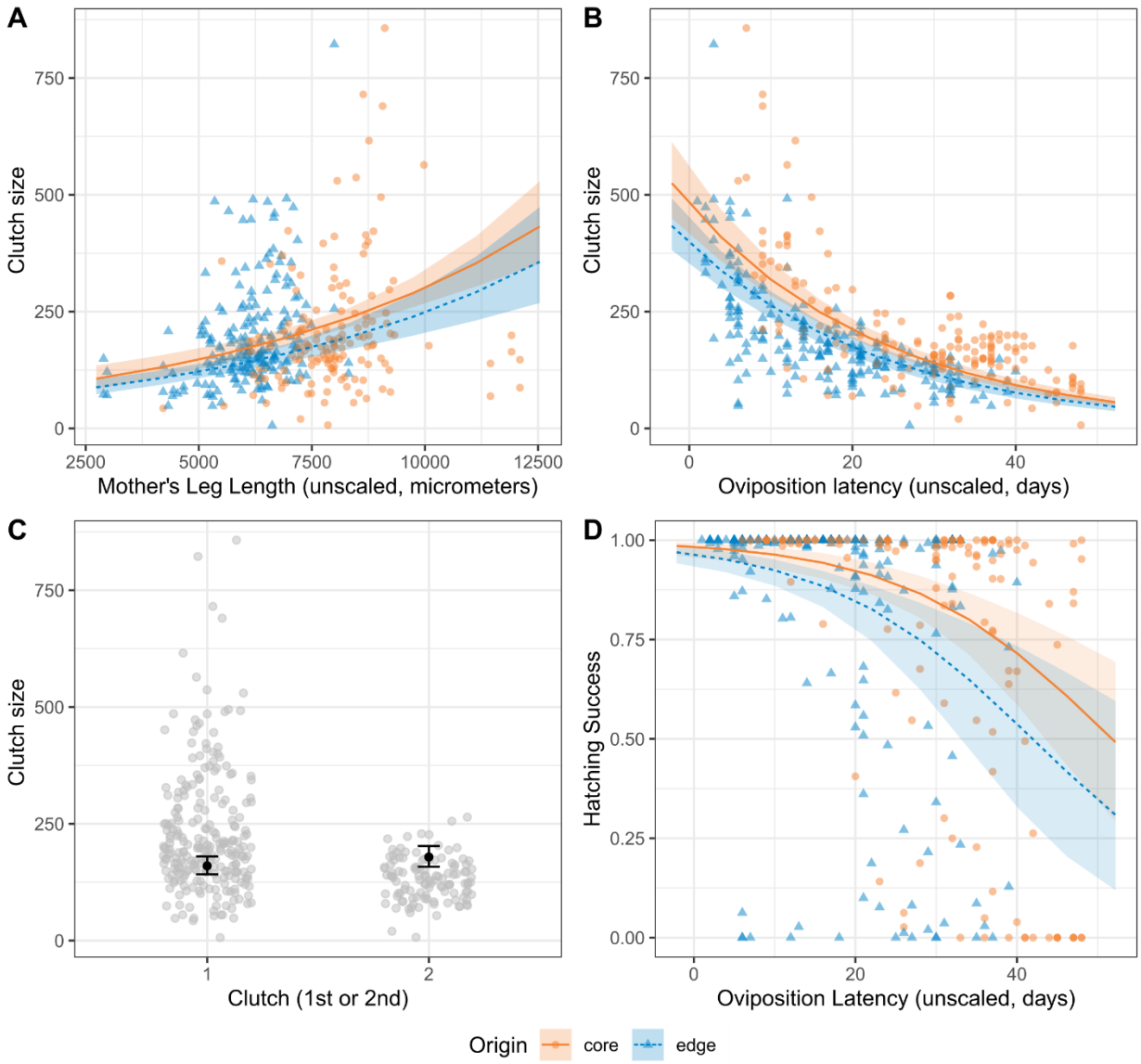

Figure S3. Clutch size and hatching success depending on mother's leg length, oviposition latency, and clutch. Transparent points represent the raw data; lines represent model predictions flanked with their 95% confidence intervals. Black points with error bars represent estimated marginal means and 95% confidence intervals for discrete predictor variables. Model predictions are back-transformed to the observed scale.

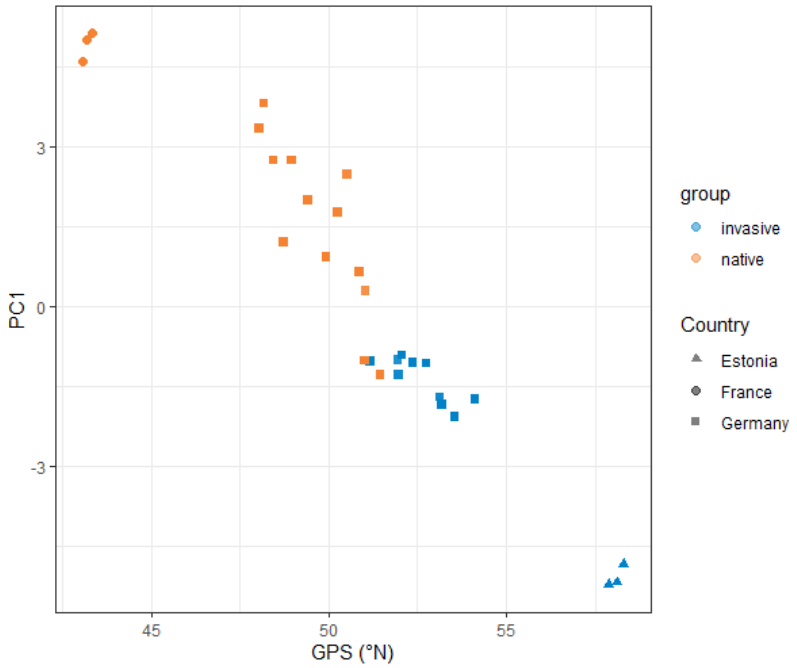

Figure S4. Environmental PC1 varies with latitude. Points represent single collecting sites, and are colored according to their assignment to "native" (orange) or "invasive" (blue) genetic clusters. Shapes represent countries.

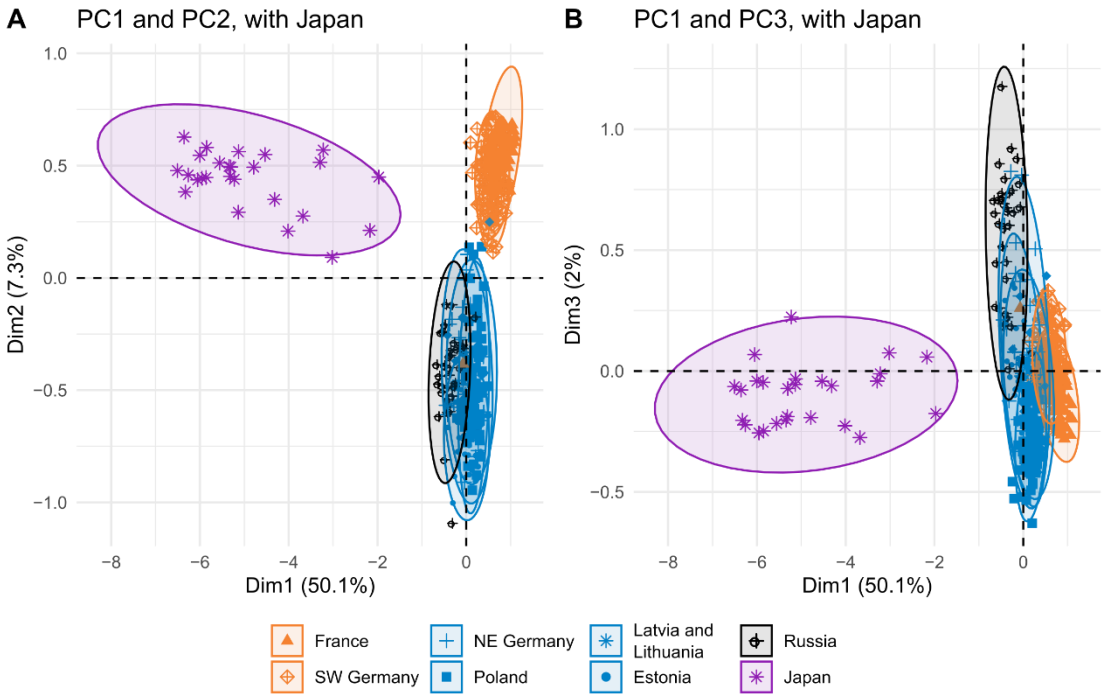

Figure S5. Principle components analysis of all populations using neutral SNPs. Ellipses represent 95% confidence intervals; points represent individual samples, with shape indicating the sampling country. Points and ellipses are colored according to the site's grouping region, Japan (purple), Russia (black), "invasive" (blue), "native" (orange).

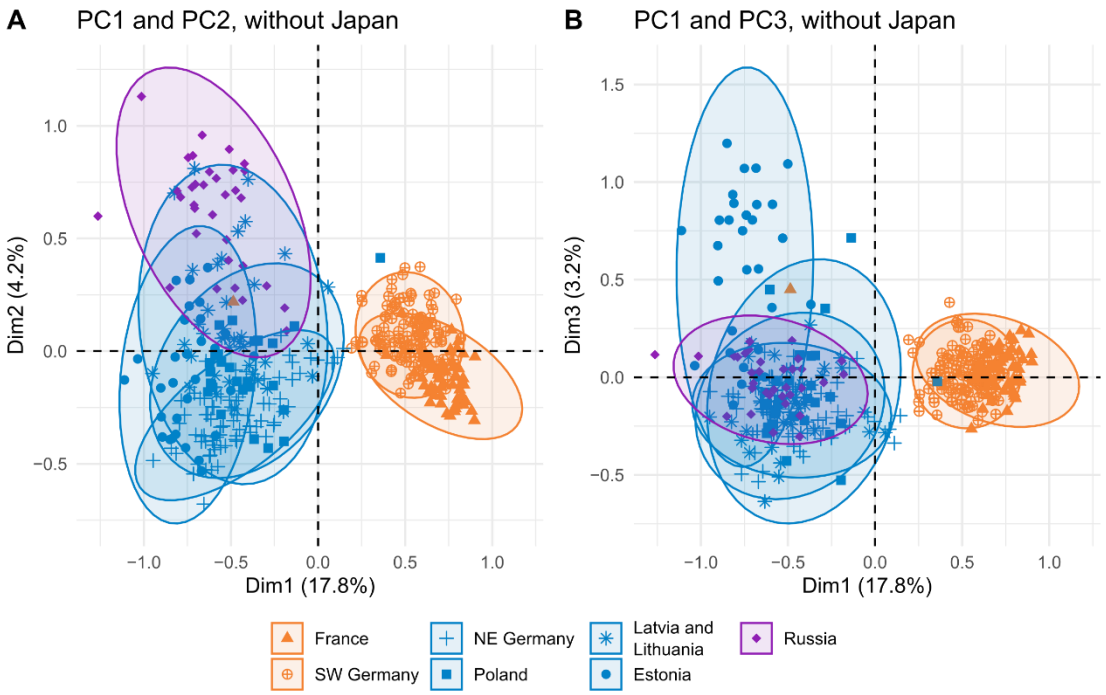

Figure S6. Principle components analysis of all non-Japanese populations using neutral SNPs. Ellipses represent 95% confidence intervals; points represent individual samples, with shape indicating the sampling country. Points and ellipses are colored according to the site's grouping region, Russia (purple), "invasive" (blue), "native" (orange).

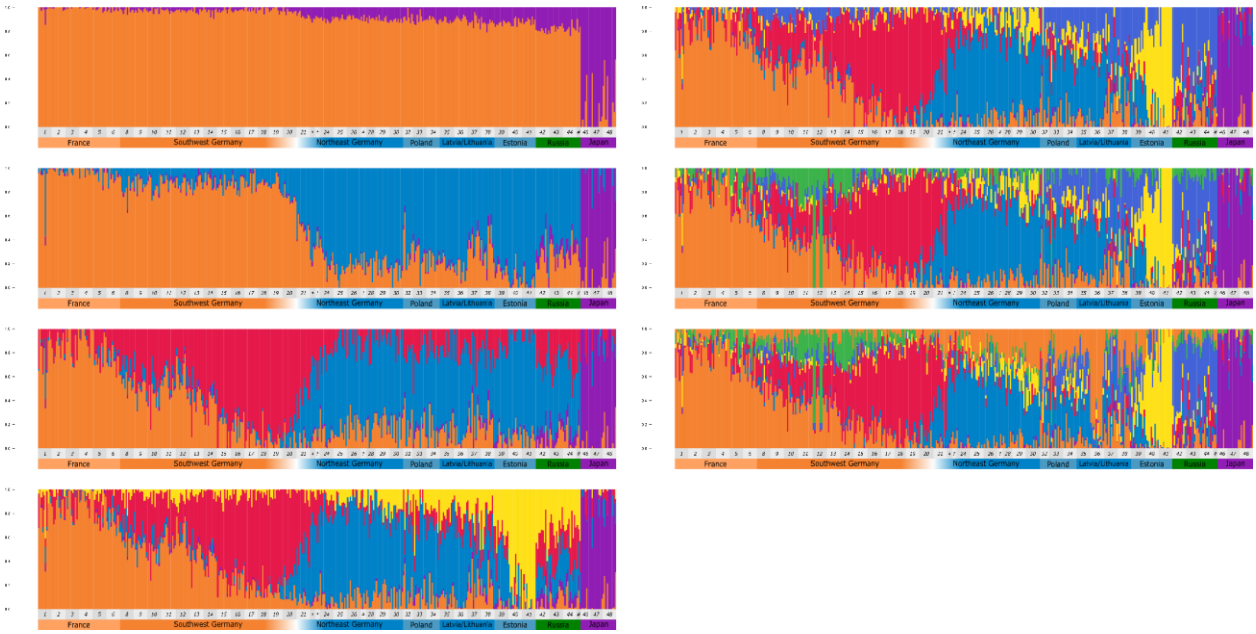

Figure S7. Stacked barplots of individual ancestry assignment, using ngsAdmix results for K=2 through K=8.

Table S1. Pairwise FST matrix for all populations. Cells are colored by value (low: yellow, high: red). Populations are numbered as in Table 1 in the main text.

	1	2	3	4	5	6	8	9	10	11	12	13	14	15	16	17	18	19	20	21	22	23	24	25	26	27	28	29	30	32	33	34	35	36	37	38	39	40	41	42	43	44	45	46	47	48
1	0	0.034	0.036	0.036	0.041	0.037	0.045	0.055	0.047	0.057	0.064	0.045	0.067	0.059	0.049	0.055	0.06	0.061	0.059	0.065	0.096	0.102	0.075	0.079	0.073	0.094	0.083	0.069	0.083	0.059	0.076	0.071	0.068	0.093	0.064	0.081	0.079	0.094	0.112	0.071	0.065	0.067	0.1	0.205	0.343	0.253
2	0.034		0	0.03	0.03	0.036	0.032	0.042	0.051	0.045	0.05	0.058	0.044	0.064	0.06	0.046	0.053	0.058	0.049	0.059	0.083	0.104	0.108	0.079	0.082	0.075	0.102	0.085	0.074	0.092	0.064	0.078	0.07	0.065	0.095	0.069	0.085	0.081	0.104	0.121	0.078	0.066	0.071	0.109	0.213	0.354	0.282
3	0.036	0.03		0	0.035	0.039	0.035	0.043	0.051	0.042	0.052	0.061	0.042	0.064	0.062	0.05	0.052	0.058	0.054	0.062	0.093	0.098	0.107	0.076	0.083	0.075	0.097	0.085	0.072	0.085	0.062	0.076	0.07	0.067	0.098	0.068	0.088	0.081	0.104	0.12	0.076	0.068	0.073	0.107	0.214	0.354	0.264
4	0.036	0.03	0.035		0	0.035	0.034	0.048	0.055	0.05	0.051	0.062	0.052	0.065	0.067	0.053	0.061	0.063	0.059	0.066	0.07	0.112	0.11	0.078	0.083	0.078	0.105	0.09	0.076	0.095	0.064	0.081	0.074	0.07	0.106	0.07	0.094	0.086	0.105	0.121	0.081	0.074	0.077	0.116	0.217	0.398	0.269
5	0.041	0.036	0.039	0.035		0	0.036	0.051	0.061	0.052	0.048	0.063	0.049	0.065	0.063	0.055	0.059	0.062	0.059	0.066	0.067	0.107	0.11	0.077	0.084	0.077	0.097	0.088	0.073	0.091	0.066	0.078	0.075	0.07	0.102	0.065	0.091	0.082	0.104	0.116	0.076	0.067	0.071	0.107	0.206	0.345	0.257
6	0.037	0.032	0.035	0.034	0.036		0	0.042	0.05	0.045	0.045	0.057	0.043	0.06	0.051	0.047	0.049	0.053	0.048	0.052	0.06	0.097	0.096	0.067	0.071	0.069	0.089	0.078	0.064	0.081	0.057	0.073	0.067	0.059	0.087	0.058	0.078	0.076	0.097	0.114	0.068	0.057	0.064	0.094	0.201	0.338	0.251
8	0.045	0.042	0.043	0.048	0.051	0.042		0	0.044	0.04	0.05	0.058	0.047	0.066	0.061	0.047	0.053	0.056	0.05	0.057	0.057	0.086	0.092	0.067	0.071	0.069	0.089	0.077	0.066	0.077	0.055	0.066	0.062	0.057	0.087	0.057	0.075	0.068	0.088	0.108	0.065	0.054	0.06	0.088	0.202	0.308	0.25
9	0.055	0.051	0.051	0.055	0.061	0.05	0.044		0	0.043	0.053	0.064	0.052	0.069	0.061	0.05	0.058	0.059	0.057	0.063	0.083	0.098	0.1	0.074	0.083	0.077	0.095	0.077	0.069	0.086	0.059	0.076	0.068	0.065	0.093	0.069	0.083	0.079	0.103	0.116	0.07	0.063	0.063	0.105	0.205	0.339	0.252
10	0.047	0.045	0.042	0.05	0.052	0.045	0.04	0.043		0	0.04	0.053	0.04	0.064	0.056	0.043	0.047	0.05	0.047	0.054	0.052	0.086	0.096	0.066	0.073	0.07	0.088	0.077	0.065	0.079	0.054	0.064	0.059	0.056	0.087	0.051	0.077	0.071	0.092	0.11	0.062	0.054	0.059	0.067	0.198	0.304	0.246
11	0.057	0.05	0.052	0.051	0.048	0.045	0.05	0.053	0.04		0	0.056	0.045	0.061	0.062	0.05	0.057	0.056	0.054	0.062	0.063	0.094	0.1	0.073	0.079	0.078	0.094	0.084	0.065	0.083	0.064	0.075	0.066	0.063	0.099	0.067	0.087	0.077	0.099	0.113	0.071	0.062	0.064	0.099	0.202	0.337	0.252
12	0.064	0.058	0.061	0.062	0.063	0.057	0.058	0.064	0.053	0.056		0	0.057	0.073	0.074	0.061	0.066	0.068	0.064	0.074	0.074	0.106	0.112	0.08	0.09	0.08	0.107	0.093	0.078	0.098	0.07	0.087	0.078	0.075	0.107	0.067	0.091	0.082	0.106	0.124	0.071	0.065	0.069	0.105	0.204	0.343	0.253
13	0.045	0.044	0.042	0.052	0.049	0.043	0.047	0.052	0.04	0.045	0.057		0	0.057	0.056	0.043	0.048	0.049	0.044	0.051	0.057	0.093	0.097	0.072	0.075	0.07	0.085	0.08	0.065	0.083	0.054	0.066	0.064	0.06	0.088	0.058	0.078	0.071	0.099	0.112	0.066	0.057	0.06	0.095	0.195	0.334	0.245
14	0.067	0.064	0.064	0.065	0.065	0.06	0.066	0.069	0.064	0.061	0.073	0.057		0.06	0.05	0.062	0.065	0.064	0.072	0.073	0.108	0.112	0.083	0.092	0.081	0.102	0.093	0.081	0.096	0.075	0.085	0.076	0.074	0.107	0.075	0.089	0.081	0.111	0.123	0.077	0.071	0.073	0.101	0.206	0.342	0.253
15	0.059	0.06	0.062	0.067	0.063	0.051	0.061	0.061	0.056	0.062	0.074	0.056	0.06		0	0.038	0.05	0.061	0.051	0.064	0.065	0.1	0.108	0.075	0.086	0.082	0.1	0.085	0.075	0.091	0.063	0.075	0.073	0.069	0.099	0.065	0.086	0.08	0.104	0.116	0.071	0.067	0.068	0.108	0.202	0.338	0.249
16	0.049	0.046	0.05	0.053	0.055	0.047	0.047	0.05	0.043	0.05	0.061	0.043	0.05	0.038		0	0.04	0.046	0.04	0.055	0.056	0.089	0.096	0.069	0.073	0.069	0.089	0.077	0.068	0.083	0.056	0.068	0.065	0.063	0.09	0.06	0.08	0.069	0.095	0.111	0.062	0.059	0.058	0.091	0.198	0.334	0.245
17	0.055	0.053	0.052	0.061	0.059	0.049	0.053	0.058	0.047	0.057	0.066	0.048	0.062	0.05	0.04		0.038	0.035	0.05	0.053	0.098	0.101	0.073	0.079	0.078	0.097	0.085	0.073	0.085	0.061	0.078	0.069	0.067	0.092	0.068	0.083	0.074	0.099	0.111	0.068	0.062	0.066	0.104	0.204	0.343	0.251
18	0.06	0.058	0.058	0.063	0.062	0.053	0.056	0.059	0.05	0.056	0.068	0.049	0.065	0.061	0.046	0.038		0	0.036	0.047	0.058	0.101	0.103	0.075	0.08	0.079	0.093	0.086	0.074	0.084	0.066	0.072	0.072	0.066	0.095	0.066	0.082	0.076	0.099	0.114	0.07	0.061	0.066	0.097	0.199	0.338	0.246
19	0.051	0.049	0.054	0.059	0.059	0.048	0.05	0.057	0.047	0.054	0.064	0.044	0.064	0.051	0.04	0.035	0.036		0	0.04	0.053	0.093	0.093	0.072	0.079	0.073	0.09	0.081	0.068	0.083	0.062	0.071	0.068	0.064	0.094	0.066	0.083	0.075	0.098	0.113	0.068	0.062	0.062	0.101	0.201	0.336	0.248
20	0.059	0.059	0.062	0.066	0.066	0.052	0.057	0.063	0.054	0.062	0.074	0.051	0.072	0.064	0.055	0.05	0.047	0.04		0	0.051	0.091	0.094	0.069	0.074	0.073	0.09	0.082	0.068	0.081	0.06	0.071	0.069	0.064	0.091	0.063	0.084	0.073	0.099	0.114	0.07	0.058	0.064	0.101	0.205	0.34	0.252
21	0.065	0.063	0.063	0.07	0.067	0.06	0.057	0.063	0.052	0.063	0.074	0.057	0.073	0.065	0.056	0.053	0.058	0.053	0.051		0	0.067	0.077	0.048	0.057	0.06	0.076	0.064	0.059	0.08	0.047	0.063	0.054	0.052	0.076	0.053	0.076	0.06	0.085	0.101	0.059	0.051	0.052	0.085	0.194	0.327	0.241
22	0.098	0.104	0.098	0.112	0.107	0.097	0.086	0.098	0.086	0.094	0.106	0.093	0.108	0.1	0.089	0.098	0.101	0.093	0.091	0.067		0	0.08	0.062	0.073	0.078	0.093	0.083	0.075	0.093	0.066	0.075	0.074	0.064	0.098	0.073	0.093	0.08	0.1	0.12	0.072	0.067	0.065	0.101	0.178	0.317	0.22
23	0.102	0.108	0.107	0.11	0.11	0.096	0.092	0.1	0.096	0.1	0.112	0.097	0.112	0.108	0.096	0.101	0.103	0.093	0.094	0.077	0.08		0	0.068	0.084	0.09	0.106	0.101	0.084	0.105	0.076	0.091	0.085	0.073	0.108	0.08	0.102	0.09	0.119	0.13	0.079	0.073	0.076	0.112	0.176	0.322	0.221
24	0.075	0.079	0.076	0.078	0.077	0.067	0.067	0.074	0.066	0.073	0.08	0.072	0.083	0.075	0.069	0.073	0.075	0.072	0.069	0.048	0.062	0.068		0	0.042	0.05	0.065	0.062	0.051	0.068	0.042	0.058	0.052	0.05	0.077	0.051	0.076	0.058	0.081	0.096	0.062	0.056	0.054	0.084	0.188	0.321	0.235
25	0.079	0.082	0.083	0.083	0.084	0.071	0.071	0.083	0.073	0.079	0.09	0.075	0.092	0.086	0.073	0.079	0.08	0.079	0.074	0.057	0.073	0.084	0.042		0	0.047	0.066	0.058	0.046	0.06	0.043	0.056	0.048	0.045	0.07	0.058	0.076	0.053	0.075	0.092	0.061	0.056	0.057	0.086	0.193	0.328	0.237
26	0.073	0.075	0.075	0.078	0.077	0.069	0.069	0.077	0.07	0.078	0.08	0.07	0.081	0.082	0.069	0.078	0.079	0.073	0.073	0.06	0.078	0.09	0.05	0.047		0	0.061	0.049	0.039	0.056	0.046	0.059	0.048	0.042	0.079	0.05	0.074	0.056	0.082	0.096	0.06	0.057	0.057	0.084	0.191	0.328	0.239
27	0.094	0.102	0.097	0.105	0.097	0.089	0.089	0.095	0.088	0.094	0.107	0.095	0.102	0.1	0.089	0.097	0.093	0.09	0.09	0.076	0.093	0.106	0.065	0.066	0.061		0	0.067	0.055	0.07	0.061	0.076	0.065	0.063	0.092	0.07	0.09	0.069	0.098	0.114	0.071	0.066	0.064	0.096	0.177	0.32	0.22
28	0.083	0.085	0.085	0.09	0.088	0.078	0.077	0.077	0.077	0.084	0.093	0.08	0.093	0.085	0.077	0.085	0.086	0.081	0.082	0.064	0.083	0.101	0.062	0.058	0.049	0.067		0	0.043	0.062	0.054	0.064	0.055	0.048	0.079	0.064	0.076	0.061	0.087	0.1	0.067	0.06	0.062	0.094	0.187	0.324	0.232
29	0.069	0.074	0.072	0.076	0.073	0.064	0.066	0.069	0.065	0.065	0.078	0.065	0.081	0.075	0.068	0.073	0.074	0.068	0.068	0.058	0.075	0.084	0.051	0.046	0.039	0.055	0.043		0.043	0.043	0.056	0.047	0.038	0.071	0.051	0.067	0.049	0.073	0.086	0.054	0.05	0.052	0.08	0.186	0.318	0.232
30	0.083	0.092	0.085	0.095	0.091	0.081	0.077	0.086	0.079	0.083	0.098	0.083	0.096	0.091	0.083	0.085	0.084	0.083	0.081	0.07	0.093	0.105	0.068	0.06	0.056	0.07	0.062	0.043		0.06	0.066	0.056	0.054	0.076	0.067	0.078	0.059	0.081	0.093	0.066	0.064	0.064	0.094	0.192	0.324	0.238
32	0.059	0.064	0.062	0.064	0.066	0.057	0.055	0.059	0.054	0.064	0.07	0.054	0.075	0.063	0.056	0.061	0.066	0.062	0.06	0.047	0.066	0.076	0.042	0.043	0.046	0.061	0.054	0.043	0.06		0.036	0.034	0.025	0.059	0.043	0.063	0.05	0.073	0.089	0.044	0.042	0.041	0.061	0.178	0.308	0.219
33	0.076	0.078	0.076	0.081	0.078	0.073	0.066	0.076	0.064	0.075	0.087	0.066	0.085	0.075	0.068	0.078	0.072	0.071	0.071	0.063	0.075	0.091	0.058	0.056	0.059	0.076	0.064	0.056	0.066	0.036		0.045	0.039	0.076	0.05	0.072	0.058	0.084	0.098	0.056	0.05	0.052	0.08	0.186	0.314	0.229
34	0.071	0.07	0.07	0.074	0.075	0.067	0.062	0.068	0.059	0.066	0.078	0.064	0.076	0.073	0.065	0.069	0.072	0.068	0.069	0.054	0.074	0.085	0.052	0.048	0.048	0.065	0.055	0.047	0.056	0.034	0.045		0	0.036	0.064	0.046	0.067	0.048	0.073	0.086	0.05	0.047	0.049	0.073	0.184	0.316	0.227
35	0.068	0.065	0.067	0.07	0.07	0.059	0.057	0.065	0.056	0.063	0.075	0.06	0.074	0.069	0.063	0.067	0.066	0.064	0.064	0.052	0.064	0.073	0.05	0.045	0.042	0.063	0.048	0.038	0.054	0.025	0.039	0.036		0	0.064	0.039	0.059	0.044	0.071	0.08	0.042	0.038	0.038	0.064	0.18	0.308	0.226
36	0.093	0.095	0.098	0.106	0.102	0.087	0.087	0.093	0.087	0.099	0.107	0.088	0.107	0.099	0.09	0.092	0.095	0.094	0.091	0.076	0.098	0.108	0.077	0.07	0.079	0.092	0.079	0.071	0.076	0.059	0.076	0.064	0.064	0	0.076	0.082	0.07	0.095	0.113	0.07	0.065	0.071	0.091	0.205	0.333	0.247
37	0.064	0.069	0.068	0.07	0.065	0.058	0.057	0.069	0.051	0.067	0.067	0.058	0.075	0.065	0.06	0.068	0.066	0.066	0.063	0.053	0.073	0.08	0.051	0.058	0.05	0.07	0.064	0.051	0.067	0.043	0.05	0.046	0.039	0.076	0	0.06	0.051	0.074	0.085	0.033	0.031	0.035	0.048	0.167	0.293	0.213
38	0.081	0.085	0.088	0.094	0.091	0.078	0.075	0.083	0.077	0.087	0.091	0.078	0.089	0.086	0.08	0.083	0.082	0.083	0.084	0.076	0.093	0.102	0.076	0.076	0.074	0.09	0.076	0.067	0.078	0.063	0.072	0.067	0.059	0.082	0.06	0	0.054	0.09	0.11	0.062	0.053	0.062	0.081	0.186	0.318	0.233
39	0.079	0.081	0.081	0.086	0.082	0.076	0.068	0.079	0.071	0.077	0.082	0.071	0.081	0.08	0.069	0.074	0.076	0.075	0.073	0.06	0.08	0.09	0.058	0.053	0.056	0.069	0.061	0.049	0.059	0.05	0.058	0.048	0.044	0.07	0.051	0.054	0	0.067	0.078	0.044	0.043	0.046	0.068	0.179	0.309	0.224
40	0.094	0.104	0.104	0.105	0.104	0.097	0.088	0.103	0.092	0.099	0.106	0.099	0.111	0.104	0.095	0.099	0.098	0.098	0.099	0.085	0.1	0.119	0.081	0.075	0.082	0.098	0.087	0.073	0.081	0.073	0.084	0.073	0.071	0.095	0.074	0.09	0.067	0	0.067	0.067	0.069	0.068	0.091	0.201	0.334	0.244
41	0.112	0.121	0.12	0.121	0.116	0.114	0.108	0.116	0.11	0.113	0.124	0.112	0.123	0.116	0.111	0.111	0.114	0.113	0.114	0.101	0.12	0.13	0.096	0.092	0.096	0.114	0.1	0.086	0.093	0.089	0.098	0.086	0.08	0.113	0.085	0.11	0.078	0.067	0	0.08	0.087	0.083	0.12	0.21	0.346	0.253
42	0.071	0.078	0.076	0.081	0.076	0.068	0.065	0.07	0.062	0.071	0.071	0.066	0.077	0.071	0.062	0.068	0.07	0.068	0.07	0.059	0.072	0.079	0.062	0.061	0.06	0.071	0.067	0.054	0.066	0.044	0.056	0.05	0.042	0.07	0.033	0.062	0.044	0.067	0.08	0	0.019	0.021	0.035	0.158	0.282	0.198
43	0.065	0.066	0.068	0.074	0.067	0.057	0.054	0.063	0.054	0.062	0.065	0.057	0.071	0.067	0.059	0.062	0.061	0.062	0.058	0.051	0.067	0.073	0.056	0.056	0.057	0.066	0.06	0.05	0.064	0.042	0.05	0.047	0.038	0.065	0.031	0.053	0.043	0.069	0.087	0.019		0	0.018	0.034	0.16	0.281	0.202
44	0.067	0.071	0.073	0.077	0.071	0.064	0.06	0.063	0.059	0.064	0.069	0.06	0.073	0.068	0.058	0.066	0.066	0.062	0.064	0.052	0.065	0.076	0.054	0.057	0.057	0.064	0.062	0.052	0.064	0.041	0.052	0.049	0.038	0.071	0.035	0.062	0.046	0.068	0.083	0.021	0.018		0	0.036	0.158	0.28	0.199
45	0.1	0.109	0.107	0.116	0.107	0.094	0.088	0.105	0.087	0.099	0.105	0.095	0.101	0.108	0.091	0.104	0.097	0.101	0.101	0.085	0.101	0.112	0.084	0.086	0.084	0.096	0.094	0.08	0.094	0.061	0.08	0.073	0.064	0.091	0.048	0.081	0.068	0.091	0.12	0.035	0.034	0.036		0	0.154	0.293	0.194
46	0.205	0.213	0.214	0.217	0.206	0.201	0.202	0.205	0.198	0.202	0.204	0.195	0.206	0.202	0.198	0.204	0.199	0.201	0.205	0.194	0.178	0.176	0.188	0.193	0.191	0.177	0.187	0.186	0.192	0.178	0.186	0.184	0.18	0.205	0.167	0.186	0.179	0.201	0.21	0.158	0.16	0.158	0.154		0	0.137	0.067
47	0.343	0.354	0.354	0.398	0.345	0.339	0.338	0.339	0.334	0.337	0.343	0.334	0.342	0.336	0.336	0.34	0.327	0.317	0.322	0.321	0.326	0.328	0.32	0.324	0.318	0.324	0.308	0.314	0.316	0.308	0.333	0.293	0.318	0.309	0.334	0.348	0.282	0.281	0.28	0.293	0.137		0	0.171	
48	0.253	0.262	0.264	0.269	0.257	0.251	0.25	0.252	0.246	0.252	0.253	0.245	0.253	0.249	0.245	0.251	0.246	0.248	0.252	0.241	0.22	0.221	0.235	0.237	0.239	0.22	0.232	0.232	0.238	0.219	0.229	0.227	0.226	0.247	0.213	0.233	0.224	0.244	0.253	0.198	0.202	0.199	0.194	0.067	0.171	

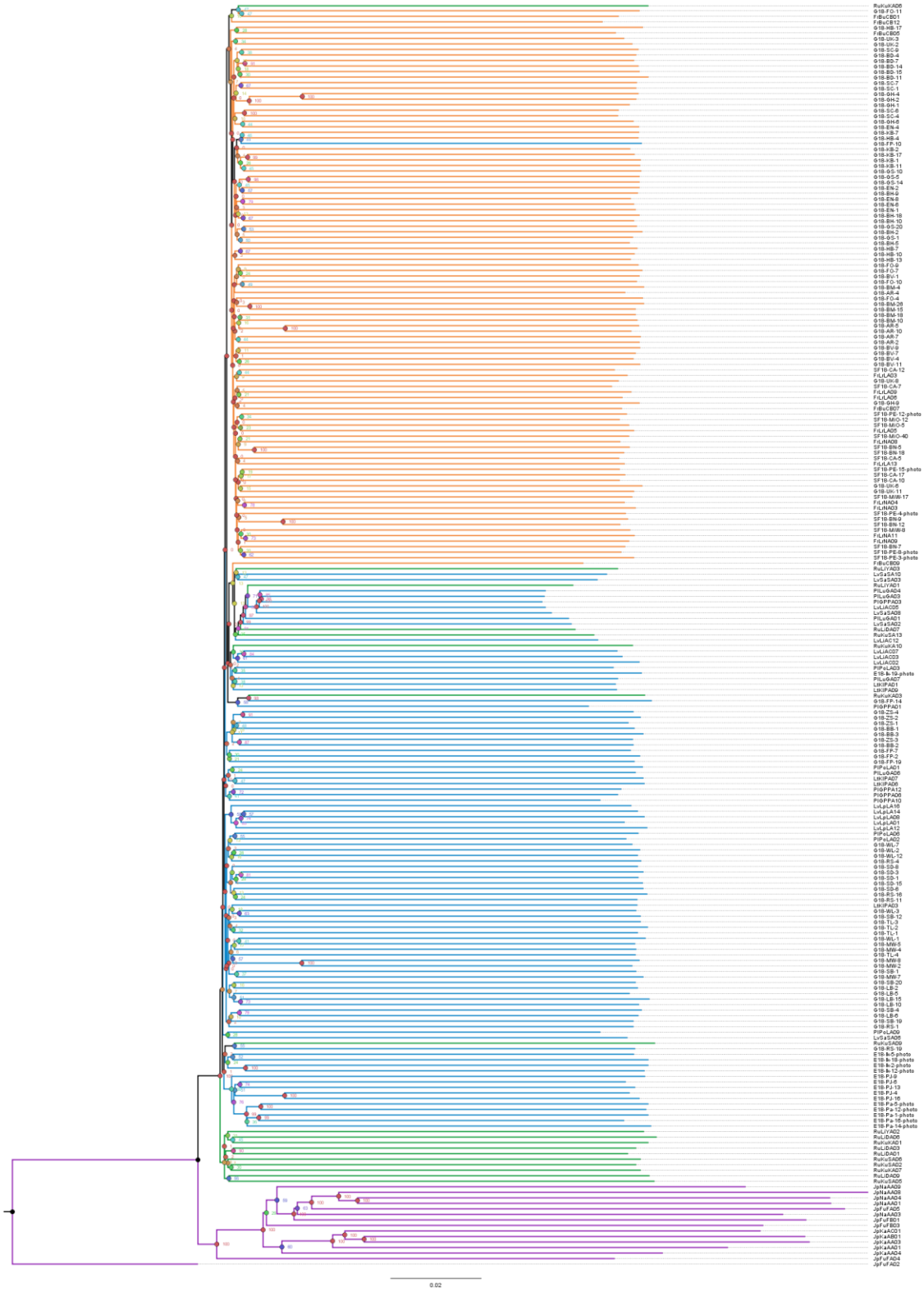

Figure S8. Phylogenetic tree based on ngsDist and FastME. Node labels are colored by bootstrap support. Branches are colored by the individual's assignment to regional groupings: Japan (purple), Russia (green), "invasive" (blue), "native" (orange).

Table S2. Model table for clutch size, if we do not include 2nd clutches or oviposition latency. Estimates are reported on the latent scale, with 95% confidence intervals. Fixed effects are considered to be significant if their confidence interval does not cross zero; these are indicated in **bold text**. Reference levels for fixed effects are given in [square brackets].

Response Variable	Sample size	Pseudo-R^2 (cond.)	Pseudo-R^2 (marg.)	Fixed effects	Estimate	2.5%	97.5%
Clutch size	244	0.230	0.185	**Origin [edge]**	0.493875	0.21490	0.772849
				Mother's leg length*	0.314927	0.21427	0.415588

*centered and scaled

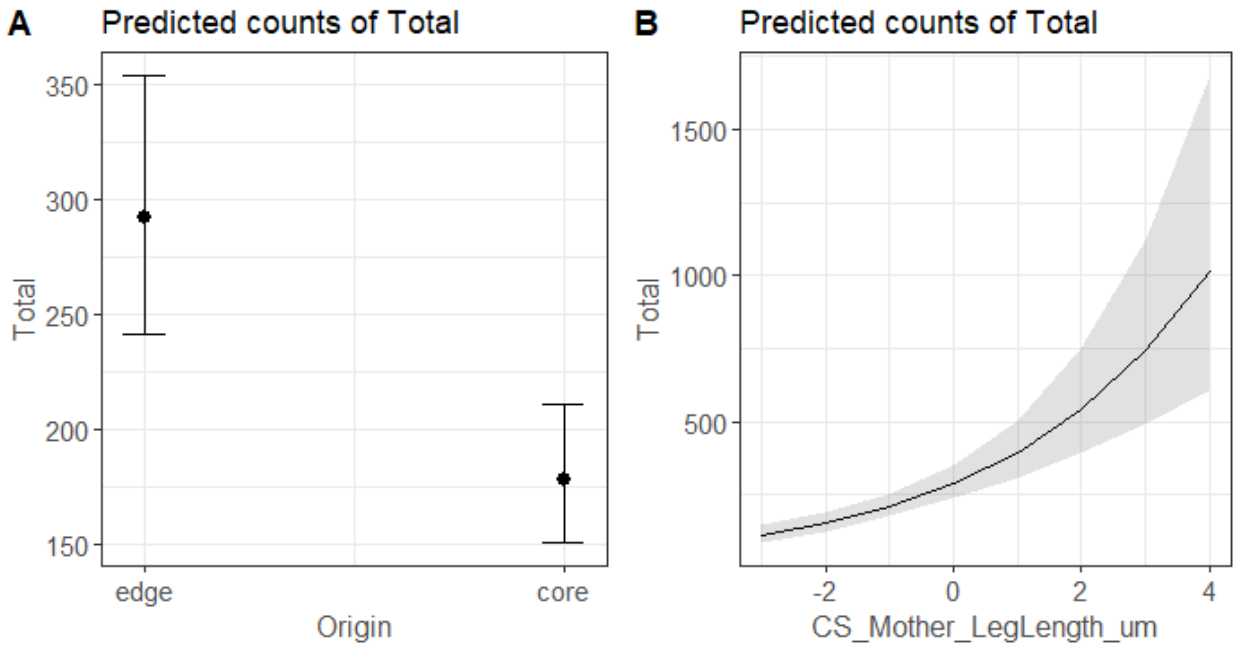

Figure S9. Model predictions for total clutch size ("Total," i.e. total number of eggs), in our supplementary exploratory model. We excluded 2nd clutches as well as the fixed effect "Oviposition latency" and only included origin (A) and mother's body size (B) as explanatory variables. The x-axis in (B) – "CS_Mother_LegLength_um" – represents centered and scaled leg length. Black points with error bars represent estimated marginal means and 95% confidence intervals for discrete predictor variables. Model predictions are back-transformed to the observed scale.

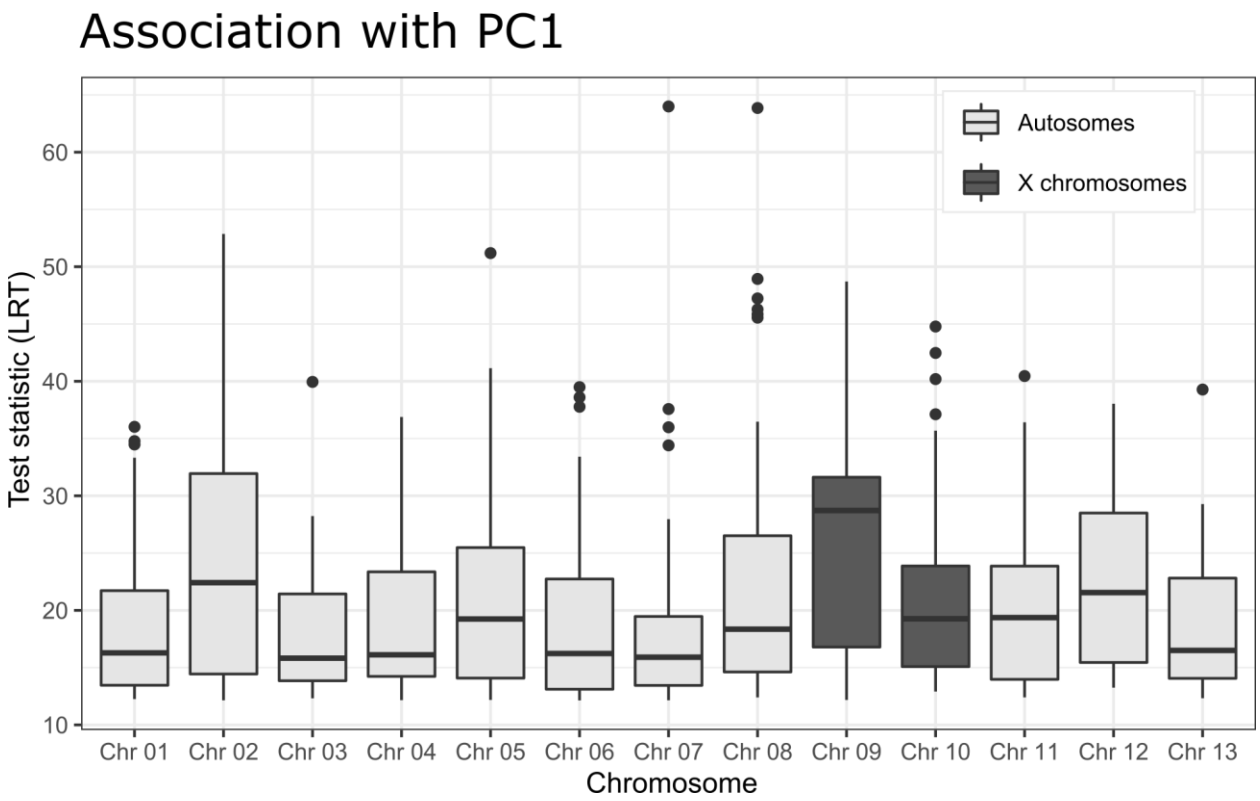

Figure S10. Boxplots of significant associations of SNPs with environmental PC1. Chromosome 9, one of the X chromosomes, shows more and stronger associations with the environment than autosomes. For the purpose of visualization, we excluded non-significant SNPs from this plot.

Supplemental File 2

Script to get Supercooling Point

By: Brian Schulze & Monica M. Sheffer

Obtain supercooling points from datalogger data

First, load libraries

```
library(openxlsx)
library(grDevices)
```

Then, set the threshold temperature change in degrees C to detect the heat of crystallization and read in the data file (edit file path to where your data is stored, or use file.choose())

```
threshold = 0.3
file = "Z:\\AllgSystZoo\\aa-
Sharing\\GrakoRESPONSE\\DataGrako2018_2019\\SupercoolingData\\MidWinterSuperc
ooling\\SC_150219_2_PA-88.xlsx"
dat = read.xlsx(file,startRow=4,colNames=F)
names= read.xlsx(file,colNames=F)[1,]
```

Now plot the data to get an overview, and then click on the plot to set new limits to zoom in on the peaks

```
cols = rainbow(ncol(dat)-1)
plot(dat$X1,dat$X2,type="l",col=cols[1],main="Click to choose limits [1. top
left; 2. bottom right]",xlab="time [sec]",ylab="temp [C弗牠]")
for(i in 3:ncol(dat))
{
  points(dat$X1,dat[,i],type="l",col=cols[i-1])
}
pos1 = locator(n=1) # top left
pos2 = locator(n=1) # bottom right
```

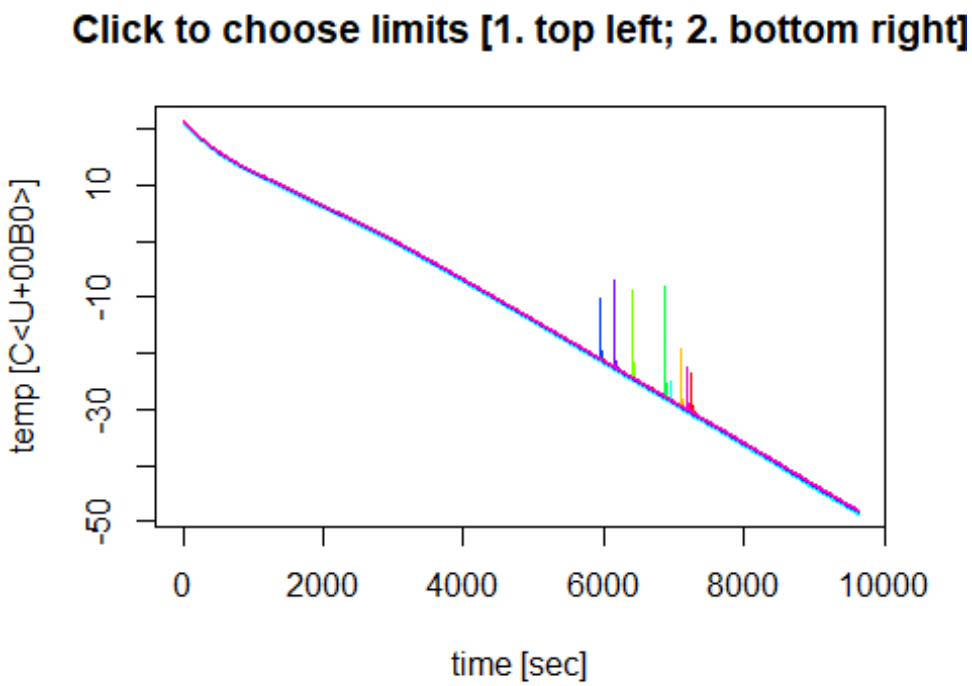

Plot the peaks with new limits obtained above, for a closer visual inspection of the data

```
#normally we click on the plots, but interactive interfaces don't work with
Rmarkdown, so we have to specify the positions manually in this example
pos1=list(x=4298.419,y=-9.202457)
pos2=list(x=7626.119,y=-33.03759)

plot(dat$X1,dat$X2,type="l",col=cols[1],xlim=c(round(pos1$x),round(pos2$x)),y
lim=c(round(pos2$y),round(pos1$y)),xlab="time [sec]",ylab="temp [C弗牠]")
for(i in 3:ncol(dat))
{
  points(dat$X1,dat[,i],type="l",col=cols[i-1])
}

#Having checked the data visually (everything looks good), now calculate the
SCPs, as well as the height of the peak and area below the curve, using the
threshold set above

scps = matrix(NA,ncol=5,nrow=ncol(dat)-1)
scps[,1] = unlist(c(names[1,-1]))
for(i in 2:ncol(dat))
{
  for(j in round(pos1$x):round(pos2$x)-1)
  {
    if((dat[j+1,i]-dat[j,i])>=threshold)
    {
```

```
      #print(paste(i-1,j,dat[j,i],dat[j+1,i],sep=" "))
      scps[i-1,2] = j
      scps[i-1,3] = dat[j,i]

      #peak height
      scps[i-1,4] = max(dat[j:(j+10),i]) - dat[j-1,i]

      #approximate area under peak
      t = (j-5):(j+60) # time of interest (5 seconds before to 60 seconds
after SCP peak)
      yt = dat[t,i]
      coeff = lm(c(dat[j-5,i],dat[j+60,i])~c(j-5,j+60))$coefficients
      area = sum(abs(coeff[2]*t+coeff[1])-abs(yt))
      scps[i-1,5] = round(area,2)
      break()
    }
  }
}
# plot and print scps
cat("SCPs:\n")

## SCPs:

for(i in 1:nrow(scps))
{
  points(scps[i,2],scps[i,3],col=cols[i],pch=16)
  cat(scps[i,1],"\t",scps[i,3],"\t",scps[i,4],"\t",scps[i,5],"\n",sep="")
}
```

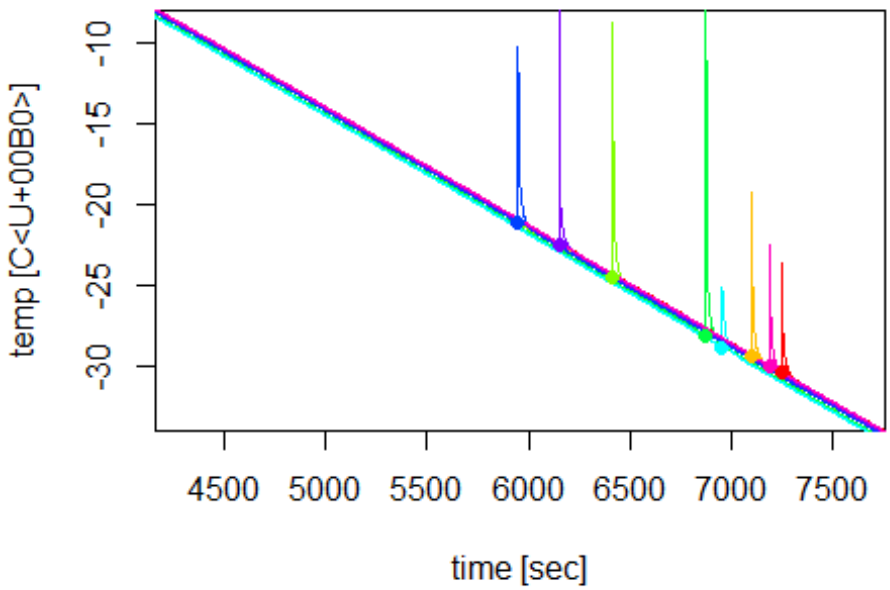


```
## E18-PA-88-A  -30.39  6.72    69.94
## E18-PA-88-B  -29.44  10.17   75.56
## E18-PA-88-C  -24.55  15.81   93.59
## E18-PA-88-D  -28.13  20.08   114.97
## E18-PA-88-E  -28.83  3.72    57.46
## E18-PA-88-F  -21.12  10.88   86.12
## E18-PA-88-G  -22.47  15.52   82.95
## E18-PA-88-H  -29.97  7.45    71.83
```

After obtaining the SCPs, we copied them into our larger dataset

```
writeClipboard(scps[,3])
```

Supplemental File 3

Script for Environmental Principle Components Analysis

By: Monica M. Sheffer

Calculate principle components to summarize environmental variation across sampling sites

First, load libraries, read and filter the data

```
library(factoextra)
library(tidyverse)
dat=read.csv("C:/Users/Uhl_4/Dropbox/Argiope_ddRAD/climate_data/output/spider
_allBioClim.csv")

#dat file has a separate row for each individual, but we just need one value
per site, so filter by distinct population numbers
dat_unique = dat %>% distinct(population_number,.keep_all = TRUE)

#we only need bioclimatic data for sites in Europe, so filter out Japan and
Russia
dat_filtered=dat_unique[which(dat_unique$Country!="Russia" &
dat_unique$Country!="Japan"),]

#group Estonia, Latvia and Lithuania into "Baltic" for cleaner plotting
dat_filtered$groups=dat_filtered$Country
dat_filtered$groups[which(dat_filtered$Country=="Estonia"|dat_filtered$Countr
y=="Lativa"|dat_filtered$Country=="Lithuania")]="Baltic"
```

Calculate and visualize the PCA

```
#calculate PCA
res.pca_noJnoR=prcomp(dat_filtered[,18:36],scale=T)

#vizualize PCA
fviz_eig(res.pca_noJnoR)
```

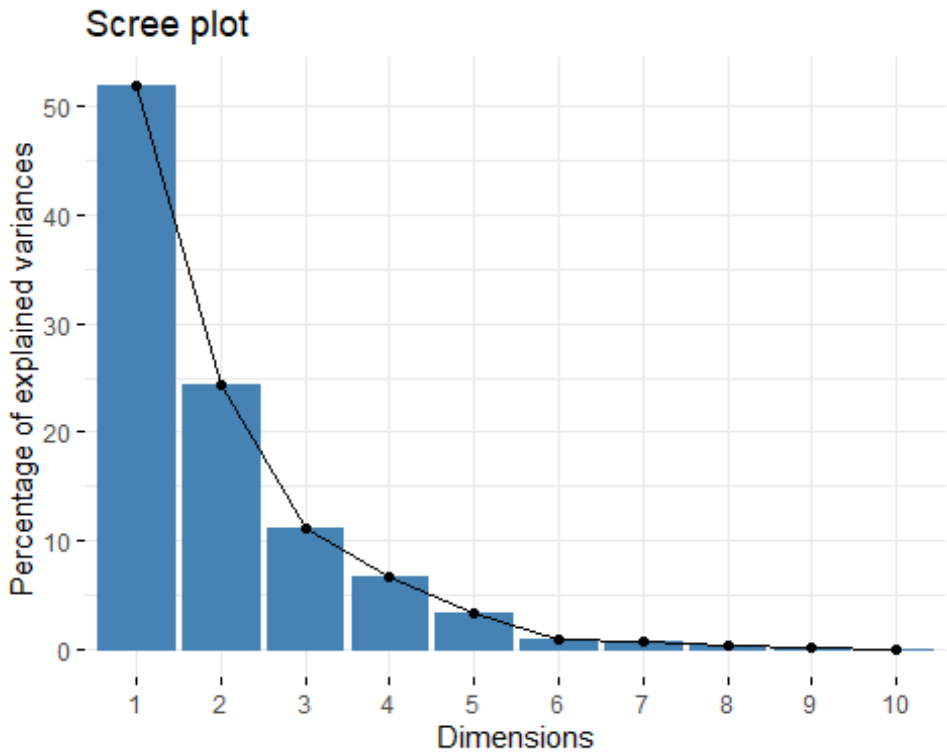


```
fviz_pca_biplot(res.pca_noJnoR,axes=c(1,2),col.ind=dat_filtered$groups,repel=
T,addEllipses = TRUE,mean.point=F,geom="point")

## Too few points to calculate an ellipse

## Warning: ggrepel: 8 unlabeled data points (too many overlaps). Consider
## increasing max.overlaps
```

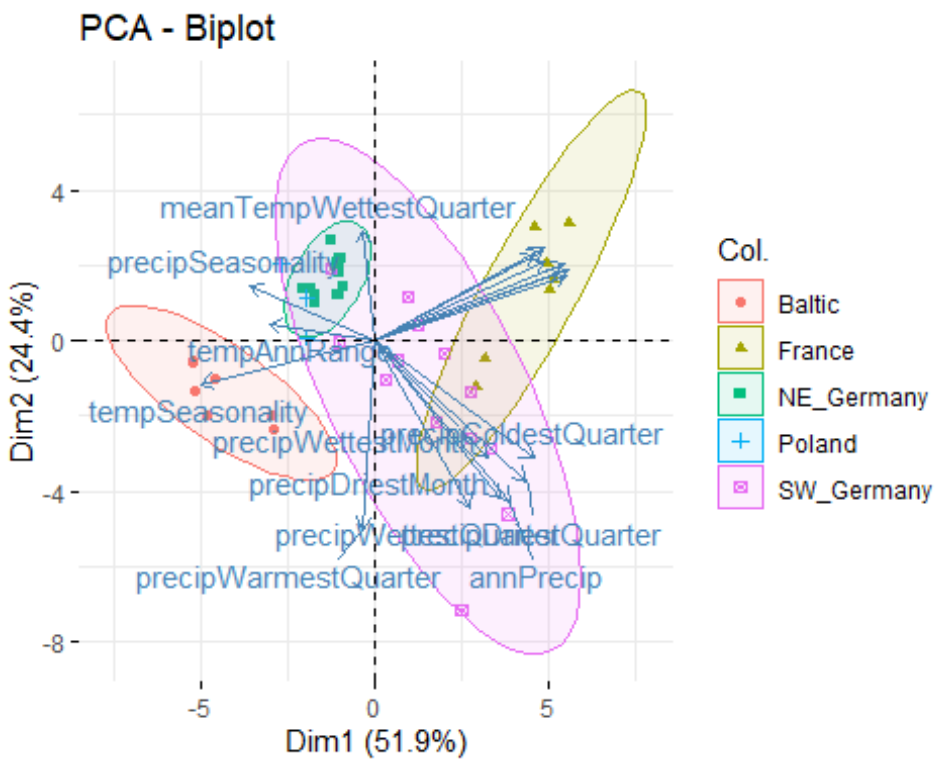


```
fviz_pca_biplot(res.pca_noJnoR,axes=c(2,3),col.ind=dat_filtered$groups,repel=
T,addEllipses = TRUE,mean.point=F,geom="point")

## Too few points to calculate an ellipse
```

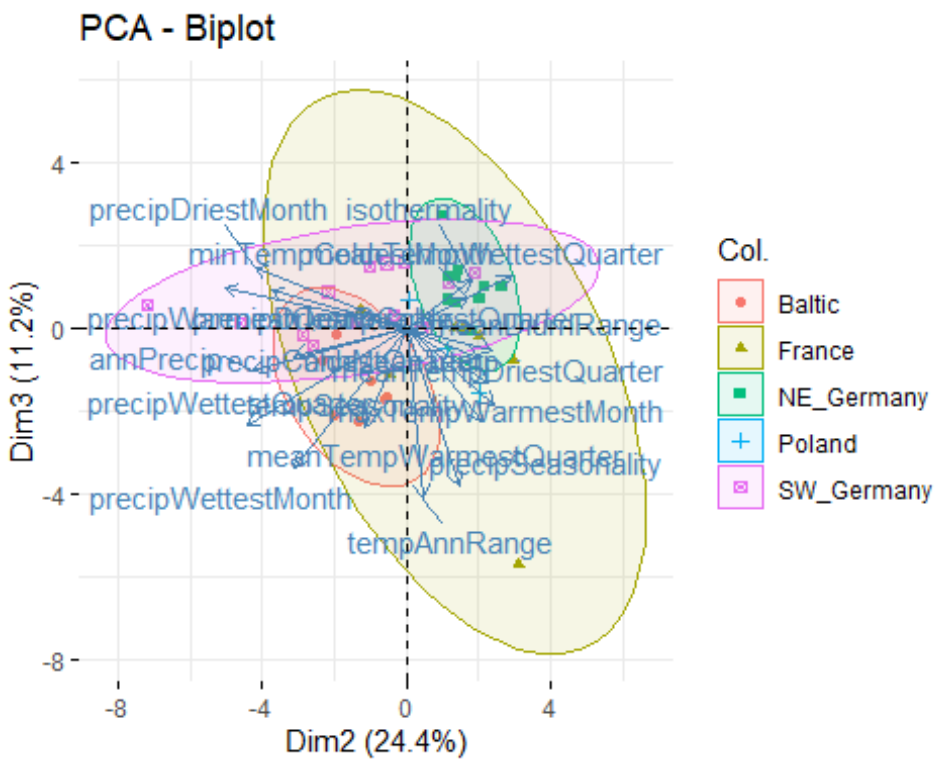


```
fviz_pca_biplot(res.pca_noJnoR,axes=c(3,4),col.ind=dat_filtered$groups,repel=
T,addEllipses = TRUE,mean.point=F,geom="point")

## Too few points to calculate an ellipse

## Warning: ggrepel: 15 unlabeled data points (too many overlaps). Consider
## increasing max.overlaps
```

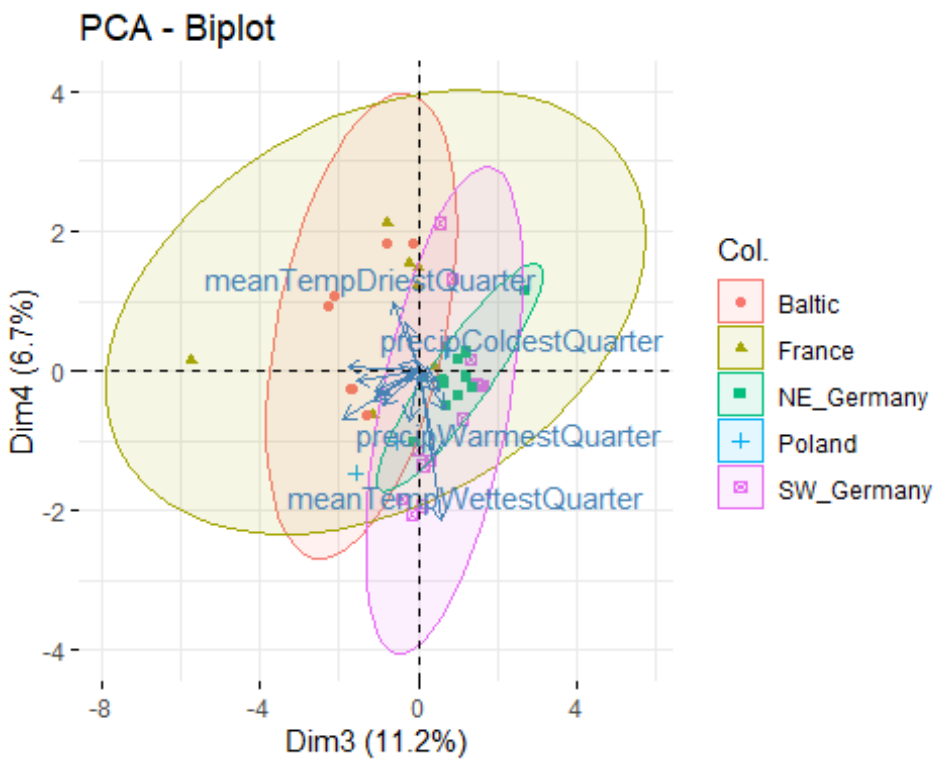


```
fviz_pca_biplot(res.pca_noJnoR,axes=c(4,5),col.ind=dat_filtered$groups,repel=
T,addEllipses = TRUE,mean.point=F,geom="point")

## Too few points to calculate an ellipse

## Warning: ggrepel: 17 unlabeled data points (too many overlaps). Consider
## increasing max.overlaps
```

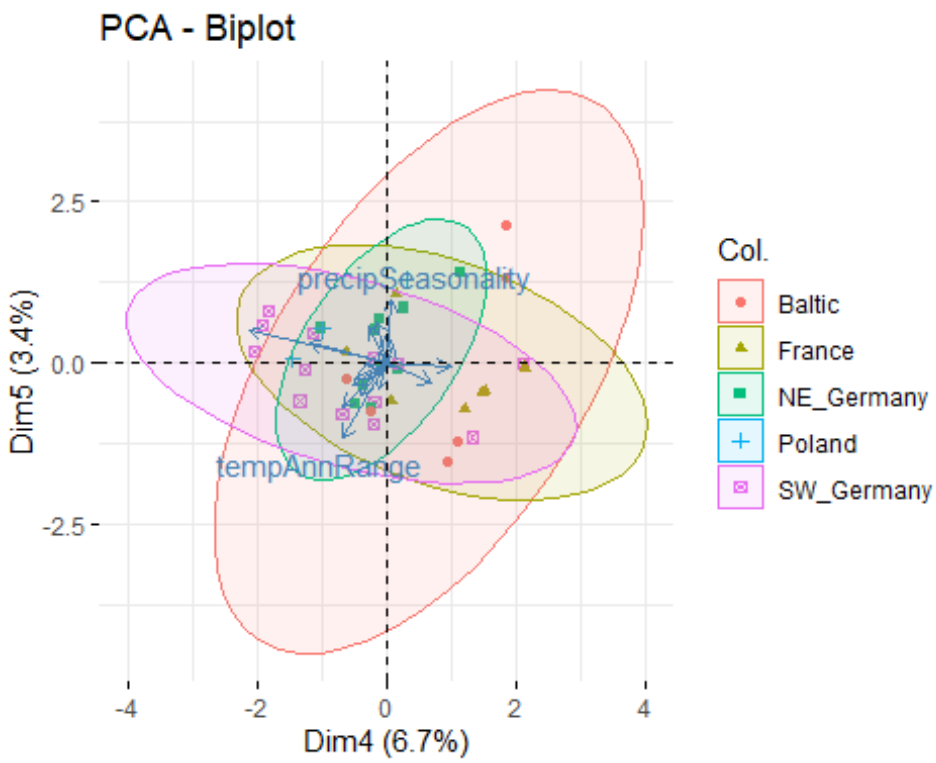

Print specific loadings of the PCs

```
sort(res.pca_noJnoR[["rotation"]][,"PC1"])

##        tempSeasonality      precipSeasonality           tempAnnRange
##             -0.27102370             -0.19418552             -0.16450314
## meanTempWettestQuarter   precipWarmestQuarter   precipWettestQuarter
##             -0.01920380             -0.01890199              0.14805015
##     precipWettestMonth      precipDriestMonth               annPrecip
##              0.17512415              0.19302953              0.20868676
##    precipDriestQuarter   precipColdestQuarter  meanTempDriestQuarter
##              0.23528249              0.24663256              0.24753941
##         meanDiurnRange    maxTempWarmestMonth meanTempWarmestQuarter
##              0.25802749              0.26150117              0.26204398
##          isothermality             annMeanTemp    minTempColdestMonth
##              0.28742502              0.29361680              0.29645808
## meanTempColdestQuarter
##              0.29975360

sort(res.pca_noJnoR[["rotation"]][,"PC2"])

##   precipWarmestQuarter   precipWettestQuarter               annPrecip
##             -0.39690373             -0.34801214             -0.33588406
##      precipDriestMonth    precipDriestQuarter   precipColdestQuarter
##             -0.33073533             -0.29354691             -0.24590297
##     precipWettestMonth        tempSeasonality           tempAnnRange
##             -0.24307533             -0.09048024              0.03506497
```

```
##      precipSeasonality    minTempColdestMonth          isothermality
##             0.11606285             0.13427019             0.14388219
## meanTempColdestQuarter            annMeanTemp meanTempWarmestQuarter
##             0.14598218             0.15910666             0.16629178
##  meanTempDriestQuarter         meanDiurnRange    maxTempWarmestMonth
##             0.17917805             0.18794679             0.19266831
## meanTempWettestQuarter
##             0.23017698
```

```
sort(res.pca_noJnoR[["rotation"]][,"PC3"])
```

```
##           tempAnnRange      precipSeasonality     precipWettestMonth
##           -0.475428324           -0.444724070           -0.390397428
##        tempSeasonality   precipWettestQuarter meanTempWarmestQuarter
##           -0.281000718           -0.273090805           -0.261345177
##    maxTempWarmestMonth  meanTempDriestQuarter              annPrecip
##           -0.217642295           -0.155451097           -0.117161640
##            annMeanTemp   precipColdestQuarter         meanDiurnRange
##           -0.086738727           -0.078688021           -0.060974214
## meanTempColdestQuarter    minTempColdestMonth    precipDriestQuarter
##            0.002638099            0.083023900            0.104256699
##   precipWarmestQuarter          isothermality meanTempWettestQuarter
##            0.113134186            0.136119231            0.145361505
##      precipDriestMonth
##            0.170342286
```

```
sort(res.pca_noJnoR[["rotation"]][,"PC4"])
```

```
## meanTempWettestQuarter   precipWarmestQuarter         meanDiurnRange
##            -0.69162758            -0.39009622            -0.22923774
##           tempAnnRange      precipDriestMonth    maxTempWarmestMonth
##            -0.22438006            -0.17408335            -0.16097378
##        tempSeasonality meanTempWarmestQuarter          isothermality
##            -0.13759165            -0.11523039            -0.09492883
##   precipWettestQuarter     precipWettestMonth    precipDriestQuarter
##            -0.09394129            -0.04957857            -0.04437050
##            annMeanTemp    minTempColdestMonth      precipSeasonality
##            -0.04433973            -0.00712530             0.02247883
## meanTempColdestQuarter              annPrecip   precipColdestQuarter
##             0.03166551             0.03238765             0.22098703
##  meanTempDriestQuarter
##             0.32012586
```

```
sort(res.pca_noJnoR[["rotation"]][,"PC5"])
```

```
##           tempAnnRange         meanDiurnRange        tempSeasonality
##            -0.52716728            -0.31030178            -0.22280938
##    precipDriestQuarter      precipDriestMonth   precipColdestQuarter
##            -0.18770326            -0.15034559            -0.14219453
##    maxTempWarmestMonth          isothermality              annPrecip
##            -0.10805523            -0.10269024            -0.02936224
```

```
##  meanTempDriestQuarter meanTempWarmestQuarter            annMeanTemp
##            -0.02144636            -0.01313582             0.07925481
## meanTempColdestQuarter   precipWarmestQuarter    minTempColdestMonth
##             0.12209270             0.13787975             0.19799805
## meanTempWettestQuarter   precipWettestQuarter     precipWettestMonth
##             0.23263255             0.25508775             0.28617036
##      precipSeasonality
##             0.44035083
```